NI

CR-165476
PWA-5708-26

NASA

Thin Film Temperature Sensors Phase III

by

H. P. Grant
J. S. Przybyszewski
R. G. Claing
W. L. Anderson

UNITED TECHNOLOGIES CORPORATION
PRATT & WHITNEY AIRCRAFT GROUP
COMMERCIAL PRODUCTS DIVISION

Prepared for

NATIONAL AERONAUTICS AND SPACE ADMINISTRATION
Lewis Research Center
Cleveland, Ohio 44135
Contract NAS3-22002

1. Report No.	2. Government Accession No.	3. Recipient's Catalog No.
NASA CR-165476		

4. Title and Subtitle	5. Report Date
Thin Film Temperature Sensors, Phase III	January 11, 1982
	6. Performing Organization Code

7. Author(s)	8. Performing Organization Report No.
H. P. Grant, J. S. Przybyszewski, R. G. Claing and W.L. Anderson	PWA-5708-26
	10. Work Unit No.

9. Performing Organization Name and Address	11. Contract or Grant No.
UNITED TECHNOLOGIES CORPORATION Pratt & Whitney Aircraft Group, Commercial Products Div. East Hartford, Connecticut 06108	NAS3-22002
	13. Type of Report and Period Covered
12. Sponsoring Agency Name and Address	Contractor Report
NATIONAL AERONAUTICS AND SPACE ADMINISTRATION Lewis Research Center Cleveland, Ohio 44135	14. Sponsoring Agency Code

15. Supplementary Notes

Project Manager: Raymond Holanda
NASA Lewis Research Center, Cleveland, Ohio 44135

16. Abstract

The third phase of development of thin film temperature sensors was completed. Efforts during this third phase consisted of further development of thin film technology, the design of a thin film thermocouple system installation suitable for engine-test evaluation, and the preparation of an engine test plan. The development of thin film technology was directed toward further improvement in film adherence, durability, accuracy, and drift characteristics. Film thickness was increased to 14 μm, and drift was reduced to less than 0.02 percent of Fahrenheit temperature per hour on actual turbine blades at 1255K (1800°F).

17. Key Words (Suggested by Author(s))	18. Distribution Statement
Sputtering Turbine Blades Thermocouple Drift Temperature Sensors Thin Film Adherence Thin Film Thermocouples	

19. Security Classif. (of this report)	20. Security Classif. (of this page)	21. No. of Pages	22. Price*
UNCLASSIFIED	UNCLASSIFIED	79	

*For sale by the National Technical Information Service, Springfield, Virginia 22161

FOREWORD

The work described in this report was accomplished by the Commercial Products Division of Pratt & Whitney Aircraft, United Technologies Corporation, under the National Aeronautics and Space Administration Contract NAS3-22002. Mr. Raymond Holanda of the NASA Lewis Research Center was the Project Manager for the program.

This report was prepared by Mr. Howard P. Grant, the Pratt & Whitney Aircraft Program Manager, Mr. John S. Przybyszewski, Mr. Richard G. Claing, and Mr. W.L. Anderson.

The contributions of Mr. Ronald Kaszycki and Mr. Richard B. Bourque of the Instrument Development Laboratory, Commercial Products Division, during the fabrication and testing of the sputtered sensor systems are gratefully acknowledged. The assistance and advice of Dr. R.L. Oglukian, Dr. W.B. Watkins, and Mr. W.W. Robinson of the Government Products Division of Pratt & Whitney Aircraft, United Technologies Corporation, are also gratefully acknowledged.

TABLE OF CONTENTS

TABLE OF CONTENTS (Cont'd.)

LIST OF TABLES

LIST OF ILLUSTRATIONS

LIST OF ILLUSTRATIONS (Continued)

SECTION 1.0

SUMMARY

The development of thin film temperature sensors has been conducted by Pratt & Whitney under a three-phase NASA program. The overall objective of this three-phase Thin Film Temperature Sensor Program was to develop a method of measuring turbine blade temperatures during engine operation without disturbing the gas flow or metal temperature profiles. This temperature measurement was to be accomplished using thermocouples that have been sputtered onto turbine blades in thin, intersecting stripes, rather than using embedded wire junctions. The program was divided into three phases to accomplish the overall objective.

Phase I, previously completed under Contract NAS3-20768, presented the analysis, design, development, fabrication, and testing of a basic temperature sensor system and the development of reliable thin-film-to-lead-wire connections. The thermocouple systems were applied to flat plate specimens of four turbine blade and vane materials and to simulated turbine blades and tested in a high temperature, low velocity exhaust gas environment. The results of this first phase of the overall program are documented in NASA CR-159782 (PWA-5526-31), Reference 1. A platinum versus platinum/10-percent rhodium thermocouple, 2 μm thick, sputtered over an insulating layer of oxidized NiCoCrAlY, was found to be the best configuration in terms of durability and accuracy during hot gas flow cyclic testing.

Phase II, previously completed under Contract NAS3-20831, applied the basic Phase I thin film technology to actual turbine blades, reduced the sensor size, and extended the test conditions to higher temperatures and gas velocities. The problem of thin film adherence to the alumina ($-Al_2O_3$) insulating layer, originally identified during Phase I, was investigated in detail under Phase II, and a procedure was established which increased the yield of successful thin film sensors. Additionally, problems of adapting the previously established fabrication procedures to actual turbine blades were discovered, and improved procedures were developed and evaluated. A useful life of about 50 hours under combustor test flow conditions was achieved. Thermocouple calibrations indicated drift of about 0.1 percent per hour. The drift was attributed to oxidation of the rhodium in the thin films. The results of this second phase of the overall program are documented in NASA CR-165201 (PWA-5604-31), Reference 2. Increased film thickness and the use of protective overcoats were recommended to reduce drift in the thermocouple systems.

The efforts during Phase III, the subject of this document, under Contract NAS3-22002 consisted of further development of thin film technology, the design of a thin film thermocouple system installation suitable for engine-test evaluation, and the preparation of an engine test plan. The development of thin film technology was directed toward further improvement in film adherence, durability, accuracy and drift characteristics. Film thickness was increased to 14 μm and drift was reduced to less than 0.02 percent per hour on actual turbine blades.

SECTION 2.0

INTRODUCTION

2.1 BACKGROUND

Turbine blade temperature measurement by blade-mounted sensors is currently accomplished by embedding thermocouples in the blade wall. The uncertainty in this method of measurement can be as high as 50K because of heat path distortion and uncertainty of exact location of the thermocouple junction. As blade wall thicknesses are decreased because of complex blade cooling schemes, the presence of embedded thermocouples becomes more adverse both from a structural and a measurement viewpoint. It is desirable to have a surface-mounted temperature sensor which does not require removal of any blade material and, at the same time, is of such minimum mass and thickness that it causes no serious heat path distortion within the blade or gas flow distortion over the blade. A thin film temperature sensor would be compatible with these considerations.

Using various thin film techniques (plating, vacuum evaporation, vacuum sputtering), a sensor can be formed by depositing layers of electrical insulating materials and metals whose thickness is only a few micrometers (μm). Successful surface thermocouples were obtained in this way by Burger in 1930 (Reference 3), Harris in 1934 (Reference 4), and Benderskey in 1953 (Reference 5). On metal parts, the technique was limited to surface temperatures below 800K due to the lack of a stable thin film insulating layer to provide reliable electrical isolation from the base metal at higher temperatures. Layers of quartz, SiO, and Al_2O_3, deposited by either vacuum evaporation or sputtering, were found to be too brittle to withstand the severe thermal stresses (up to 3.5×10^9 Pascals; 500,000 pounds per square inch) induced by the mismatch of temperature coefficients of expansion between the insulating layer and base metal.

Recent work on thin films at Pratt & Whitney is summarized in Table I. The work described in columns 1 and 2 was performed by Dils (Reference 6), using solid FeCrAlY test pieces oxidized in air to form an insulating layer of aluminum oxide. An additional amount of aluminum oxide was then sputtered on this grown aluminum oxide. The thermocouple legs were then sputtered on this insulator, and tests at 1350K were performed. This combination of fabrication methods and materials was able to withstand high temperatures. Thermal electromotive force (emf) was within 1.5 percent of standard reference Type S wire thermocouples, while a 600K temperature gradient was imposed along the length of the thin film. Drift was generally less than 0.01 percent per hour at constant temperature, over a period of 150 hours (Reference 7).

TABLE I

REVIEW OF PRATT & WHITNEY AIRCRAFT EXPERIENCE WITH SPUTTERED THIN FILM SENSORS ON MCrAlY SUBSTRATES AT HIGH TEMPERATURES

	1	2	3	4	5	6	7	8
Date	1972 - 75	1975	1975 - 76	1976	1976	1977	1979	1980
Type of Sputtered Sensor	Thermocouples	Thermocouples	Thermocouples	Strain gage	Erosion samples	Thermocouples	Thermocouples	Thermocouples
Sputtered Film	Pt/Pt-10% Rh	Pt/Pt-10% Rh	Pt/Pt-10% Rh	Platinum	Platinum	Pt/Pt-10% Rh	Pt/Pt-10% Rh	Pt/Pt-10% Rh
Film Thickness	2 to 12 μm	2 to 12 μm	2 μm	2 μm	2 μm	2 μm	2 μm	2 μm
Substrate Coating	---	---	NiCoCrAlY	NiCoCrAlY	NiCoCrAlY	NiCoCrAlY	NiCoCrAlY CoCrAlY	NiCoCrAlY
Base Material	FeCrAlY	FeCrAlY	MAR-M-200 + hafnium	Hastelloy X	B1900 + hafnium	B1900 + hafnium	MAR-M-509 B1900 + hafnium IN100 MAR-M-200 + hafnium	MAR-M-200 + hafnium
Lead-Wire-to-Film Connection	Strap weld	Strap weld	Fired platinum paste	Fired platinum paste	None	Fired paste	Hot compression bond	Hot compression bond
Configuration	Erosion bars, rods & airfoils	Cylinder	Flat bar	Strain bar	JT9D 1st-stage turbine blades	JT9D 2nd-stage turbine vanes	Flat bars	JT9D 1st-stage turbine blades
Test Facility	Lab combustor	Lab combustor	Lab furnace	Lab furnace	Operating engine	Operating engine	Furnace and torch	Combustor, 1 atm
Time Above 1250K, Each Sensor	100 hours	180 hours	170 hours	32 hours	150 hours	60 hours	60 hours	60 hours
Cycles to 1250K, Each Sensor	100	20	6	1			30	71
Reference Publications	(6) (7)	(7)	---	---	---	---	(1)	(2)
Remarks	20 specimens tested	Instrumented specimen for proof of calibration stability	Instrumented specimen for proof of calibration stability	Strain test specimen	Engine erosion test	Metal temperature and heat transfer coefficient	Developed lead wire attachments and ran extended hot calibrations of thin film thermocouples in hydrocarbon flame	Platinum adherence improved and reversible drift mechanism identified

The work described in columns 3, 4, 5, and 6 of Table I was performed by Przybyszewski (unpublished). In furnace tests on flat specimens (column 3), a typical turbine blade material (MAR-M-200 plus hafnium) was coated with a typical alumina-forming protective material (NiCoCrAlY); then platinum versus platinum/10-percent rhodium thermocouples, 2 μm thick, were sputtered on a furnace-grown Al_2O_3 layer and tested to 1250K to demonstrate the feasibility of use on standard engine hardware. Film strain gages were also tested (column 4), and film erosion samples were prepared and tested (column 5) to further evaluate possible applications and assess potential problems. The strain gage tests demonstrated the feasibility of miniaturization of instrument sensor systems with pattern line widths down to 75 μm, and the erosion tests proved the capability of thin film metal coatings to survive under engine conditions without prohibitive deterioration. Finally, an engine test of thin film thermocouple devices was performed with sensors mounted on turbine vanes (column 6). Although problems occurred with the thin-film-to-lead-wire connections, the sensors on the vanes survived engine operating conditions for 60 hours in most cases. No calibration data were obtained from this experiment.

The work in column 7 of Table I was performed under Phase I, Contract NAS3-20768, of the on-going three-phase NASA program. Results are reported in Reference 1. Reliable lead wire attachments were developed, feasibility of sputtered thermocouples on four different turbine blade and vane alloys was demonstrated, and eight sputtered thermocouple systems on flat bars were cycled 30 times to 1250K, with total time of 60 hours at 1250K for each, in a low velocity oxyacetylene flame. Average life was 42 hours, with less than 4 percent drift in calibration. Initial thermal electromotive force was between 1.4 percent above and 3.6 percent below reference Type S wire thermocouples, with temperature gradients of up to 400K applied along the length of the thin films. Drift was generally downward at less than 0.1 percent of Fahrenheit temperature per hour. The primary failure mode was loss of adherence of platinum films. A literature search and some preliminary experiments resulted in several recommendations for improving adherence.

The work in column 8 of Table I was conducted under Phase II, Contract NAS3-20831, of the three-phase NASA program. Results are reported in Reference 2. The technology for sputtering 2 μm thin film platinum versus platinum/10-percent rhodium thermocouples on alumina-forming coatings was improved and extended to applications on actual turbine blades. Good adherence was found to depend upon achieving a proper morphology of the alumina surface. Problems of adapting fabrication procedures to turbine blades were uncovered, and improvements were recommended. Testing at 1250K at one atmosphere pressure was then extended to a higher Mach number (0.5) in a combustor flow for 60 hours and 71 thermal cycles. The mean time to failure was 47 hours accumulated during 1-hour exposures in the combustor. Calibration drift was about 0.1 percent per hour, attributable to oxidation of the rhodium in the thin films. It was found that the drift could be reversed by raising the temperature of the entire film system to 1370K. This behavior was attributed to the high-temperature decomposition of oxides of rhodium into pure rhodium and oxygen, as reported in Reference 8 and 9. An increase in film thickness and application of a protective overcoating were recommended to reduce drift during actual engine testing.

2.2 OBJECTIVES

The objectives of the Phase III program, the subject of this document, under Contract NAS3-22002 were as follows:

- Confirm the drift mechanism by performing additional drift tests on the Phase II blades, and by testing thermocouple systems comprised of platinum film versus platinum wire and platinum/10-percent rhodium film versus platinum/10-percent rhodium wire.

- Optimize system design and fabrication procedures on actual turbine blades to further improve the durability and accuracy under engine environmental conditions. Parameters to be investigated included film thickness, overcoatings, orientation angles during sputtering, and film routing on blades.

- Design an engine installation of thin film thermocouple systems on turbine blades, and define the requirements for a quantitative intercomparison test, in an engine test program, of several techniques for measurement of blade surface temperature (optical pyrometer, wire thermocouples, thin film thermocouples).

- Demonstrate reduced drift on actual turbine blades.

The goals for durability and accuracy throughout the three phases of the program were: 75 percent survival rate for the 50-hour steady state portion of the test program, initial calibration accuracy of the thin film thermocouples within 1.5 percent of Fahrenheit temperature, and drift of less than 5 percent of Fahrenheit Temperature during the test program.

SECTION 3 0

TECHNICAL APPROACH

3.1 THIN FILM SENSOR

The thin film thermocouple structure selected, based on the experience described in Section 2.1, is illustrated in Figure 1. A section through one leg of the thermocouple is shown.

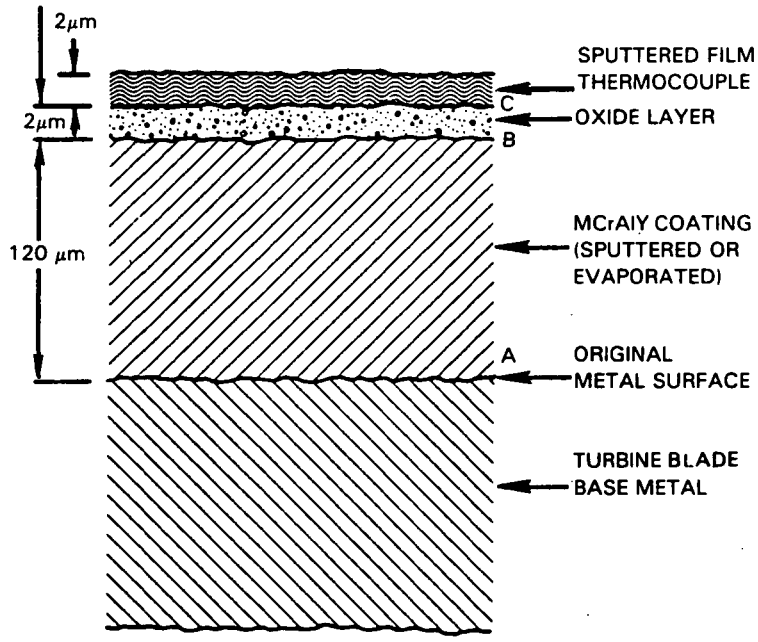

Figure 1 Thin Film Thermocouple Cross-Section. When properly grown and filled by sputtering, the dense oxide layer is an excellent insulator and is mechanically tough and adherent.

The thermocouple legs are platinum and platinum/10-percent rhodium. This thermocouple is designated Type S by ANSI Standard MC 96.1 and is metallurgically the simplest of those recommended for service up to 1800K.

The key ingredient in the structure shown in Figure 1 is the alumina forming "MCrAlY" coating. The coating composition is typically 18 percent Cr, 12 percent Al, 0.5 percent Y, and the balance "M", where "M" is selected for best compatibility with the turbine blade material. "M" may be Fe, Ni, Co, or a combination of Ni and Co. The attractive property of this coating is that at high temperatures in air, a dense layer of Al_2O_3 forms on the surface. When properly grown and filled by sputtering an additional amount of Al_2O_3 onto the surface, this Al_2O_3 coating is an excellent insulating material with high dielectric breakdown voltage. In addition, this oxide layer is mechanically tough and adherent, resisting erosion and spalling through extended temperature cycling and exposure to high velocity gas flows.

The MCrAlY coatings, when properly formulated, are ductile, so that severe mechanical and thermal strains beyond the yield point are not transmitted to the hard oxide layer. The strains within the Al_2O_3, therefore, remain within the elastic and buckling limits.

When the oxide layer eventually spalls or erodes, a new protective oxide soon grows to take its place. It is this property that provides extended corrosion protection. The useful life of a thin film sensor sputtered onto the oxide is ended when the first oxide spalling occurs.

The bond at "A" in Figure 1, between the MCrAlY coating and the turbine blade material, is partially chemical in nature and is enhanced by heat treatment to promote diffusion and solid solution in the interface region.

The strong bond at "B" in Figure 1, between the oxide layer and the MCrAlY material, has been the subject of extensive study and may be explained by the presence of the yttrium which combines with other constituents of the coating to form yttride "pegs" extending into the grain boundaries of the coating.

The bond at "C" in Figure 1, between the noble metal film and the oxide layer, is not intrinsically strong. Good adherence of the noble metal film requires special care in fabrication, as discussed in Section 3.3.

3.2 THIN-FILM-TO-LEAD-WIRE CONNECTION

In the engine test of sample sputtered films, lead-wire connections had been fabricated by oversputtering the sensor lead films onto lead wires embedded in insulated platform holes and reinforced by application of fired platinum paste (Engelhart Industries No. 6869). These lead-wire connections failed early. Subsequently, during the Phase I development program (Reference 1), a number of alternative techniques for lead-wire attachment were investigated, and a successful hot compression bonding technique was developed. This technique was then used throughout the Phase I and Phase II tests of sample thermocouple systems (furnace cycling, vibration tests, and combustor exhaust gas-stream tests) with excellent results. This bonding technique is described in Reference 1.

3.3 ADHESION OF THIN FILMS

The adhesion of thin film materials to the supporting material must be sufficient to withstand the mechanical and thermal strains that are expected to occur during operation of an instrumented part. The adhesion of thin films is affected by a number of factors including surface cleanliness and chemical activity of the two materials at the interface. If the two materials can form a chemical bond without foreign material contamination, the adhesion generally is good. If there is limited chemical activity (such as with platinum on alumina), certain steps must be taken to achieve adequate adhesion.

One method that has been successfully used is to deliberately roughen the surface of the substrate by grit blasting to promote a mechanical type of adhesion. Adhesion occurs because some of the sputtered film material enters re-entrant crevices on the roughened surface if the crevices are clean. Cleanliness of the roughened surface is, therefore, very important.

In Phase I, it was found that a dew point higher than 280K (48°F) during either masking or sputtering prevented satisfactory adhesion of platinum films, probably as a result of adsorption of water vapor on the roughened substrate surface. Note that the use of cleaning solvents that readily evaporate can cool the surface sufficiently to cause condensation of water vapor on the surface when the dew point is high.

To ensure good adhesion of platinum films, the amount of water vapor in the environment must be minimized until the sputtered films have been deposited. The amount of water vapor in both the masking and sputtering environments must therefore be monitored and controlled.

Adhesion is also affected by the sputtering process parameters. The sputtered material has a substrate-arrival energy which results in physical embedding of the sputtered material into the substrate. However, the maximum arrival energy that can be achieved is limited by the maximum temperature rise (caused by electron bombardment during sputtering) which the masking materials can tolerate.

There is evidence (Reference 10) that adherence is also a function of sputtered surface orientation relative to the sputtering source target. Sputtering, in general, is not a line-of-sight process, and material can be deposited on all faces of a solid object simultaneously. However, in regions of grazing incidence or on hidden surfaces, arrival energy and the resulting adherence may be reduced.

In summary, the bond at "C" in Figure 1, between the oxide layer and the noble metal, is not inherently strong and is quite dependent on the physical characteristics of the surface, surface cleanliness, the amount of water vapor present during fabrication, and the sputtered surface orientation. Fortunately, an extremely strong bond is not required because the sensor coefficient of expansion matches that of the oxide reasonably well. Adequate adherence can be attained by careful attention to the factors already identified.

3.4 OVERCOATINGS

No overcoating of the thin film thermocouples was originally planned because the platinum and platinum/10-percent rhodium films were thought to be resistant to corrosion and erosion, based on results obtained during previous engine experiments (Table I, columns 5 and 6). However, these results did not include calibration accuracy comparisons. Phase I and Phase II calibration data revealed thin film thermocouple drift which was at least partially attributable to selective oxidation of rhodium. Investigation of oxygen-barrier overcoatings was therefore included in the Phase III program.

Page Intentionally Left Blank

SECTION 4.0

SENSOR SYSTEM SPECIFICATIONS

During the design and development of the thin film temperature sensor systems to meet the goals of the program, special consideration was given to the following four major specifications: size, accuracy, reliability, and environment. These specifications are defined in the contract. This section presents a description of these contractual specifications. All specification goals were met, and the methods by which these goals were achieved are discussed in Sections 6.0, 7.0 and 8.0.

4.1 PHYSICAL SIZE

The maximum permissible value of five physical dimensions of the thin film sensor system are specified in the contract. These dimensions are:

	mm	Inch
Measurement-Zone Size	1.3	0.050
Film Width	1.3	0.050
Film Thickness	0.015	0.0006
Lead Wire Cable Connection Size	3.2	0.12
Connection Protrusion Above Surface	0.25	0.010

The specification also required that the lead wire cable be capable of withstanding a temperature of 1140K (1600°F).

4.2 ACCURACY

The following accuracy specification goals are defined in the contract (the percentages are based on temperature expressed in degrees Fahrenheit):

1. Accuracy of reference wire thermocouples, $\pm$0.75 percent.

2. Reference wire thermocouple maximum drift, 1 percent during the full testing program (60 hours).

3. Agreement of thin film thermocouples with reference wire thermocouples, initial calibration prior to start of testing program, $\pm$1.5 percent.

4. Thin film thermocouple maximum calibration drift goal, 5 percent during the full testing program (60 hours).

4.3 RELIABILITY

The contract specified the failure rate goal for the thin film thermocouple system, due to any failure which renders the system inoperative, as 25 percent

or less during the full testing program (60 hours). In addition, any sensor that degraded to a condition outside of accuracy limits during the testing program was to be considered as a failure.

4.4 ENVIRONMENT

The required design of a thin film thermocouple system installation suitable for engine-test evaluation inherently must be capable of withstanding the environment which exists in an operating engine, including temperature gradients, hydrocarbon fuel, thermal cycling, gravitational loading, vibration, high pressure, and high Mach number, as well as a maximum thermocouple junction temperature of 1250K (1800°F).

SECTION 5.0

SENSOR-SYSTEM ENGINE INSTALLATION CRITERIA

5.1 OVERVIEW

This section describes design considerations for engine installation of a temperature measurement system using thin film thermocouples. This installation design was conducted to provide a perspective of the entire measurement system and to identify the effects of critical restraints and requirements on measurement system durability and accuracy. The design defined a thin film thermocouple installation on the first-stage turbine blades of a large high-bypass ratio turbofan engine (Pratt & Whitney's JT9D). This installation design included:

- Provisions for intercomparison of thin film thermocouple data with optical pyrometer and wire thermocouple measurements.
- A Pratt & Whitney telemetry system for transmission of thermocouple signals from the rotating shaft to the stationary data acquisition system.

The Engine Test Plan, presented in more detail in the Appendix, includes transient operation from idle to take-off power, steady state operation at various power settings, and start-up and shutdown cycles. The following engine test conditions were selected:

- Twenty-five hours at intermediate power settings (30 to 80 percent of maximum rated power).
- Ten hours at a turbine inlet temperature of 1370K (2000°F)
- One hour at 100 percent of rated power (take-off thrust).
- Twenty start-up/shutdown cycles.

A schematic of the thermocouple system installation is provided in Figure 2. Details of lead wire installation, the telemetry system requirements, optical pyrometer requirements, and measurement system uncertainty are discussed in the following sections. The thin film installations on the blades are described in Section 6.7.

5.2 LEAD WIRE INSTALLATION

Routing of trunk lead wires is shown in Figure 2 for the installation in a JT9D engine. Installation methods would be similar for other two-spool high bypass ratio turbofan engines. Trunk leads, which connect the telemetry system to the high-pressure turbine hub, run the entire length of the high-pressure compressor. These leads must be installed during high-pressure compressor assembly. A duplex cable with glass fiber wrap and ISA Type "S"

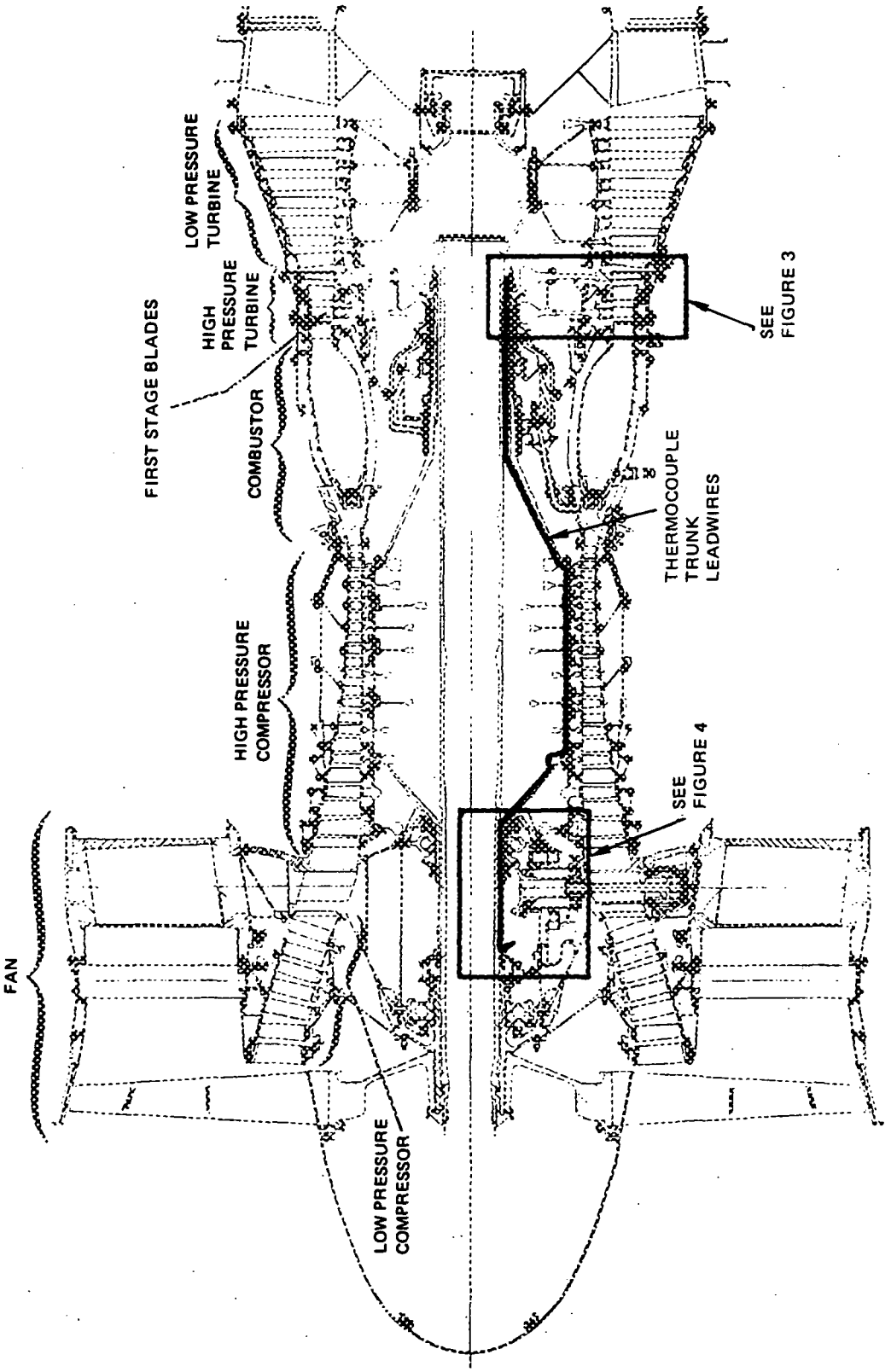

Figure 2 JT9D Engine Instrumentation. Trunk leads connect the thin film thermocouple lead wires with the telemetry system.

extension wire having a temperature rating of 810K (1000°F) is required. The cable is held in place with epoxy cement, aluminum tape, ceramic cement, and welded Invar straps at various locations.

High-pressure turbine lead wire routing from the trunk lead termination at the turbine hub to the turbine blades is shown in detail in Figure 3. These leads are of bare wire (ISA Type "S") held in place with ceramic cement to withstand disk temperatures up to 920K (1200°F). Turbine leads are spliced to the trunk leads using silver solder.

Connection of the forward ends of the trunk leads to the telemetry system tag board, shown in Figure 4, are made with soft solder. Signal and power cables are routed to the engine exterior through a hollow strut in the intermediate case.

5.3 TELEMETRY SYSTEM

Transfer of temperature signals from the engine rotor is accomplished in this installation design by a rotating telemetry system. Each thermocouple signal telemetry transmitter module will accept six thermocouple signals and generate a repetitive (2-millisecond) series of pulses, the magnitude of the pulses corresponding to the six temperature levels. Also included are pulses for synchronization, zero, calibration, and module temperature (cold junction reference). The pulse signals are transmitted by a frequency modulated radio frequency carrier signal to the stationary receiver. The signal is demodulated and demultiplexed to reproduce the temperature signals. Excellent accuracy is attained through use of the composite pulse series method. Because the zero, calibration level, and module temperature are applied to each 2-millisecond series, zero and sensitivity changes with temperature and centrifugal force are measured, and corrections may be applied automatically during data processing.

5.4 OPTICAL PYROMETER

An optical pyrometer is a stationary sensor which detects the detailed temperature profile of all blade surface elements which pass its view. The purpose of the pyrometer in this design is to provide a separate blade surface temperature measurement for comparison to the thin film thermocouples. It is, therefore, necessary to place some thin film sensors at locations which will be viewed by the pyrometer. Other thin film sensors are placed at locations not accessible to the line of sight of the optical pyrometer to provide temperature information not previously available.

5.5 WIRE THERMOCOUPLES

A few conventional surface-mounted wire thermocouples are included in the installation design for intercomparison with the thin film thermocouples and the optical pyrometer.

Trunk leads and turbine module leads to the blades are installed exactly as for the thin film thermocouples. The wire thermocouples are attached to the turbine blade airfoil by flame spray techniques, as described in Section 6.7.

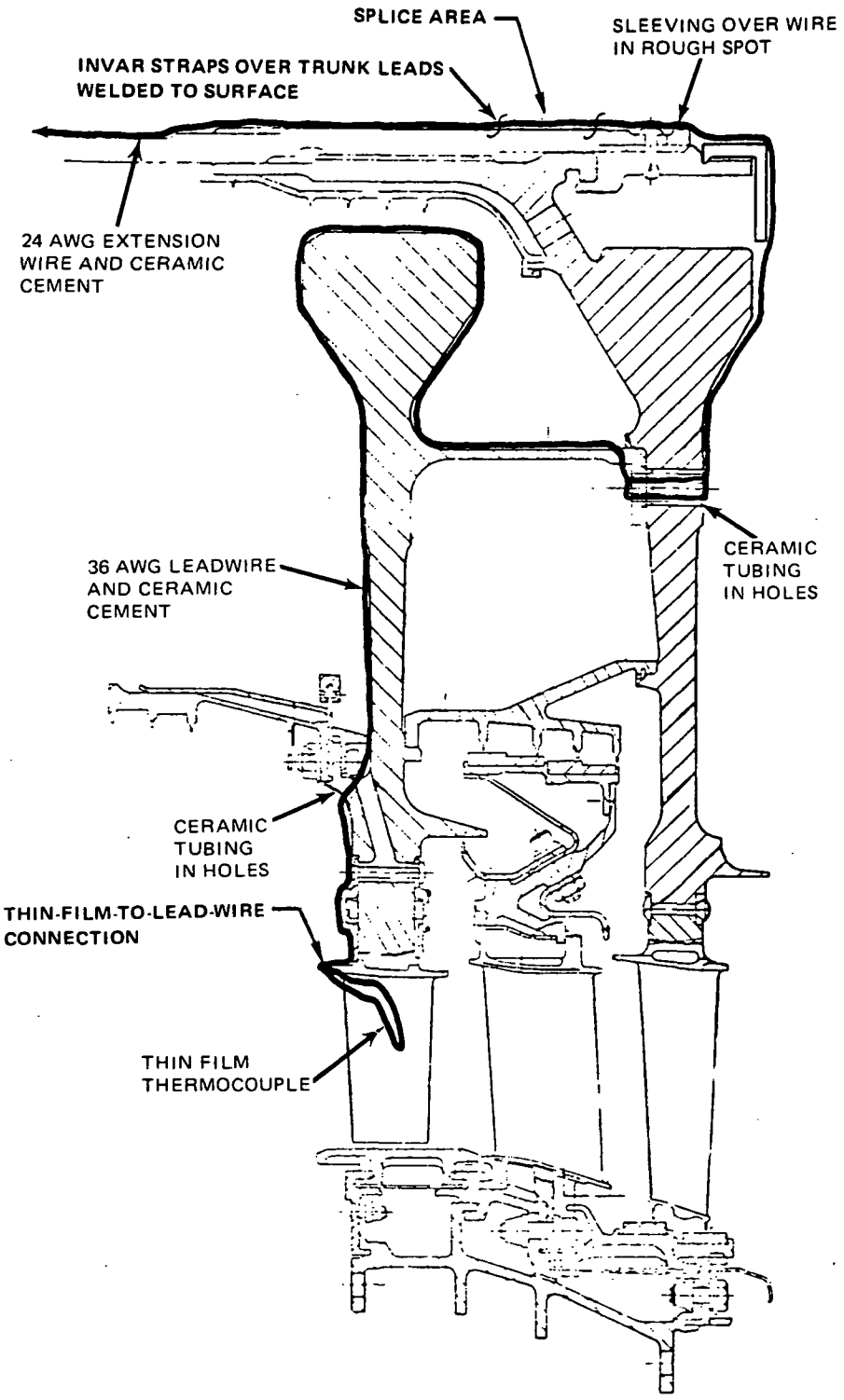

Figure 3 High-Pressure Turbine Instrumentation. Lead wires routed along and attached to the rotating disk connect the thin film thermocouples with the trunk leads.

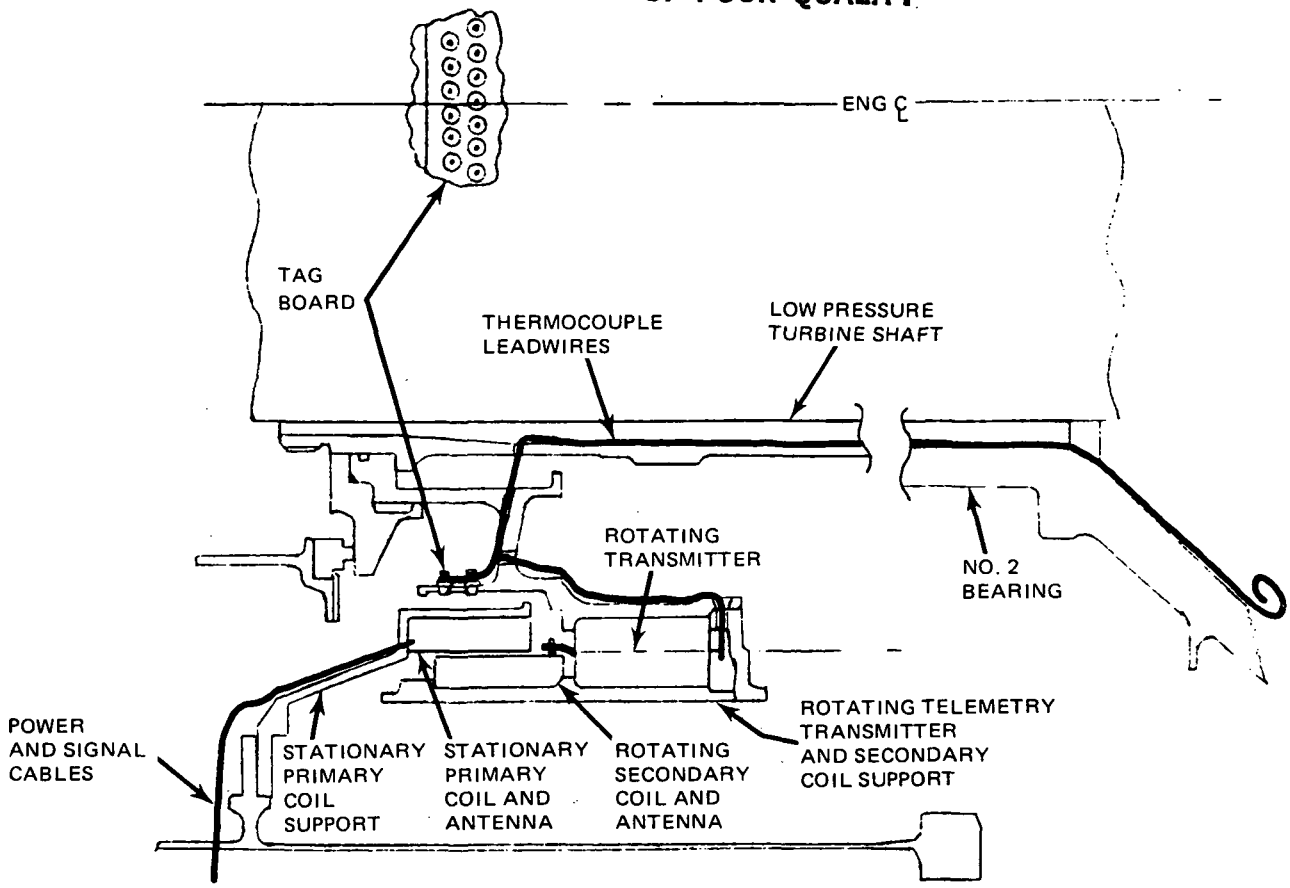

Figure 4 Lead Routing to the Telemetry System. A rotating frequency-modulated radio transmitter provides temperature data with high accuracy.

Several locations on the turbine airfoil are instrumented with a wire thermocouple immediately adjacent to a thin film thermocouple. A location favorable to wire thermocouple accuracy is at a point of maximum blade wall thickness and boundary layer thickness (low thermal gradients). Some favorable and some unfavorable locations are included in the installation design.

5.6 MEASUREMENT UNCERTAINTY

To determine the expected uncertainty of thin film thermocouple measurements during engine testing, it is necessary to combine the uncertainty of all elements in the system including the telemetry and recording systems. Table II lists the uncertainty for each element and the combined (root mean square) uncertainty. The expected uncertainties for optical pyrometer system measurements (from References 11 and 12) and wire thermocouple system measurements are determined in the same way and listed in Table II. At the bottom of the table the total uncertainty of intercomparison of the measurements during an engine test are summarized. The uncertainty is estimated to be in the range of ±1.4 to ±3.5 percent, depending on the engine operating point, location on the blade, and the method of comparison (reference wire thermocouple or pyrometer). All uncertainties are based on two standard deviation error bands so that 95 percent of all measurements are expected to fall within the stated uncertainty.

TABLE II

TEMPERATURE MEASUREMENT UNCERTAINTIES

	Percent Engine Test Uncertainty		
	Worst Operating Condition	Best Operating Condition	
A. Thin Film Thermocouple (at start of test)			
Calibration Traceability (including extension leads)	0.50	0.50	
Telemetry	1.00	1.00	
Automatic Data System	0.25	0.25	
$[\Sigma(A_i{}^2)]^{1/2}$	1.14	1.14	
B. Reference Wire Thermocouple			
Wire Material Traceability (including extension leads)	0.50	0.50	
Temp. Gradient on Blade	0.90	0.45	
Temp. Gradient above Blade	3.00	0.30	
Telemetry	1.00	1.00	
Automatic Data System	0.25	0.25	
$[\Sigma(B_i{}^2)]^{1/2}$	3.34	1.27	
C. Optical Pyrometer System			
Temp. Gradient on Blade	0.60	0.30	
Optics Cleanliness	0.30	0.30	
Blade Surface Emissivity	0.50	0.50	
Blade Reflections	1.20	0.20	
Analyzer (Detector, Digitizer)	0.25	0.25	
Plotter	0.25	0.25	
$[\Sigma(C_i{}^2)]^{1/2}$	1.5	0.8	
$[\Sigma(A_i{}^2 + B_i{}^2)]^{1/2}$	3.5	1.7	Note 1
$[\Sigma(A_i{}^2 + C_i{}^2)]^{1/2}$	1.9	1.4	Note 2

Note 1: Expected uncertainty in intercomparison of thin film thermocouple and wire thermocouple

Note 2: Expected uncertainty in intercomparison of thin film thermocouple and optical pyrometer

SECTION 6.0

SENSOR SYSTEM FABRICATION AND TEST PROCEDURES

6.1 OVERVIEW

To meet the technology improvement objectives of the current Phase III program, thin film thermocouple systems on several sets of test pieces were subjected to various tests. Table III lists the test pieces and test procedures employed. Sections 6.2 through 6.7 describe the test pieces and test procedures in detail.

TABLE III

PHASE III TEST PIECES AND TEST PROCEDURES

Test Pieces	Figure Number	Film Description	Test Procedure	Report Section
Turbine Blades No. 1 and 3, previously combustor tested in the Phase II program	6	Thin film thermocouples, 2 μm thick, Pt vs. Pt/10%-Rh	Drift before and after 1 hour bake at 1370K	6.3
Flat bars	7	Pt film, 5 μm thick	Drift; film vs. Pt wire, with no pre-bake	6.4
Flat bars	7	Pt/10%-Rh film, 5 μm thick	Drift; film vs. Pt/10%-Rh wire after 1 hour bake at 1370K	6.4
Flat bars	7	Overcoatings, 5 μm thick	Mechanical and thermal tests of overcoatings	6.5
Optical flats and prisms vs. sputtering	8	Pt films 1 μm thick (maximum)	Measure film thickness vs. sputtering distance and surface angle	6.6
Turbine Blades No. 41, 42, 43, 44 Concave side	10	Thin film thermocouples less than 2 μm thick	Drift after 1 hour bake at 1370K	6.7
Turbine Blades No. 43, 46 Convex side	10	Pt/10%-Rh films, 14 μm thick	Drift after 1 hour bake at 1370K	6.7

6.2 SPUTTERING CONFIGURATIONS AND PARAMETERS

During the thin film temperature sensor program, two sputtering facilities, one with a planar (flat disk) target and the other an S-gun (truncated conical) target, were used. Figure 5 compares the two configurations.

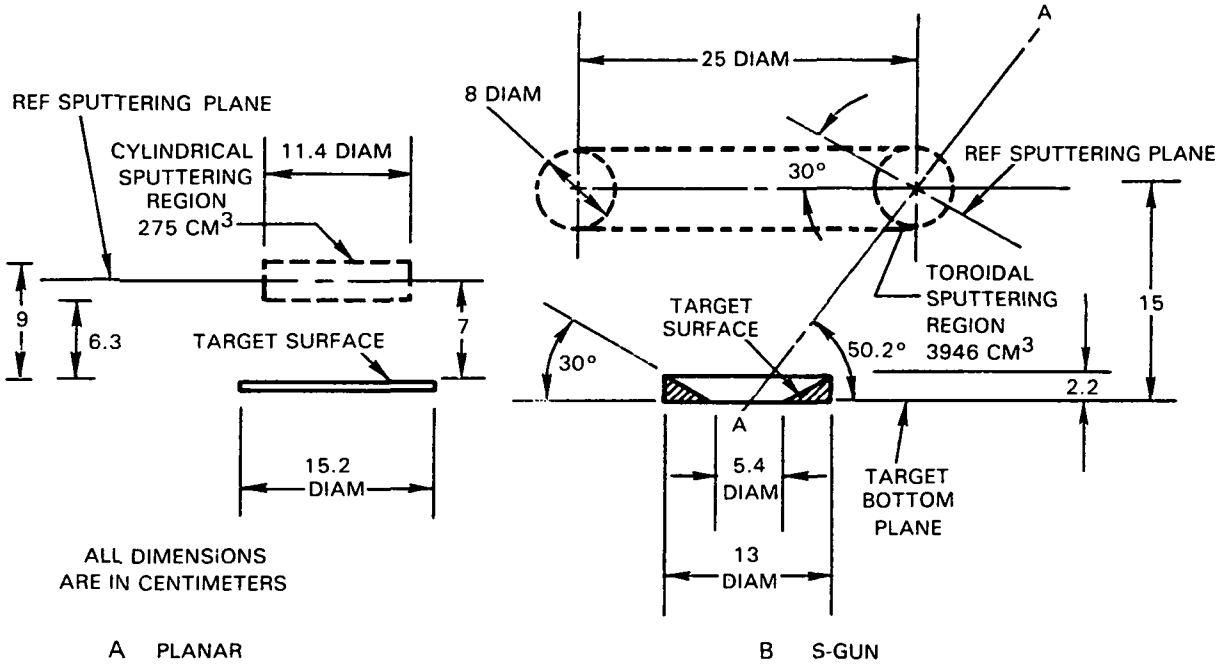

Figure 5 Comparison of Sputtering Facilities. The planar sputtering configuration has the advantage of simplicity and target availability, while the S-gun configuration has greater capacity and versatility.

The planar sputtering configuration (Figure 5) has a simple 15.2-cm diameter target that is readily available commercially in a variety of materials. However, the small sputtering region permits the simultaneous sputtering of only two to four turbine blades, and the sputtering rate must be low to avoid overheating of the photoresist materials used in masking. The so-called "S-gun" sputtering facility (Figure 5) has a complex conical target in a magnetron configuration. These conical targets are more difficult to fabricate, are more expensive, and are not readily available commercially in some materials. However, the much larger sputtering region will accommodate the simultaneous sputtering of up to 20 turbine blades, and much higher sputtering rates may be used without overheating the work piece as a result of reduced electron bombardment of the work piece provided by the magnetron configuration.

The planar facility was used exclusively during the Phase I program (Reference 1) and for most sputtering during the Phase II program (Reference 2). However, some specimens used during the Phase II program were sputtered in the S-gun facility for comparison with those sputtered in the planar facility. Thin film thermocouple systems sputtered with the S-gun were found to be equal

to or better than the specimens from the planar facility in both durability and calibration accuracy. Both sputtering facilities were used during the current Phase III program, and the sputtering facility for each test specimen is identified in the following Sections 6.3, 6.4, and 6.5.

Nominal sputtering parameters are listed on Table IV. All sputtering was conducted at radio frequency (13.56 megaHertz) with no DC bias applied to the test pieces. The measure of power generated is the DC self bias that appears at the target which is included on Table IV. The sputtering rates listed are for flat plate work pieces placed in the reference sputtering plane of Figure 5.

TABLE IV
Sputtering Parameters

Sputtered Material	Target Material	Target Type	Target Self Bias (DC Volts)	Gas Composition	Gas Pressure (Pascal)	Sputtering Rate on Ref. Sputtering Plane of Fig. 5 (μm/hr)
Al_2O_3	Al_2O_3	S-gun	800	Ar + 5% O_2	0.33	0.21
Al_2O_3	Al_2O_3	Planar	1100	Ar + 5% O_2	0.66	0.12
Si_3N_4	Si	S-gun	400	N_2	0.33	0.21
Si_3N_4	Si	Planar	1500	N_2	0.66	0.12
Pd/30%-Mo	Pd/Mo Composite	Planar	900	Ar	0.66	0.60
Pt	Pt	S-gun	800	Ar	0.33	1.50
Pt	Pt	Planar	800	Ar	0.66	0.45
Pt/10%-Rh	Pt/10%-Rh	S-gun	800	Ar	0.33	1.50
Pt/10%-Rh	Pt/10%-Rh	Planar	800	Ar	0.66	0.45

6.3 DRIFT REVERSIBILITY PROGRAM

During the Phase II program (Reference 2), it was found that turbine blade surface temperature readings of the 2 μm thin film thermocouple systems on three turbine blades in the as-fabricated condition (see Figure 6) were low by 5 to 36 percent of the temperature gradient on the airfoil. These results were from initial oven tests during which the airfoil temperature was maintained near 1250K and the thin-film-to-lead-wire connection at the platform was near 750K.

Two of the Phase II blades (Blades No. 1 and 3) were subsequently exposed to 60-hour combustor tests during which the airfoils were maintained between 1100K and 1250K and the platforms were near 750K. The temperature reading error changed further with time, during the combustor tests, by several percent in 60 hours.

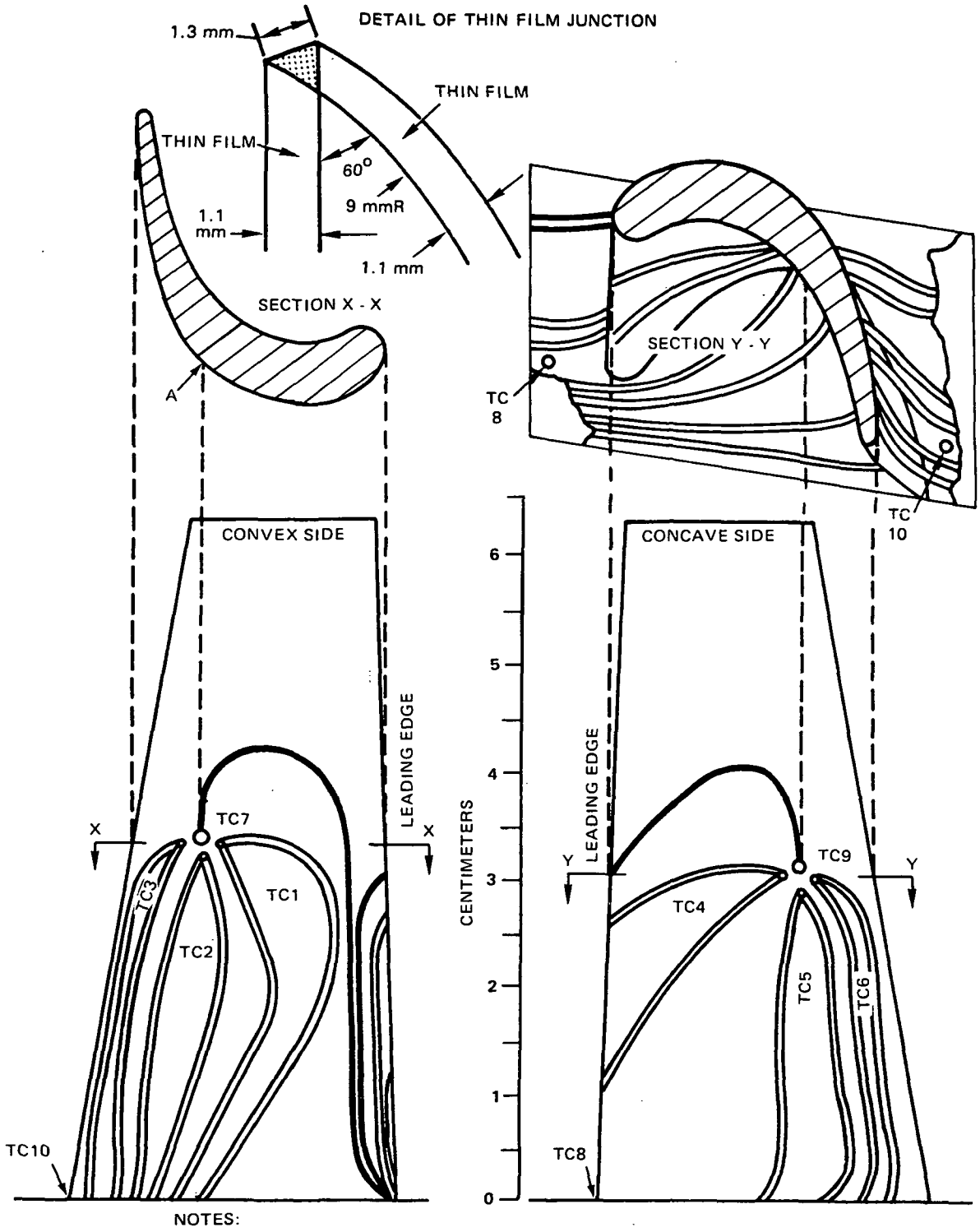

NOTES:

1. MAX. WIDTH OF THIN FILMS IS 1.3 mm
2. MIN. RADIUS OF THIN FILM STRIPE PATTERN IS 9 mm
3. ALL THIN FILM T/C JUNCTIONS WITHIN 5 mm DIA. OF/REF. T/C
4. TC8, TC9, TC10 ARE REFERENCE WIRE THERMOCOUPLES

Figure 6 Phase II Thin Film Temperature Sensor Pattern and Detail of Thin Film Junction.

Following a suggestion from the Government Products Division of Pratt & Whitney, the third blade (Blade No. 2), which had not been combustor tested, was then baked isothermally at 1370K for 1 hour to decompose oxides of rhodium. When this blade was put back into the standard oven temperature gradient, it was found that the temperature reading errors, previously at about 20 percent, had been reduced to less than 1.5 percent. Subsequently, this error increased with time in the oven by some 15 percent in 50 hours.

The reversibility of the drift on Blade No. 2 by baking at 1370K was strong evidence of the oxidation of rhodium. According to References 8 and 9, rhodium oxides decompose at high temperatures to form pure rhodium. (Rh_2O_3 decomposes above 1166K; RhO decomposes above 1280K.) Further evidence of rhodium oxidation was the gradual darkening of the platinum/10-percent rhodium films in the oven tests and combustor tests followed by a return to a bright metallic luster after baking at 1370K.

To further confirm the drift mechanism and to determine whether the reversal of drift could be accomplished even after the 60 hours of combustor testing, thin film thermocouple system No. 6 on Blade No. 1 and system No. 2 on Blade No. 3 (Figure 6) were repaired and subjected to additional oven testing during the current Phase III program. Each blade was subjected to the following tests, a, b, c, and d, involving 61 hours of oven testing of each blade:

a) Each system was visually examined before and after each test and photographs were taken where appropriate.

b) The thin films were maintained for 10 hours in the following thermal condition (hereinafter referred to as the standard temperature profile): a nominal temperature gradient of 500K, with the sensing point on the airfoil maintained at a nominal 1250K and film-to-lead connection temperature maintained at a nominal 750K, as determined by reference wire thermocouple. Thin film thermocouples and reference wire thermocouples were monitored continuously. The tests were conducted in a laboratory oven with a chamber size of 10 cm x 10 cm x 23 cm. The opening to the oven was closed except for a slot large enough to allow the airfoil to be inserted in a horizontal position. The root of the blade was cooled by blowing air over the root fir tree. The thermocouples were connected to multichannel thermocouple chart recorders containing reference cold junctions and calibrated for ANSI type S thermocouples to 1366K (2000°F) with an accuracy of ±10K. A Lewis thermocouple switch permitted manual selection of any one thermocouple reading on a precision digital temperature indicator with traceable accuracy of ±5K with ANSI type S thermocouples. Resistance to ground was checked periodically with a low voltage ohmmeter (with all other recording instruments disconnected).

c) The blades were then placed in an isothermal oven with temperature maintained for one hour at 1310K to 1370K over the entire film length.

d) After Test c, the blades were again placed in the standard temperature profile. The thermocouples were monitored continuously for 50 hours.

6.4 FILM VS. WIRE DRIFT TESTS

The principal objective of this test was to determine whether the observed drift in calibration of the Type S thin film thermocouple systems arose entirely in platinum/10-percent rhodium film (rhodium oxidation), or partly in the platinum film and partly in the platinum/10-percent rhodium film. To accomplish these objectives, a number of special thermocouple systems were fabricated and tested. Each system consisted of a film of a single material (platinum or platinum/10-percent rhodium) with lead wires attached at each end.

Platinum wires were attached at each end of each platinum film, platinum/10-percent rhodium wires were attached at end of each platinum/10-percent rhodium film. The thermolectric voltage was then monitored while a large temperature gradient was imposed on each film over a time period long enough to establish a drift trend.

A second objective was to take a first step in the study of the effect of surface-to-volume ratio of films and wires on drift rate. Therefore, the films employed were 5 μm thick, for comparison with the previous 2 μm thick films.

Sample films of platinum and platinum/10-percent rhodium alloy were sputtered on six flat-surfaced test bars as shown in Figure 7. Each bar was 8.1 cm long and served as a simulated blade surface on which the thin films were deposited. The bar material was PWA 659 (MAR-M-200+Hf) with a 100 μm thick coating of electron beam vapor deposited PWA 270 alumina forming NiCoCrAlY. Each coated bar was oxidized in air for 50 hours at 1300K to form a layer of Al_2O_3. Additional Al_2O_3 was sputtered onto the surface to achieve a total Al_2O_3 thickness of 2 μm. On this surface, the metal films were sputtered.

Two platinum films 5 μm thick were sputtered on each of three bars (Bars 1, 2, and 3). Two platinum/10-percent rhodium films 5 μm thick were sputtered on each of three bars (Bars 4, 5, and 6). The flat face of the test bar was placed in the reference sputtering plane of Figure 5, in the S-gun unit. Sputtering parameters of Table IV were used. Platinum lead wires were hot compression bonded (at 1140K) to the platinum films. Platinum/10-percent rhodium lead wires were hot compression bonded (at 1140K) to the platinum/10-percent rhodium films. Bars 1, 2, 4, and 5 were placed in an oven in the standard temperature gradient for 8 to 20 hours. Reference wire thermocouples were used to monitor the temperature at the lead-wire-to-film connections. Thermal emf generated by the lead wire and film systems was monitored. Resistance to ground (bar material) was measured from time to time during the oven tests.

The lead wires were 0.075 mm in diameter and extended out of the oven to a terminal block where they were attached to heavy extension wires of like material. Since the ratio of surface area to volume of 0.075 mm wires is 3.75 times smaller than the ratio of surface area to volume of 5 μm film (See Table V) oxidation of the lead wires would not significantly alter the drift rate observed in oven tests.

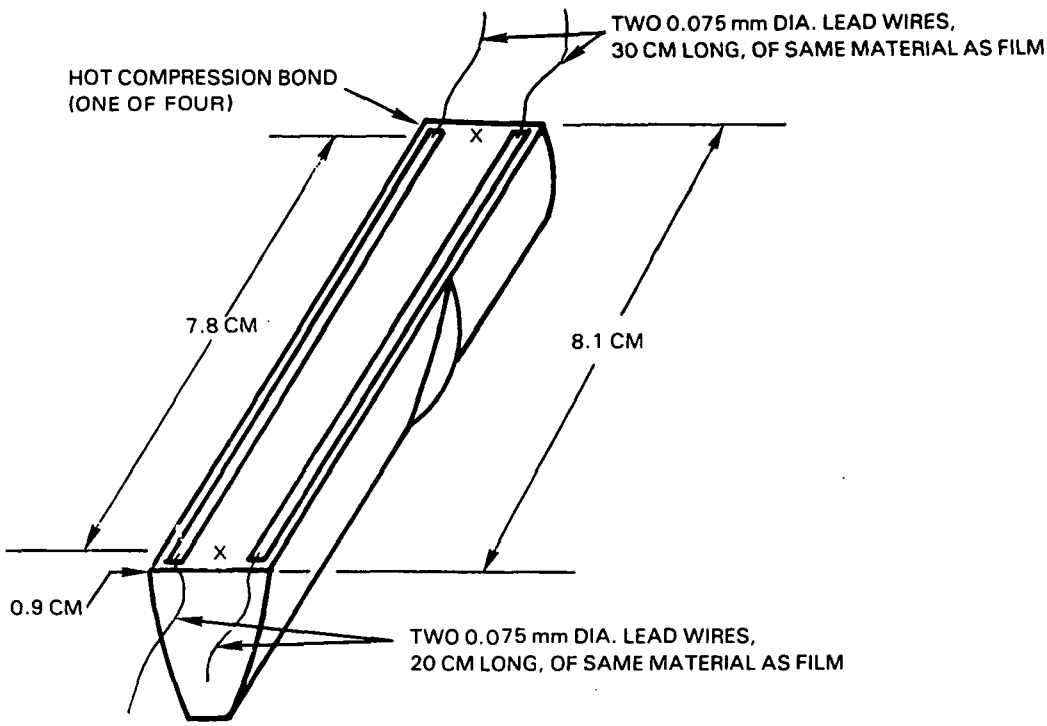

NOTE 1 BASE MATERIAL: PWA 659 (MAR-M-200) PLUS PWA-270 (NiCoCrAlY) COATING

NOTE 2 X'S INDICATE THE POSITIONS OF REFERENCE WIRE THERMOCOUPLES

BAR NUMBER	FILM MATERIAL	FILM THICKNESS (μm)	FILM WIDTH (mm)
1	Pt	5	1
2	Pt	5	1
3	Pt	5	1
4	Pt/10%-Rh	5	1
5	Pt/10%-Rh	5	1
6	Pt/10%-Rh	5	1

Figure 7 Film vs. Wire Test Bars. Tests were conducted on platinum film vs. platinum wire and platinum/10%-rhodium film vs. platinum/10%-rhodium wire.

TABLE V

RATIO OF SURFACE AREA TO VOLUME
FOR SELECTED WIRES AND FILMS

Wires		Films	
Diameter, mm	Ratio, mm^2/mm^3	Thickness, mm	Ratio, mm^2/mm^3
0.250	16	0.0625	16
0.125	32	0.014	71.4
0.075	53.3	0.005	200
0.0625	64	0.002	500

Bars 1, 2, 4, and 5 were used in the film vs. wire drift tests. Bars 3 and 6 were spares which were not drift tested but were used later in the overcoating evaluations.

6.5 OVERCOATING EVALUATION PROGRAM

Previous tests had identified rhodium oxidation as one probable source of thin film thermocouple calibration drift. Overcoating the think film systems with a material which acts as an oxygen barrier was therefore a logical approach to reducing drift. The overcoat material selected must be thermoelectrically inactive, electrically non-conducting, and compatible mechanically and chemically with both of the thin film materials. (Note that it would not be possible to overcoat the Pt/10% Rh film without the overcoat also coming into contact with the Pt film at the film junction). Three overcoating materials were selected for trial: Al_2O_3, Si_3N_4, and oxidized Pd/30-percent Mo. The first two are familiar high-temperature insulating materials selected on the basis of experience (including successful experience in overcoating experimental thin film strain gages for service to 920K under Contract NAS3-21262). The third candidate was selected as the result of an observation during trials of possible strain-gage alloys under Contract NAS3-21262. It was observed that metallic films 1.2 μm thick of the alloy Pd/30-percent Mo were transformed to dense black adherent, non-conducting films by exposure at 920K for one hour. (It was assumed that oxidation of the molybdenum was the principal mechanism).

An overcoating thickness of 5 μm was selected for all candidate overcoats since this was the least thickness that provided good pin-hole free electrical insulation with sputtered Al_2O_3 and Si_3N_4 on steel and titanium alloy compressor blades in Contract NAS3-21262.

After completion of the film versus wire drift tests, four of the test bars (Bars 2, 3, 5, and 6 of Figure 7) were selected for overcoating evaluations. Bar 2 and Bar 5, which had been drift tested, were heat treated at 1370K in air for 1 hour to decompose oxides of rhodium. Bar 3 and Bar 6, which were

not drift tested, were used in the as-fabricated condition, after hot compression bonding of lead wires (2 hours at 1140K). All metal films were bright and clean in appearance with a metallic luster.

Three candidate overcoating materials (Al_2O_3, Si_3N_4, and Pd/30-percent Mo) were then sputtered separately, 5 μm thick, on selected portions of the four bars, as listed in Table VI. Sputtering parameters used in overcoating are shown in Table IV. The Al_2O_3 was sputtered in the S-gun facility; Si_3N_4 and Pd/30- percent Mo were sputtered in the planar facility. During sputtering the flat face of the test bar was placed in the reference sputtering plane of Figure 5.

Drift testing of the overcoated film systems was planned, for comparison with drift testing of the uncoated systems.

TABLE VI

MATRIX OF OVERCOATING TEST SPECIMENS

Test Bars		Overcoating Materials		
Bar No.	Thin Film Type and History	Al_2O_3	Si_3N_4	Oxidized Pd/30%-Mo
2	Pt After Drift Test and Heat Treatment		Two Films Overcoated	
3	Pt As-Sputtered	Two Films Overcoated		
5	Pt/10%-Rh After Drift Test & Heat Treatment	One Film Overcoated		One Film Overcoated
6	Pt/10%-Rh As-Sputtered		Two Films Overcoated	

Note: Overcoatings were 5 m thick.

6.6 SPUTTERING DISTANCE AND ORIENTATION PROGRAM

The objective of this task was to establish the effect of height above the sputtering target, and orientation of the surface during sputtering, on the sputtering rate attained in the large S-gun sputtering unit. Available data (Reference 10) indicated that the sputtering behavior was more directional in the S-gun than in the planar diode unit. Since film thickness could have a significant effect on drift due to oxidation, the effects of height and orientation on film thickness for each element of a complex blade surface could be important.

Two special sample pieces were sputtered, one at a time, in successive runs, with platinum for 0.5 hour in the S-gun sputtering unit. Standard sputtering parameters were used (see Table IV). Each sample was a 15.2-cm diameter quartz optical flat with two quartz prisms mounted on the surface to be sputtered, as shown in Figure 8. The prisms provided surfaces oriented at 30, 45, 60, and 90 degrees relative to the optical flat. The surface of the optical flat was oriented in a plane parallel to the reference sputtering plane of Figure 5B, centered on the Reference A-A axis. This configuration is shown in Figure 9.

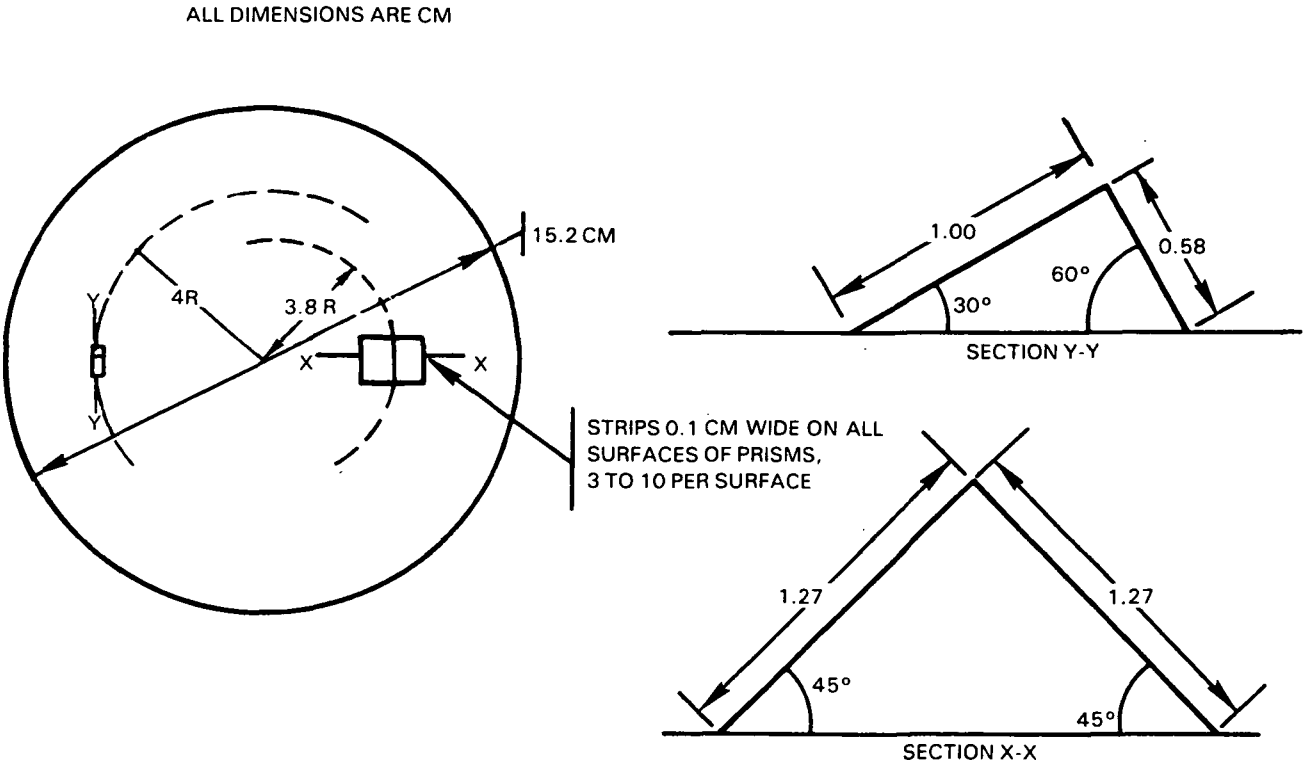

Figure 8 Configuration of the Samples for the Sputtering Distance and Orientation Program. Each sample was a 15.2-cm diameter optical flat with two prisms mounted on the surface to be sputtered.

Sample No. 1 was positioned at a distance of 12 cm above the target bottom plane and sample No. 2 was positioned at 18 cm. The spatial distances and orientations, therefore, simulated all locations which would be encountered on a typical turbine blade of complex shape and average size during sputtering.

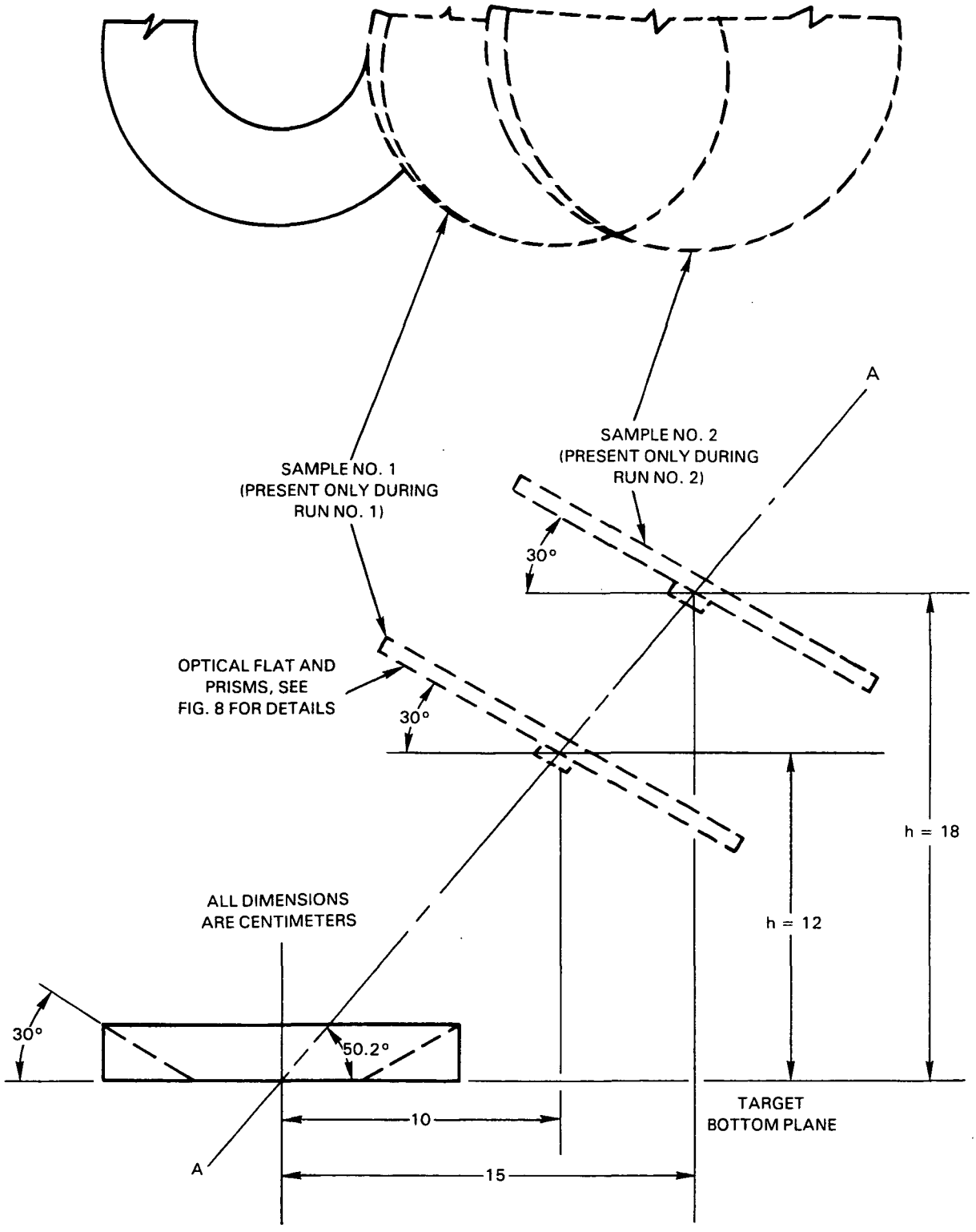

Figure 9 Position of the Samples in the Sputtering Distance and Orientation Program. The positions of the sample were selected for uniform thin film deposition.

The disk and flats were masked to produce stripes of platinum 1 to 2.5 mm wide and spaced 2 to 5 mm apart. After sputtering and removal of the masks, platinum thickness profiles were measured with a Talysurf profiler by traversing each optical flat surface along a line defined by the intersection of a target radial plane and the optical flat surface. In addition, platinum film thicknesses on each of the sloped prism surfaces were measured by the same technique.

Platinum film adherence was tested on each quartz flat and on each surface of each quartz prism. The procedure used was the tape removal test. A 2-cm length of Dodge Industries tape, No. 2045-5, was pressed firmly in place on the thin film and then removed by pulling the tape vertically. The test typically provides a pass/fail evaluation of thin film adherence. If a small portion of the film is removed by the tape, film adherence is judged to be marginal.

6.7 TURBINE BLADE SENSOR INSTALLATION AND TEST PROGRAM

6.7.1 Overview

The objective of this task was to establish the accuracy and drift characteristics of thin film thermocouple systems with design optimized for an engine test application and with Pt/10%-Rh film thickness increased to minimize oxidation effects. After completion of the tests described above, thin film thermocouple systems were therefore designed and installed on six additional first-stage turbine blades. Static oven calibration and drift tests of several of these systems were conducted (Table VII).

TABLE VII

MATRIX OF TURBINE BLADE SENSOR INSTALLATIONS AND TESTS

Batch	Blade No.	Film Description (Concave Side of Airfoil)	Location of Film-to Lead-Wire Connection	Film Description (Concave Side of Airfoil)	Procedure
1	41	2 Thin Film TC Pt vs Pt/10%-Rh	a		Drift
1	42	2 Thin Film TC Pt vs Pt/10%-Rh	b		Drift
1	43	2 Thin Film TC Pt vs Pt/10%-Rh	a		Drift
1	44	2 Thin Film TC Pt vs Pt/10%-Rh	b		Drift
2	46		c	2 Pt/10%-Rh Film 14 μm Thick	Drift
2	43		c	2 Pt/10%-Rh Film 14 μm Thick	Drift

The blades were identical to the blades used in the drift reversibility program (Figure 6). The blade material is MAR-M-200 plus Hf. The blades are first-stage turbine blades of a large fan-jet engine (JT9D) in the 200kN (25-ton) thrust class.

Design considerations are discussed in Section 6.7.2, fabrication of a first batch of blades (concave side of blades 41, 42, 43, and 44, Figures 10A through 10D) that met all the objectives except film thickness is described in Section 6.7.3, fabrication of a second batch of blades with thick Pt/10%-Rh films (convex side of blades 43 and 46, Figures 10E1 and 10E2) is described in Section 6.7.4, and testing procedure is described in Section 6.7.5.

6.7.2 Design Considerations

Location of Lead-Wire-to-Film Connections

To survive the centripetal accelerations of up to 30,000 g experienced at the blade platform, the lead wire connections to the films must be located under the platform or on the platform radial edge. Inertial loading due to the mass of the lead wire then exerts only compressive or small shear forces on the wire-to-film bond.

Note that the preferred location for the extension leads from the first-stage blades in the JT9D engine high-pressure turbine (Figure 3) is on the upstream face of the first-stage rotor disk. This location avoids blind fits during assembly (i.e., the leadwork is always visible during the assembly of the module consisting of first-stage and second-stage stator and rotor). The preferred location for film-to-lead-wire attachment on the blade is therefore under the leading edge of the blade platform. Two other possible locations are under the platform side edges, midway between leading edge and trailing edge, and under the trailing edge of the platform. Either of these two latter arrangements requires rework of solid ribs under the platform to provide grooves or holes through which the extension lead wires may then pass forward.

On some blades in the present program, the lead wire connections were made underneath the platform leading edge. On other blades, the lead wire connections were made on the top of the platform or even on the airfoil to simplify the fabrication process and provide extra film systems for laboratory tests at low cost. The configurations fabricated are described in Sections 6.7.3 and 6.7.4.

Routing of Films on Blades

Selection of the film path from the point of temperature measurement on the airfoil to the point of lead wire attachment under the platform is governed by the conflicting requirements of durability and cost of total system fabrication.

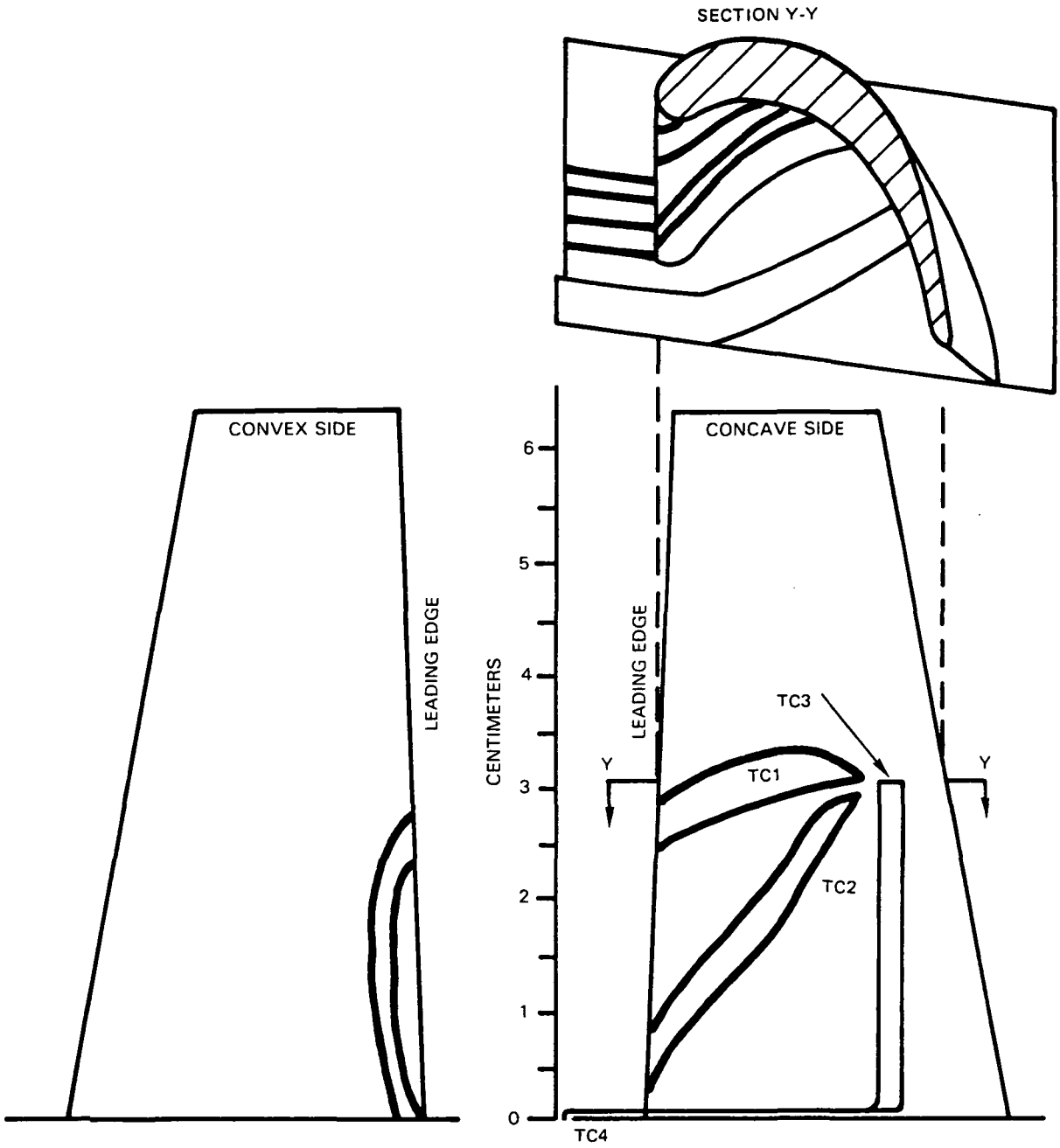

NOTES:
1. MAX. WIDTH OF THIN FILMS IS 1.3 mm
2. MIN. RADIUS OF THIS FILM STRIPE PATTERN IS 9 mm
3. ALL THIN FILM T/C JUNCTIONS WITHIN 5 mm DIA. OF REF. T/C
4. TC3, TC4, ARE REFERENCE WIRE THERMOCOUPLES

Figure 10A Thin Film Sensor Patterns on Turbine Blade No. 41.

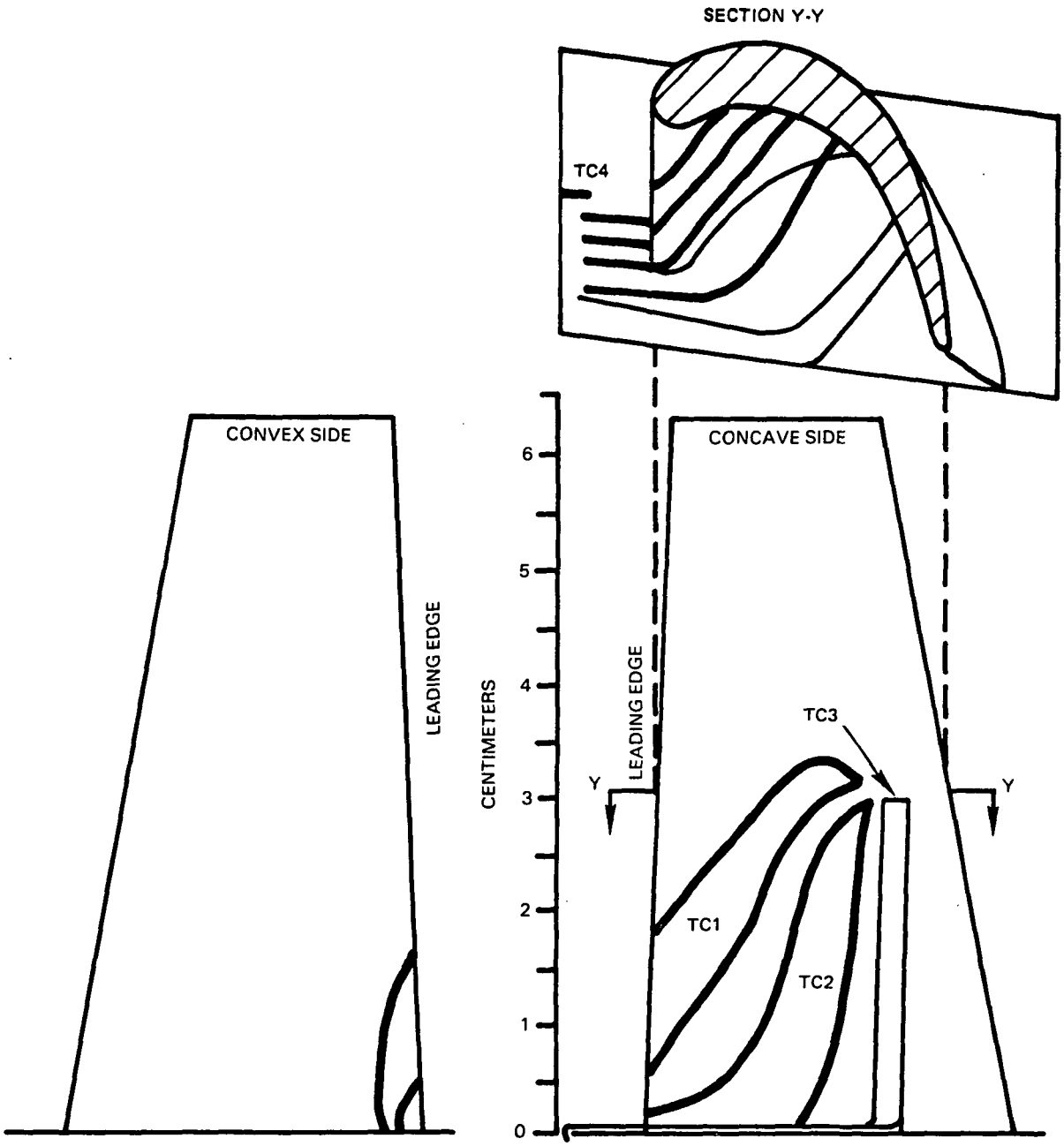

NOTES:
1. MAX. WIDTH OF THIN FILMS IS 1.3 mm
2. MIN. RADIUS OF THIS FILM STRIPE PATTERN IS 9 mm
3. ALL THIN FILM T/C JUNCTIONS WITHIN 5 mm DIA. OF/REF. T/C
4. TC3 AND TC4 ARE REFERENCE WIRE THERMOCOUPLES

Figure 10B Thin Film Sensor Patterns on Turbine Blade No. 42.

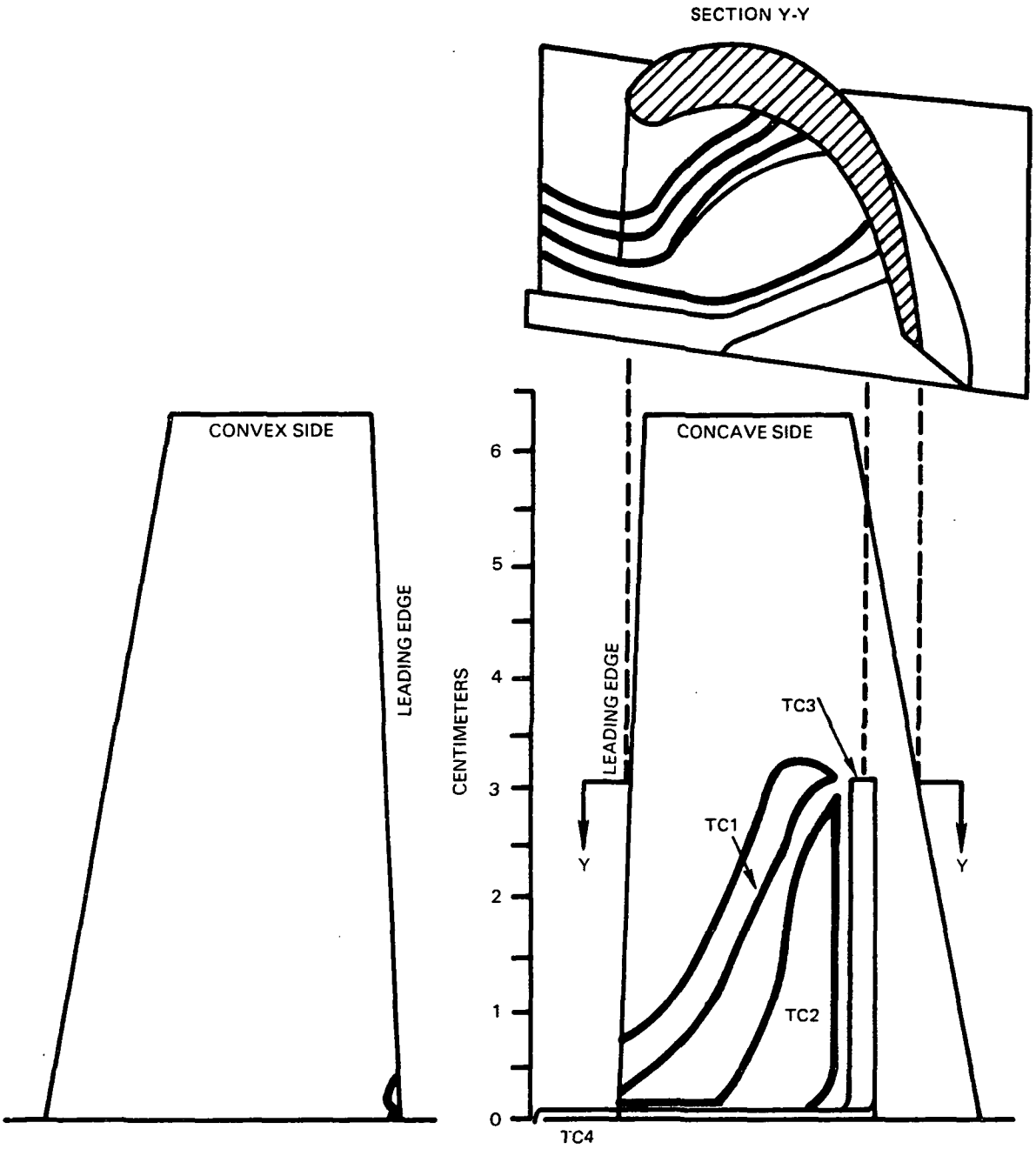

NOTES:
1. MAX. WIDTH OF THIN FILMS IS 1.3 mm
2. MIN. RADIUS OF THIS FILM STRIPE PATTERN IS 9 mm
3. ALL THIN FILM T/C JUNCTIONS WITHIN 5 mm DIA. OF/REF. T/C
4. TC3 AND TC4 ARE REFERENCE WIRE THERMOCOUPLES

Figure 10C Thin Film Sensor Patterns on Turbine Blade No. 43.

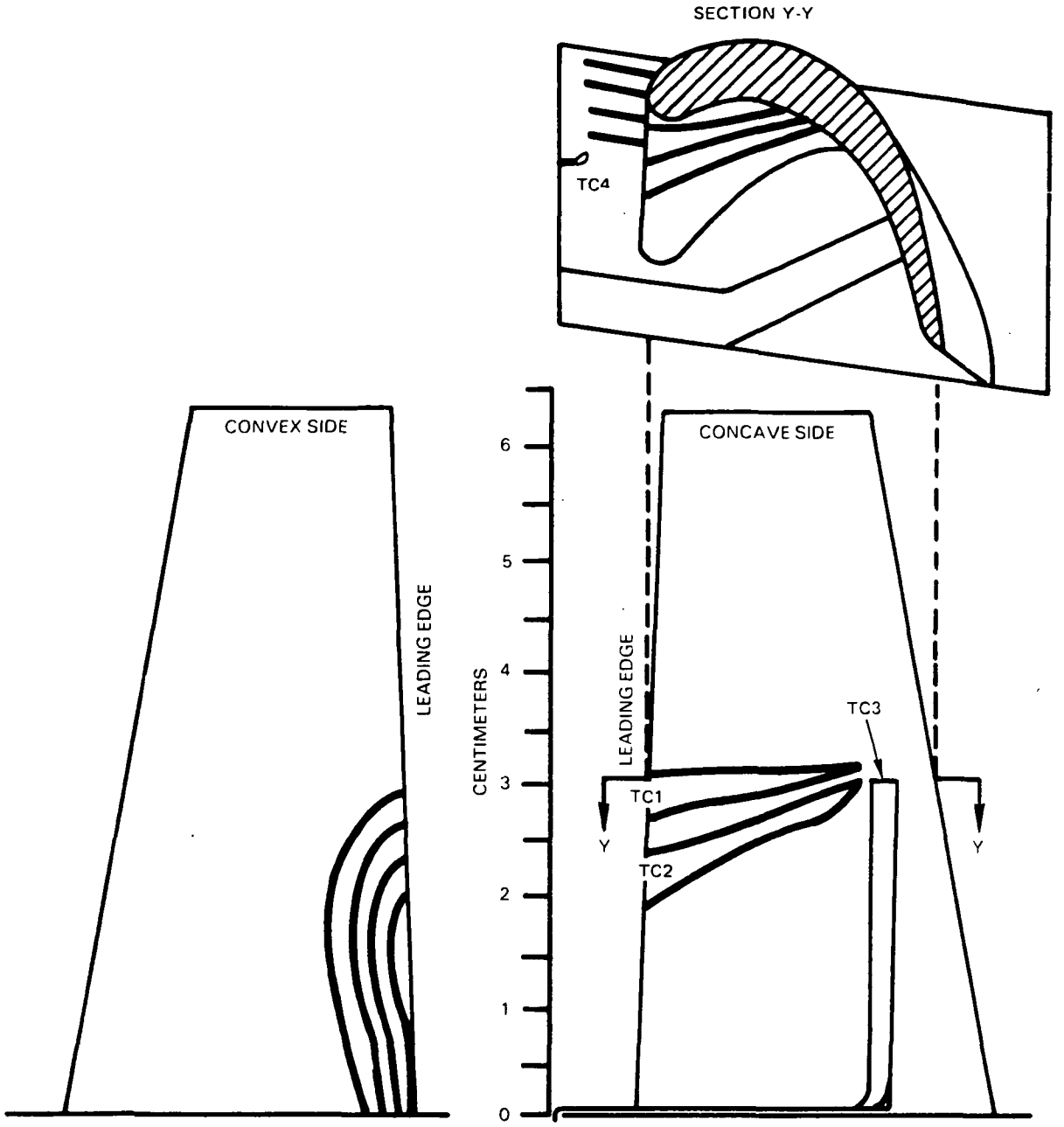

NOTES:
1. MAX. WIDTH OF THIN FILMS IS 1.3 mm
2. MIN. RADIUS OF THIS FILM STRIPE PATTERN IS 9 mm
3. ALL THIN FILM T/C JUNCTIONS WITHIN 5 mm DIA. OF REF. T C
4. TC3 AND TC4 ARE REFERENCE WIRE THERMOCOUPLES

Figure 10D Thin Film Sensor Patterns on Turbine Blade No. 44.

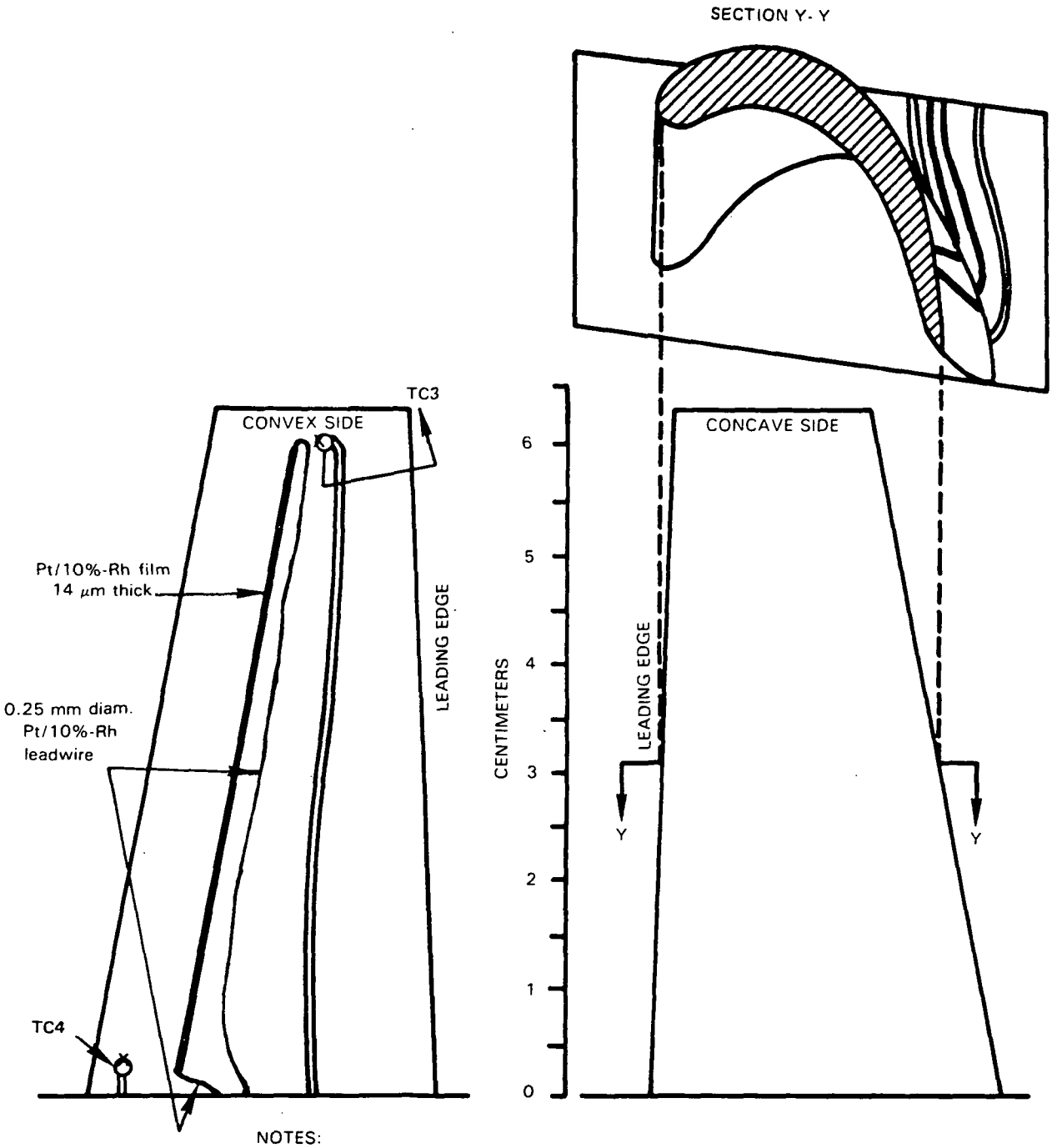

NOTES:

MAX. WIDTH OF THIN FILMS IS 1.3 mm

ALL THIN FILM T/C JUNCTIONS WITHIN 5 mm DIA. OF REF. T/C

TC3 AND TC4 ARE REFERENCE WIRE THERMOCOUPLES

Figure 10E1 Thin Film Sensor Patterns on Turbine Blade No. 46, Convex Side.

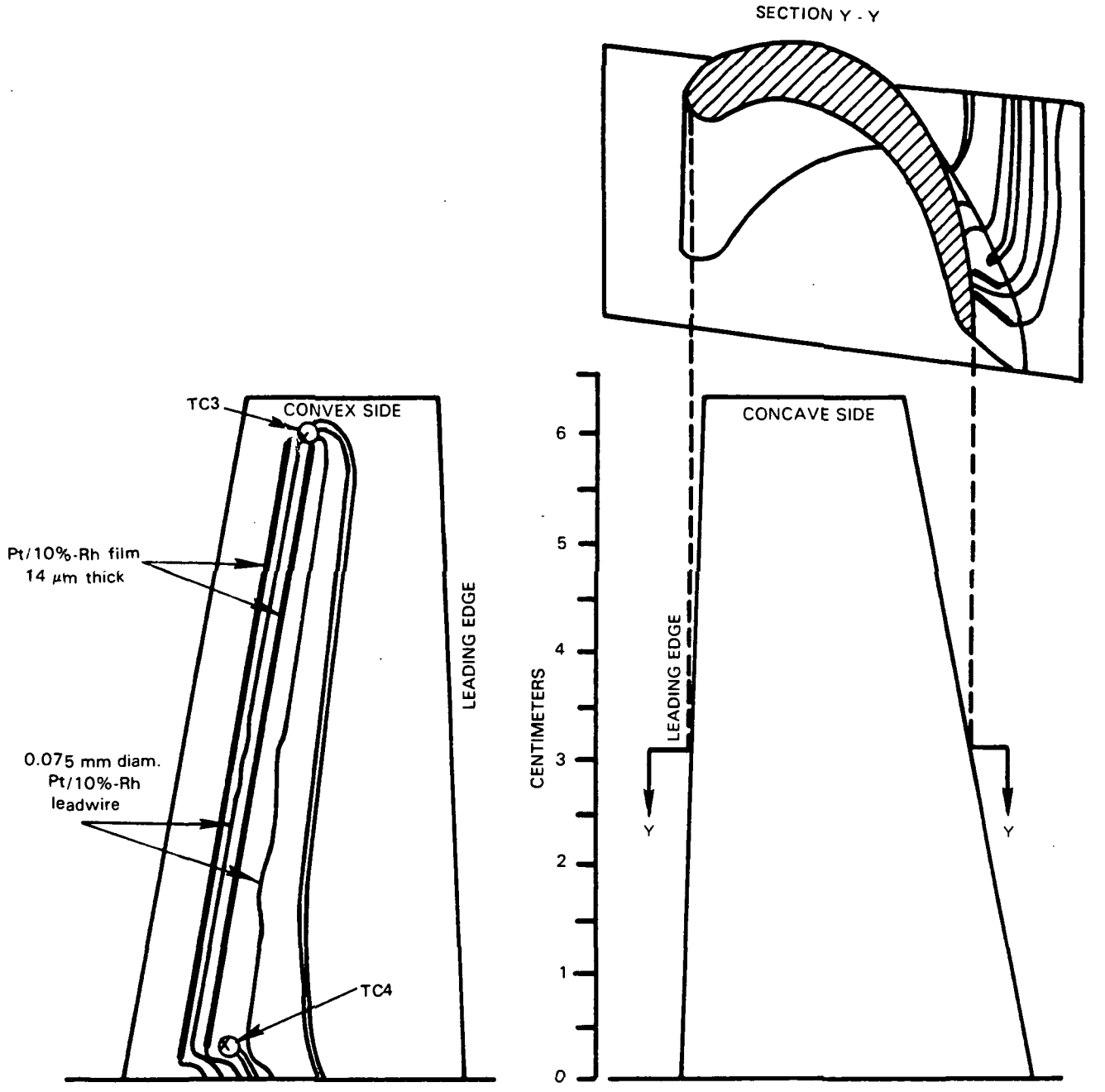

NOTES:

MAX. WIDTH OF THIN FILMS IS 1.3 mm
ALL THIN FILM T/C JUNCTIONS WITHIN 5 mm DIA. OF REF. T/C
TC3 AND TC4 ARE REFERENCE WIRE THERMOCOUPLES

Figure 10E2 Thin Film Sensor Patterns on Turbine Blade No. 43, Convex Side.

To minimize the cost of modification of the blade structure, the lead wire attachment must be made under the platform leading edge. The only rework of the blade in this case is to machine radii on the platform leading edge to avoid sputtering across sharp edges. The film configuration becomes complex in this case, however, since the films must be extended to the platform leading edge. There is room on the platform top for only a few films to pass forward through the region adjacent to the blade leading edge root. In multiple film installations, some films must therefore be routed forward on the airfoil to, or around, the blade leading edge before descending to the platform. These films pass through regions of sharp complex curvature of blade surface. In these regions, good continuity and adherence of films is more difficult to achieve (Reference 2) than on flatter regions, due to masking problems (poor adherence of tape masks on sharply concave surfaces) and sputtering orientation problems (avoiding grazing incidence on some portions of the film path). In such regions, the masking procedure often requires several attempts before success is achieved. A tape mask not in firm contact with the blade results in a ragged-edged film pattern and even discontinuous films. In addition, the sputtering process must employ several successive orientations to assure favorable incidence on all elements of the blade surface. (Continuous rotation in one or two planes during sputtering would be optimum. The facilities available during the present program did not include continuous rotation capability.)

In the alternative configuration, to minimize the cost of film fabrication, the lead wire attachment must be made on or under the side edge of the blade platform. The film routing is greatly simplified in this case. Masking is more straightforward. Sputtering can usually be accomplished with no more than two orientations (or rotation in a single plane). The cost of modification of the blade structure increases, however. The modification includes machining of shallow notches on the platform side edges to provide an edge surface region not in contact with the platform of the adjacent blade, machining of radii in these notched areas, and machining of grooves or holes in solid ribs under the platform through which lead wires may be routed to the front face of the turbine disk. The machining must be accomplished without removing material in highly stressed regions.

Both types of installation had been achieved in earlier trials, and both were considered feasible for the reported program. On the first batch of blades fabricated in the current program, the films were routed to the platform leading edge area. Some of these films extended around the platform leading edge to lead wire connections under the platform. These blades are described in Section 6.7.3. On the second batch of blades, the films were routed spanwise, directly from the point of temperature measurement on the airfoil to the blade root fillet region, following the path on the blade that would be used for film systems designed for platform side edge lead wire attachment. These blades are described in Section 6.7.4.

Control of Film Thickness

Increasing the film thickness was expected to reduce the drift in calibration by reducing the ratio of film surface area to volume, and therby reducing the effect of selective oxidation of rhodium. To attain a desired film thickness, sputtering times and sputtering orientations were selected by performing an analysis based on the results of the sputtering distance and orientation program (Section 7.4.5). The analysis is a tedious procedure. A proposed blade orientation is selected. Then, along a proposed film path on the blade, several locations are selected, representative of the extremes of orientation angle of blade surface element relative to two perpendicular axes (x, y) in the sputtering plane of Figure 5. For each of the several blade surface elements, the angles a_{xz} and a_{yz} subtended with the two reference axes were determined as sketched in Figure 11, thus completely specifying the orientation in space of this surface element. The angle θ is then calculated from $\tan^2 \theta = \tan^2 a_{xz} + \tan^2 a_{yz}$. Since the sputtering rate is known from equation (1) of Section 7.4.5 as a function of distance and θ, then for any arbitrarily selected position of the blade in the sputtering unit, the sputtering rate for each of the selected surface elements could then be determined. By trial and error a set of orientations and sputtering times was selected that resulted in a predicted film thickness (at each of the several locations) which was equal to or greater than the minimum desired thickness.

6.7.3 Fabrication of Blades 41 Through 44, Concave Side

On this first batch of blades (41, 42, 43, 44, concave side, shown in Figure 10A, B, C, D) two designs were developed. The designs were designated Type 1 and Type 2.

For the Type 1 design, the blade had two film sensors on the concave side of the airfoil plus one reference wire thermocouple installed on the airfoil in a location which permitted direct comparison with the thin film thermocouples. Film-to-lead connections were made underneath the platform leading edge. A second reference wire thermocouple was installed immediately adjacent to the film-to-lead connections to permit monitoring connection temperature.

Type 2 was like Type 1 except that film-to-lead connections and platform reference wire thermocouple were located on the gas path side (top) of the platform leading edge. This design permitted fabrication of the entire film length in fewer sputtering operations to reduce the cost of preliminary evaluation of thicker films in static tests on actual turbine blades.

The design thickness of Pt/10%-Rh films on blades 41 and 42 was 8 μm, and on blades 43 and 44 was 13 μm, to provide data for comparison with results obtained earlier with 2 μm films and 5 μm films. The design thickness of Pt films on all four blades was 9 μm , arbitrarily selected to gain experience with the integrity of platinum films thicker than the 2 μm and 5 μm platinum films previously used.

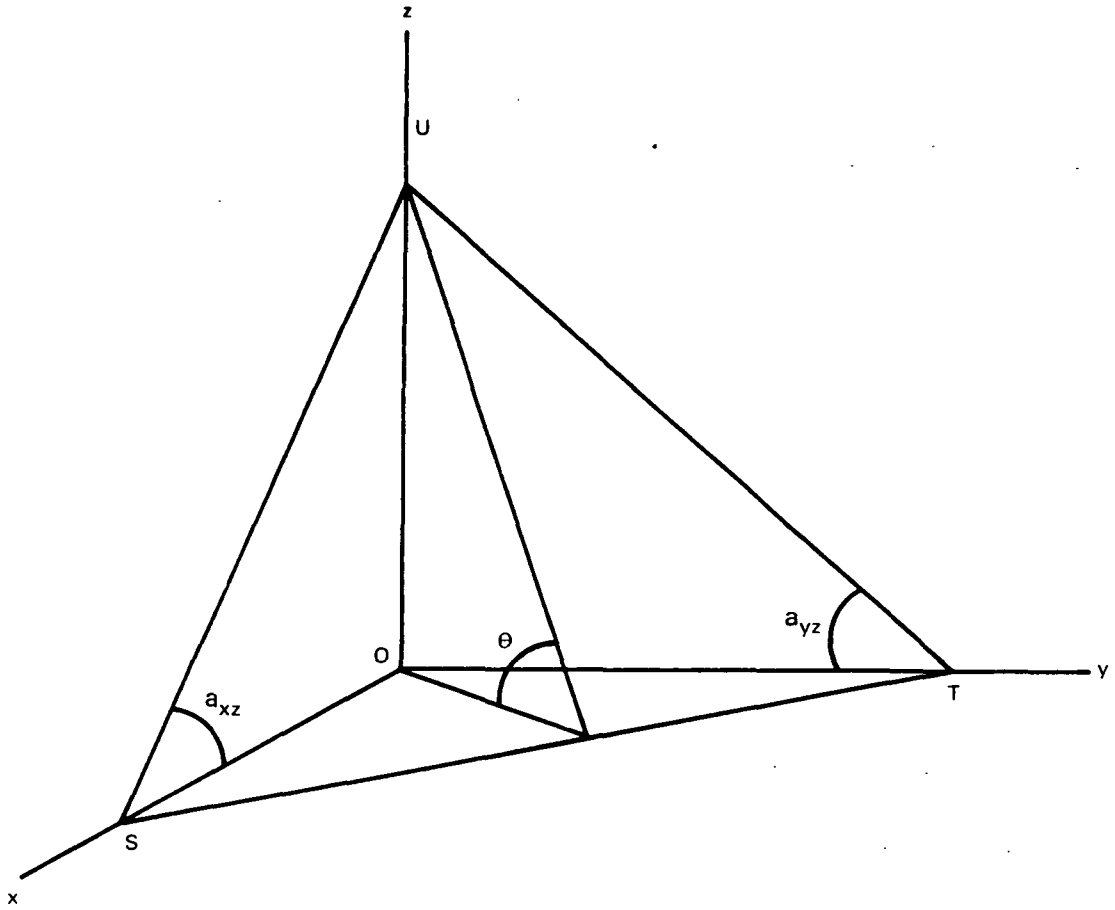

Figure 11 Orientation Angles a_{xz}, a_{yz} and θ of a Blade Surface Element Plane (S-T-U) with respect to the reference sputtering plane x-o-y. The relation between these angles is $\tan^2 \theta = \tan^2 a_{xz} + \tan^2 a_{yz}$.

The presence of the reference wire thermocouple lead wires on the platform in design types 1 and 2 severely limited the space available for film leads. The flame sprayed Al_2O_3 insulation and overcoat of these lead wires in fact occupies most of the available space on the top surface of the platform beside the blades, as shown in Figure 10A through 10D. There is room for at most one film lead on the platform between the blade leading edge root and the flame sprayed area. No success was achieved in many preliminary attempts to mask a pattern which routed two film leads on the platform and two on the airfoil close to the platform in the leading edge fillet area (these two descending to the platform after rounding the leading edge). The extremely complex surface shape in the blade leading edge area near the platform led to poor adhesion of the tape used for masking and a ragged-edged (and discontinuous) sputtered film.

The patterns finally used on blades 41, 42, 43, and 44 shown in Figures 10A through 10D represent various compromises adopted in achieving reliable masking. The fabrication sequence was as follows, beginning with the blade in its bill-of-materials machined form, before application of any corrosion-resistant coatings. First the blade platform leading edge was remachined slightly to produce a smooth semicircular cylindrical surface for routing of lead films from top to bottom of the platform. Then the usual initial polishing of all surfaces was carried out (Reference 2). At this point, at the request of the engine test groups a packed aluminide coating (PWA 273) was then applied to all exterior surfaces, followed by the usual PWA 270 NiCoCrAlY coating (Reference 2). The packed aluminide has been found to enhance the durability of the NiCoCrAlY in engine tests and had been found to have no deleterious effect on thin film thermocouple systems in lab tests. Both coatings were applied in a vendor facility under closely controlled conditions.

After NiCoCrAlY coating, the usual thin film fabrication process was interrupted to install the flame-sprayed reference wire themocouples. In this process the entire blade is masked with a flame-spray resistant tape except for the area to be flame sprayed. The exposed regions are grit blasted to remove all coatings, flame sprayed with a base coat of nickel aluminide (Metco 443) and then an insulating layer of Al_2O_3 (Rokide H). The wire thermocouple is then ladder taped in place and flame sprayed with a bond coat of Rokide H. The ladder tape is then removed and additional Rokide H is flame sprayed to bury all exposed lead work and produce a smoothly faired installation 0.3 to 0.5 mm thick.

After installation of the flame-sprayed wire thermocouples, the thin film fabrication was completed using the procedure of Reference 2, including polishing and grit blasting of the NiCoCrAlY surface, heat treatment of the NiCoCrAlY, oxidation of the NiCoCrAlY, sputtering of Al_2O_3, and masking and sputtering of Pt and Pt/10%-Rh.

Sputtering of the film patterns was accomplished for design type 1 (blades 41, 43) using three successive fixed orientations in the S-gun sputtering unit. The procedure described in Section 6.7.2 was used in selecting the orientations. These planned orientations are shown in Figure 12. For design Type 2 (blades 42, 44) the third orientation was omitted.

Lead wires of 0.075 mm diameter about 2 cm long were hot compression bonded to each film and these lead wires were tweezer welded to the 0.125 mm diameter conductors of Type S sheathed ceramo extension cables. The sheath of the extension cable was strap welded under the platform leading edge and all exposed lead wires were coated and bonded to the blade with ceramic cement (SermeTel P-1). After curing of the cement the entire blade assembly was baked at 1370K for one hour to decompose any oxides of rhodium.

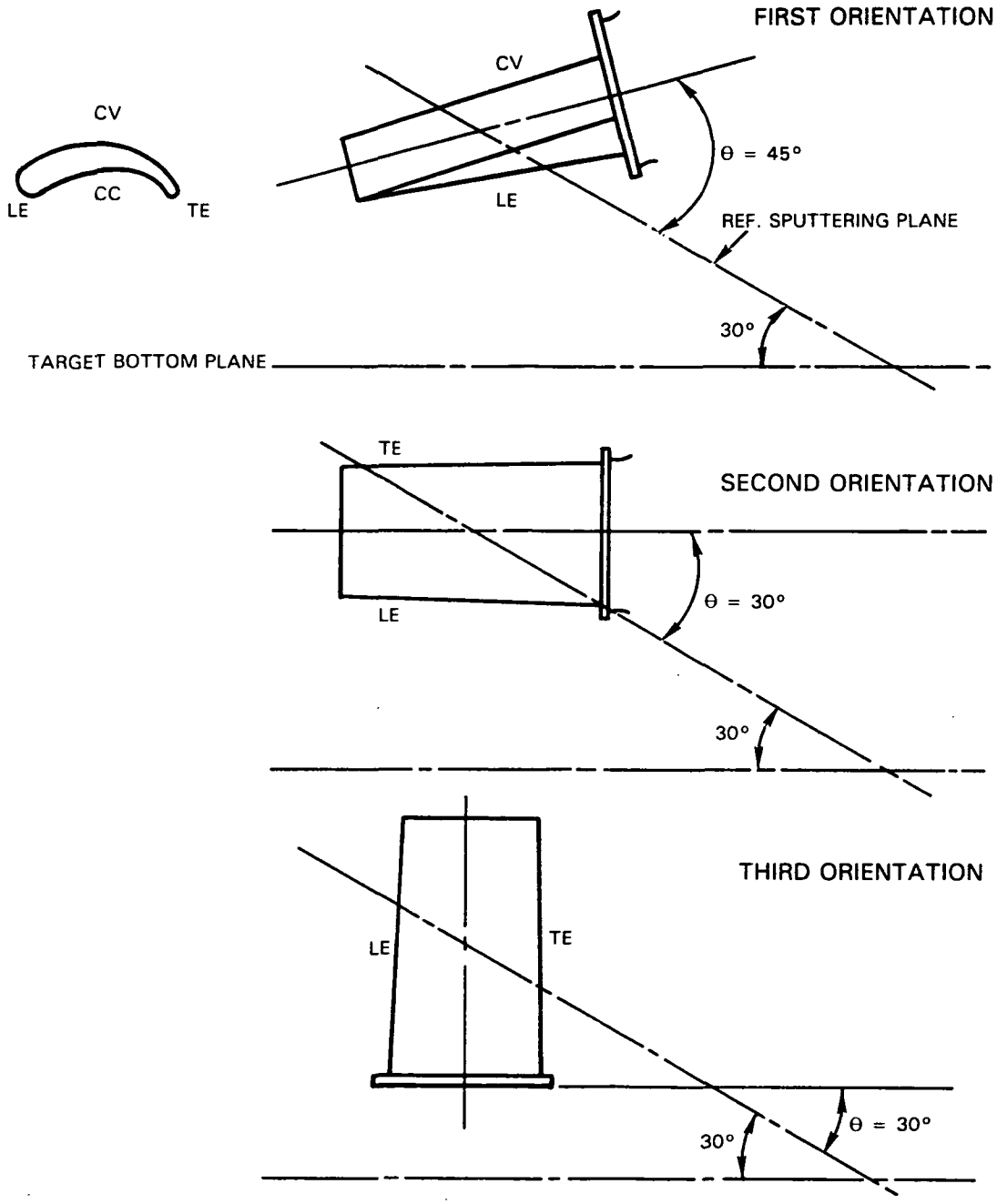

Figure 12 Planned Orientations During Sputtering of Batch 1.

After completion of all tests of the first batch of thermocouple systems (described above) it was learned that there had been a serious error in orientation procedure during the sputtering of the batch. The target bottom plane had been used, rather than the sputtering plane of Figure 5, in establishing orientation angle when installing the blades. The actual sputtering orientations had therefore been 30^{0} larger than planned, as shown in Figure 13. The value of θ was therefore actually about 75 degrees on most

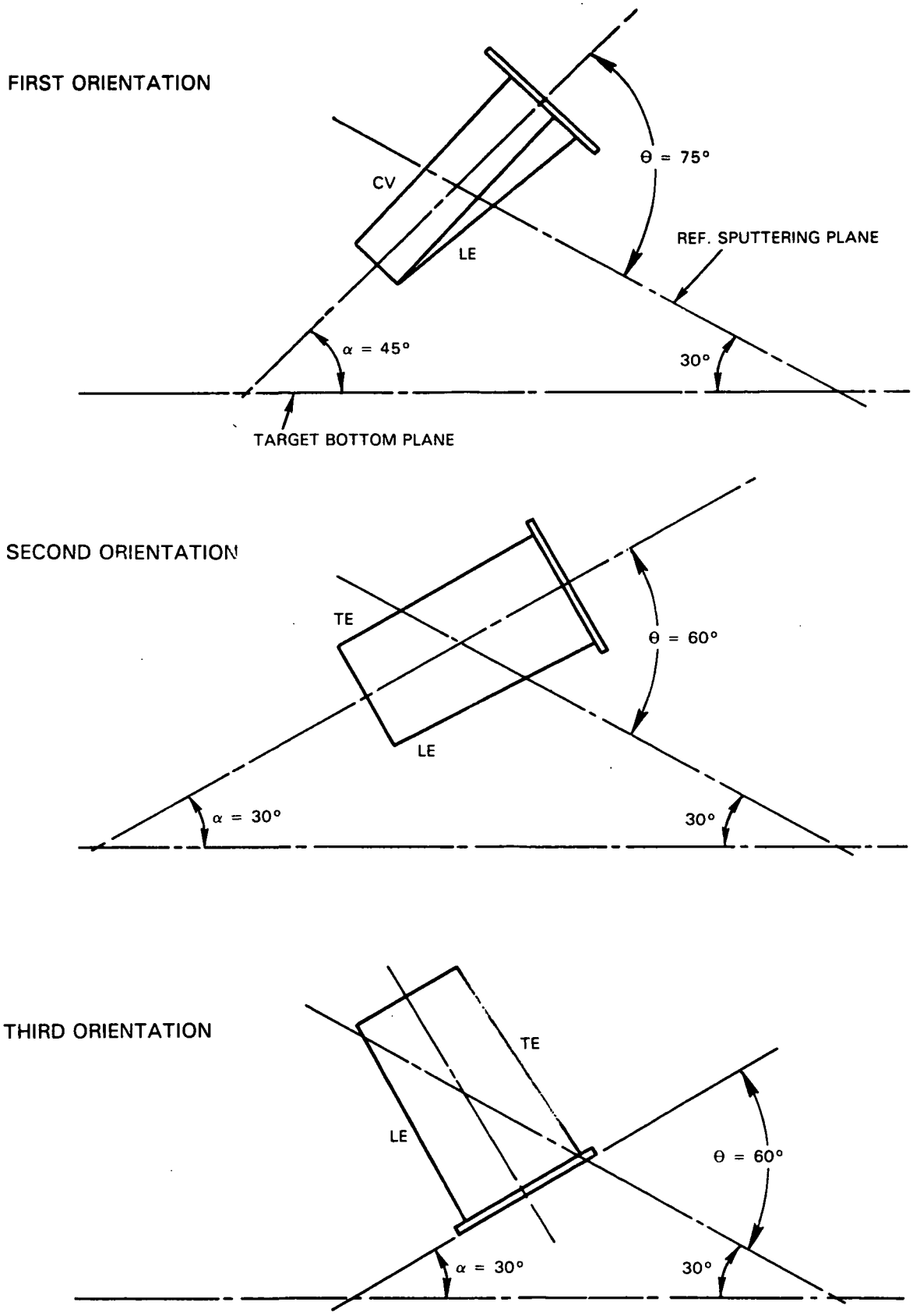

Figure 13 Actual Orientations During Sputtering of Batch 1. Angle α was set to 45, 30, and 30 degrees, rather than angle θ .

of the airfoil concave surface (first orientation). Since there is a tolerance of several degrees in setting the orientation, and since the sputtering rate varies rapidly with angle when the angle approaches 90 degrees (see later discussion in Section 7.4.5) it was impossible to estimate the effective film thickness within a factor of three. It was nevertheless clear that the films in some areas were at least several times thinner than planned and would not provide the desired extension of data into the region of Pt/10%-Rh films thicker than 2 μm.

6.7.4 Fabrication of Blades 43 and 46, Convex Side

To explore the effects of rhodium oxidation on thicker films, a second batch of films was fabricated and tested on the convex side of blades 43 and 46. The film systems consisted simply of Pt/10%-Rh films 14 μm thick on the airfoil only, extending spanwise from near the tip to near the root (Figure 10E). A single sputtering orientation was entirely adequate in fabricating these films. After fabrication of these films the blades were baked at 1370K for one hour to decompose any oxides of rhodium. On each of these blades, Pt/10%-Rh lead wire systems were then attached to each end of the Pt/10%-Rh films (Figure 10E). On blade 43 the lead wire system consisted of 0.075 mm Pt/10%-Rh lead wires extending from each end of each film to connections outside the furnace. On blade 46 the lead wire system consisted of a 1 cm length of .075 mm Pt/10%-Rh wire extended with a 20 cm length of 0.25 mm Pt/10%-Rh wire. The 0.25 mm diameter was selected because the ratio of surface area to volume of 0.25 mm wires is 4.45 times smaller than the ratio of surface area to volume of 14 μm films, ensuring that oxidation of the long lead wires would not significantly alter the drift rate observed in oven tests. Reference wire thermocouples were welded to the blade surface adjacent to each end of the film (one near blade root and one near blade tip).

6.7.5 Test Procedure

The blade assemblies described in Sections 6.7.3 and 6.7.4 were drift tested using the calibration oven and instrumentation described in Section 6.3, with the sensing point on the airfoil maintained at a nominal 1250K and film-to-lead connection temperature maintained at a nominal 750K. All thermocouple readings were monitored as described in Section 6.3. Resistance to ground (blade material) was checked periodically with a low voltage ohmmeter (with all other recording instruments disconnected). The results of the tests are presented in Section 7.5.

SECTION 7.0

RESULTS

7.1 DRIFT REVERSIBILITY PROGRAM

In Figure 14, the errors observed during oven drift tests of the three blades, before and after baking at 1370K for 1 hour, are presented. In all cases, after the entire thin film from sensing point to film-to-lead connections is subjected for one hour to a temperature of 1370K, in the range where rhodium oxide is reduced to rhodium, the error in calibration is reduced significantly. This result is further support for the hypothesis of Reference 2 that the drift in calibration is largely due to gradual conversion of rhodium in the platinum/10-percent rhodium film to thermoelectrically inactive oxides at temperatures below 1170K and reconversion of the oxides to pure rhodium at temperatures above 1170K.

On the blades with previous exposure to combustor flow for 60 hours (Blades 1 and 3), the subsequent recovery toward zero error is less complete than on the blade not previously exposed to combustor flow (Blade 2).

Note in Figure 14 that heat treatment of Blade 2 had reduced the error to 1.5 percent of Kelvin temperature, while the same heat treatment of Blades 1 and 3 reduces the error to 2.5 percent of T. It is hypothesized that the oxidation of rhodium takes place at or near the film surface, removing rhodium from solution locally, to produce the observed gray to black surface discoloration. If this is the case then during the oxidation process rhodium continuously diffuses toward the surface due to the gradient in the rhodium concentration. The process would be reversed during decomposition of the oxide at temperatures above 1166K.

The less complete recovery of Blades 1 and 3 may be due to loss of rhodium through spalling of rhodium oxide during the 50-hour combustor tests. Further support for this premise is provided by the observation that the rate of calibration drift during the final oven tests (Figure 14) is larger for Blades 1 and 3 than for Blade 2. The larger drift rate suggests that the films on Blades 1 and 3 are thinner due to loss of film material by spalling of rhodium oxide during the 70 temperature cycles to 1250K of the combustor tests. Erosion of the rhodium oxide during combustor tests is not believed to be a major cause of oxide loss, because the recovery of the systems tested on blades 1 and 3 was about the same, even though one system was on the concave side (blade 1), where high erosion would be expected, and one was on the convex side (blade 3). Thinner films of initially oxide-free platinum/rhodium films are expected to display more rapid thermoelectric drift for the same rate of conversion of rhodium to oxides, because of increased surface-to-volume ratio.

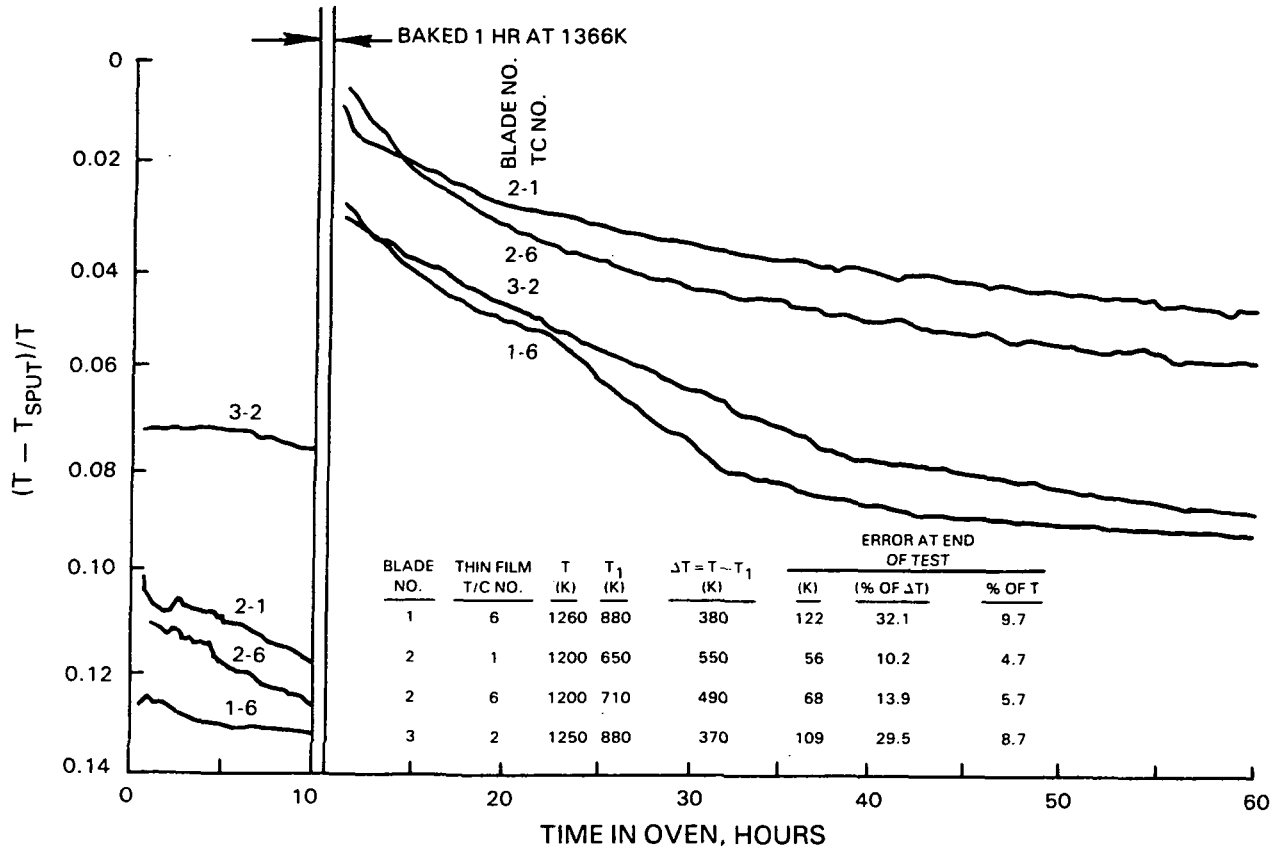

BLADE NO.	THIN FILM T/C NO.	T (K)	T_1 (K)	$\Delta T = T - T_1$ (K)	ERROR AT END OF TEST (K)	(% OF ΔT)	% OF T
1	6	1260	880	380	122	32.1	9.7
2	1	1200	650	550	56	10.2	4.7
2	6	1200	710	490	68	13.9	5.7
3	2	1250	880	370	109	29.5	8.7

Figure 14 Comparison of Thin Film Thermocouple Calibration Drift for Blades 1, 2, and 3. Blades 1 and 3 were previously combustor tested for 60 hours; Blade 2 was previously oven tested for 50 hours. T and T_1 are the Kelvin temperatures measured with Type S wire thermocouples adjacent to the film junction and the film to leadwire connection, respectively. T_{SPUT} is the Kelvin temperature indicated by the thin film system, assuming Type S response.

The recovery of Blade 3 was nearly identical to that of Blade 1 (2.5 percent of T), as would be expected.

It is interesting to note in Figure 14 that the initial error (after combustor tests but before isothermal heat treatment at 1370K) was 13 percent of T for Blade 1 and 7 percent of T for Blade 3. The difference is presumably attributable to the difference in degree of oxidation of the platinum/10-percent rhodium films due to different temperature distributions along the films during the combustor tests. On Blade 1, the film tested was No. 6 on the concave side (1250K maximum temperature during combustor tests). On Blade 3, the film tested was No. 2 on the convex side (1100K maximum temperature during combustor tests). To explain the larger error on Blade 1 on the basis of rhodium oxidation, it would have to be shown that this film on the hotter

side of the blade was oxidized to a greater degree. Visual examination of the blades does not prove or disprove this hypothesis. About the same degree of darkening is evident on both of the platinum/rhodium films, though it does appear that the darkening extends over a greater length of the film on the hotter side.

A photograph taken before the heat treatment at 1370K of Blade 3 (Figure 15) shows the gray discoloration of all platinum/10-percent rhodium films after exposure to temperatures between 900K and 1200K. A photograph after the heat treatment at 1370K (Figure 15) shows that the discoloration has largely disappeared.

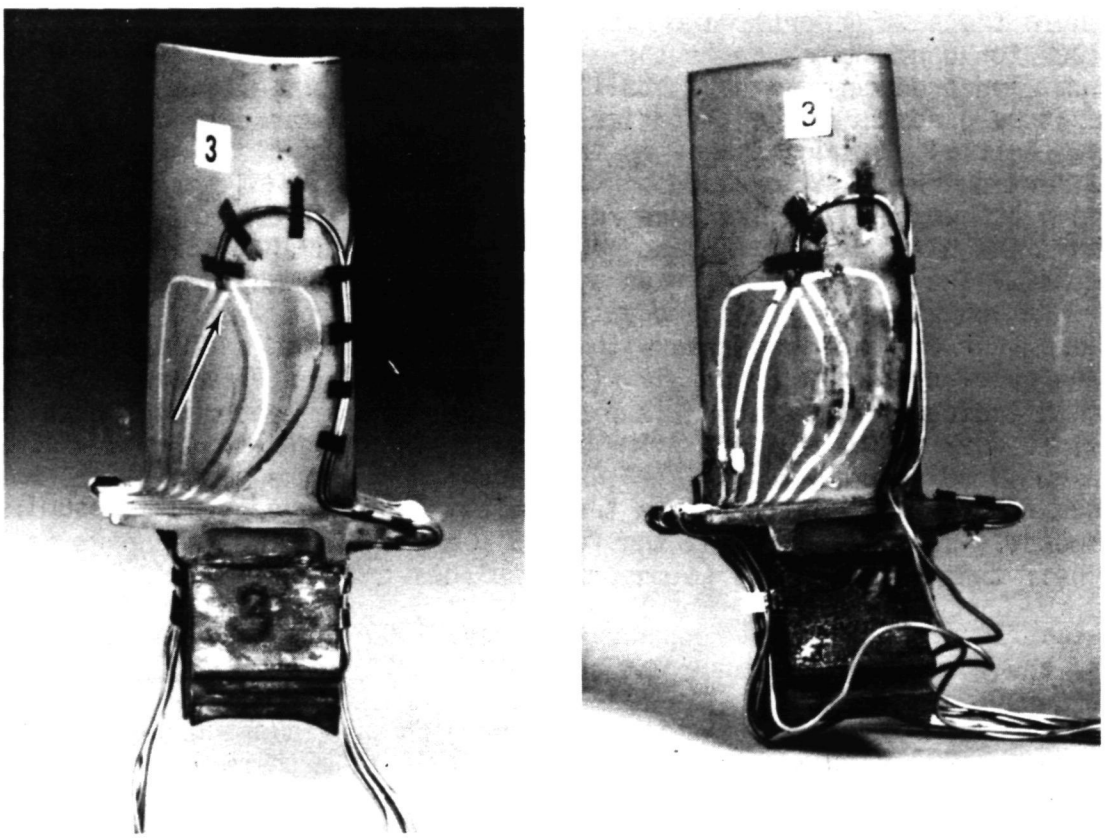

Figure 15 Thin Film Thermocouple Systems on Blade 3: After the 60-hour Combustor Test of the Phase II Program [left] (Reference 2) and (B) After Subsequent Bake at 1370K for 1 hour [right]. For each thermocouple pair, the film on the right is platinum/ 10-percent rhodium; the arrow indicates the thermocouple retested during Phase III. (80-444-0462-B; 80-441-0808-E)

7.2 FILM VS. WIRE DRIFT TESTS

Three different 5 μm platinum film versus 75 μm platinum wire thermocouple systems on two bars (Figure 7) were exposed in air in the standard temperature gradient (nominal 1250K at one end of the film, nominal 750K at the other end) for eight hours. Thermocouple voltage generated was monitored. There was no net drift in thermocouple output for any of the three platinum systems during this period. Small output voltages existed in all film systems throughout the tests (in the direction which would cause a low reading in a Type S thermocouple system if the platinum wire were replaced with the platinum film tested). The average magnitude of this offset for the three films were -70 μV, -40 μV, and -40 μV (corresponding to temperature errors of -6K, -3.5K, and -3.5K, which are within the accuracy of standard thermocouple wire). The electrical resistance to ground was above 5000 ohms throughout the tests, and the film resistances were about 10 ohms.

Four different 5 μm platinum/10-percent rhodium film versus 75 μm platinum/10-percent rhodium wire thermocouple systems on Bars 4 and 5 were tested in the same general way. The bars in this case were thermally soaked at 1370K for one hour in an isothermal oven to decompose any oxides of rhodium and produce a bright metallic luster before insertion in the standard temperature gradient. The test time in the gradient was extended to 22 hours. Initial output voltages in these four thermocouple systems were all in the direction which would cause a high reading in a Type S thermocouple system if the platinum/rhodium wire were replaced with the platinum/rhodium film tested. The offsets were +2K and +4K for one bar and +12K and +14K for the other bar. The output of all four systems drifted downward relative to a Type S calibration at nearly the same rate. In Figure 16 the drift in calibration of these four films is compared with the drift of the thin film thermocouple systems on blade 2 from Figure 14. (Since it was shown in reference 2 that the error in indicated temperature is proportional to the temperature gradient $(T-T_1)$ from end to end of the film, the data are presented in Figure 16 in the normalized form $(T-T_{sput})/(T-T_1)$, where T_{sput} is the temperature deduced from the thin film system thermoelectric voltage output, assuming type S response.) The drift rate of the four 5 μm films on the test bars is less than half that of the 2 μm films on the blades.

The electrical resistance to ground was above 3000 ohms throughout these tests, and the film resistance was about 10 ohms.

The results of these tests are in agreement with previous indications that the principal source of the drift in the Type S thin film thermocouple systems is in the platinum/10-percent rhodium films. The drift rate is approximately in inverse proportion to the thickness of the platinum/10-percent rhodium films. All of these findings are consistent with the hypothesis that oxidation of rhodium is the principal source of the calibration drift.

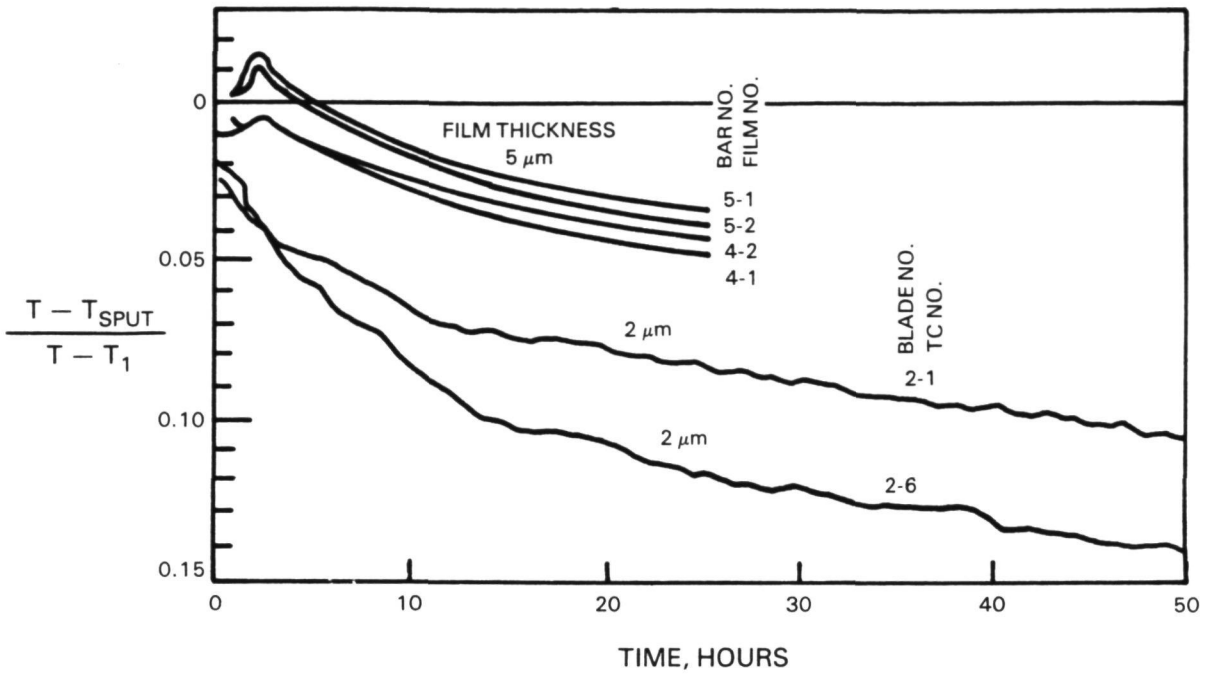

Figure 16 Comparison of Calibration Drift for 5 μm and 2 μm Films. Error, expressed as a fraction of the temperature gradient ($T - T_1$) imposed on the film, is plotted against time. All films were heat treated at 1370K for one hour before start.

7.3 OVERCOATING EVALUATION PROGRAM

The three candidate overcoating materials (Al_2O_3, Si_3N_4, and Pd/30-percent Mo) were sputtered separately, 5 μm thick, on sample platinum films and sample platinum/10-percent rhodium films on the test bars listed in Table VI. The intention was then to conduct drift testing for comparison with the drift test results of uncoated films. Serious mechanical or electrical problems were observed with all three coating materials as described in the following paragraphs. As a result, drift tests were not conducted.

Al_2O_3 overcoatings on the test bars with platinum and platinum/10- percent rhodium films were adherent and clear as sputtered but bubbled and peeled (only in the region directly on the metal films) when temperature was cycled to 1250K (Figure 17A). Dr. F. T. Turner of Varian Corporation was then consulted. He suggested that a heated substrate or a direct current bias during sputtering would be helpful and cited success with Al_2O_3 over silicon to 1270K using these techniques. Pratt & Whitney's Government Products Division has reported some success with a combination of direct current bias sputtering of Al_2O_3 plus a thick coating of another (proprietary) material before cycling to 1250K. It is evident that further development would be required to achieve an overcoating of Al_2O_3 that is durable to 1250K.

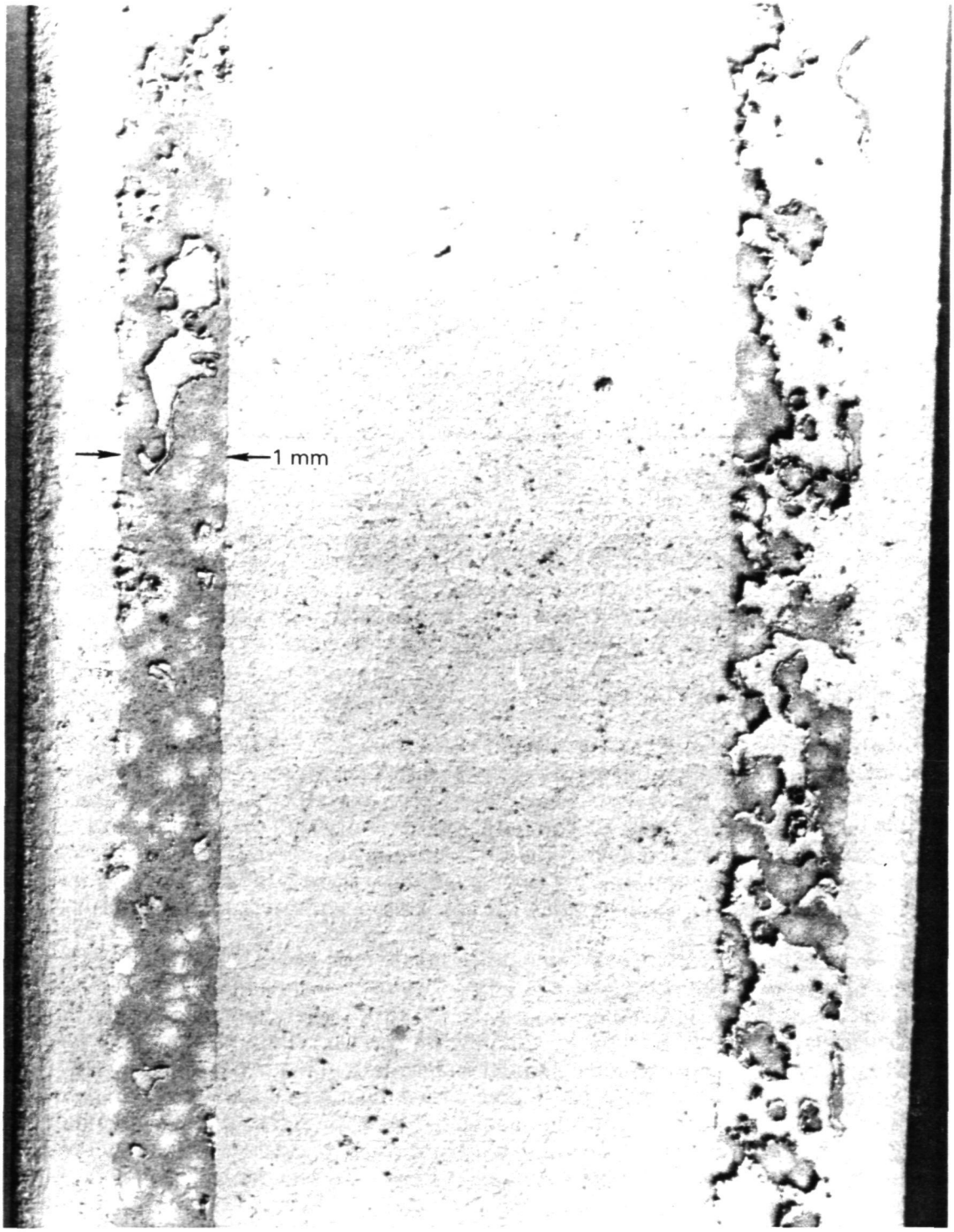

Figure 17A Sputtered Pt/10%Rh Films, Overcoated With Sputtered Al_2O_3, Are Shown After Cycling to 1250K. The Al_2O_3 overcoat has buckled and peeled in the regions directly on the metal films, removing portions of the metal films.

Si_3N_4 overcoatings adhered firmly to the Al_2O_3, platinum, and platinum/10-percent rhodium films on the test bars, but the overcoating resulted in lifting of the metal films from the test bars during sputtering (Figure 17B). The Si_3N_4 films were sputtered from a silicon target in nitrogen in the planar sputtering system, using the procedure which has been uniformly successful in thin film strain gage system fabrication under Contract NAS3-21262; where overcoating of thin metal films of nickel/30-percent chromium and copper/40-percent nickel was accomplished on Si_3N_4 insulating layers. It is possible that, in the sputter overcoating of thin film thermocouples with Si_3N_4, enough heat is generated to break the (weak) noble-metal-to-Al_2O_3 bond. Sputtering in the S-gun facility, with its lower electron heating, might be more successful. However, a silicon target for the S-gun was not available. This possibility could be explored in another program.

Overcoatings of Pd/30-percent Mo were adherent to the Al_2O_3 and platinum/10-percent rhodium. The film systems remained intact during cycling to 1250K. As expected, the platinum/10-percent rhodium films were short-circuited by the overcoating in the as-sputtered condition. In addition, short circuits to ground were observed in the platinum/10-percent rhodium systems. It was planned initially, based on experience with 1 μm thick films of Pd/30-percent Mo in Contract NAS3-21262, to soak the thermocouple system at high temperature until the Pd/Mo film became a nonconducting layer as a result of oxide growth. A long series of bake-outs (48 hours at 1250K, 24 hours at 1030K, 4 hours at 1420K) did not produce the desired result. Although the outer surface of the Pd/Mo developed a durable insulating layer, the short circuits from platinum/10-percent rhodium films to ground persisted. It is possible that the 5 μm film thickness reaches a stable (and still conductive) state beyond which the oxidation rate is extremely slow. The 1 μm films of Contract NAS3-21262 had become a durable insulating material after one hour at 920K. Further experimentation with thinner films of Pd/30-percent Mo might be fruitful.

7.4 SPUTTERING DISTANCE AND ORIENTATION PROGRAM

The results of the sputtering distance and orientation program for the S-gun sputtering system are presented in Figures 18 and 19 as film thickness versus lateral position and versus surface angle, respectively.

7.4.1 Thickness Variation with Height Above Target (h)

Film thickness at the center of the flat disk decreases from 1 μm at a height above the target (Figure 9) of 12 cm to 0.6 m at a height of 18 cm. Film thickness is therefore approximately proportional to the -1.25 power of the height above the target .

7.4.2 Thickness Variation with Lateral Position

Figure 18 shows that at the 12-cm height, film thickness varies less than 1 percent with radius over the center $\pm$5 cm of the 7.6-cm radius disk, along the line sampled. As the disk edge is approached, film thickness decreases gradually and is 5 to 10 percent smaller at a radius of $\pm$7 cm compared to thickness near the center.

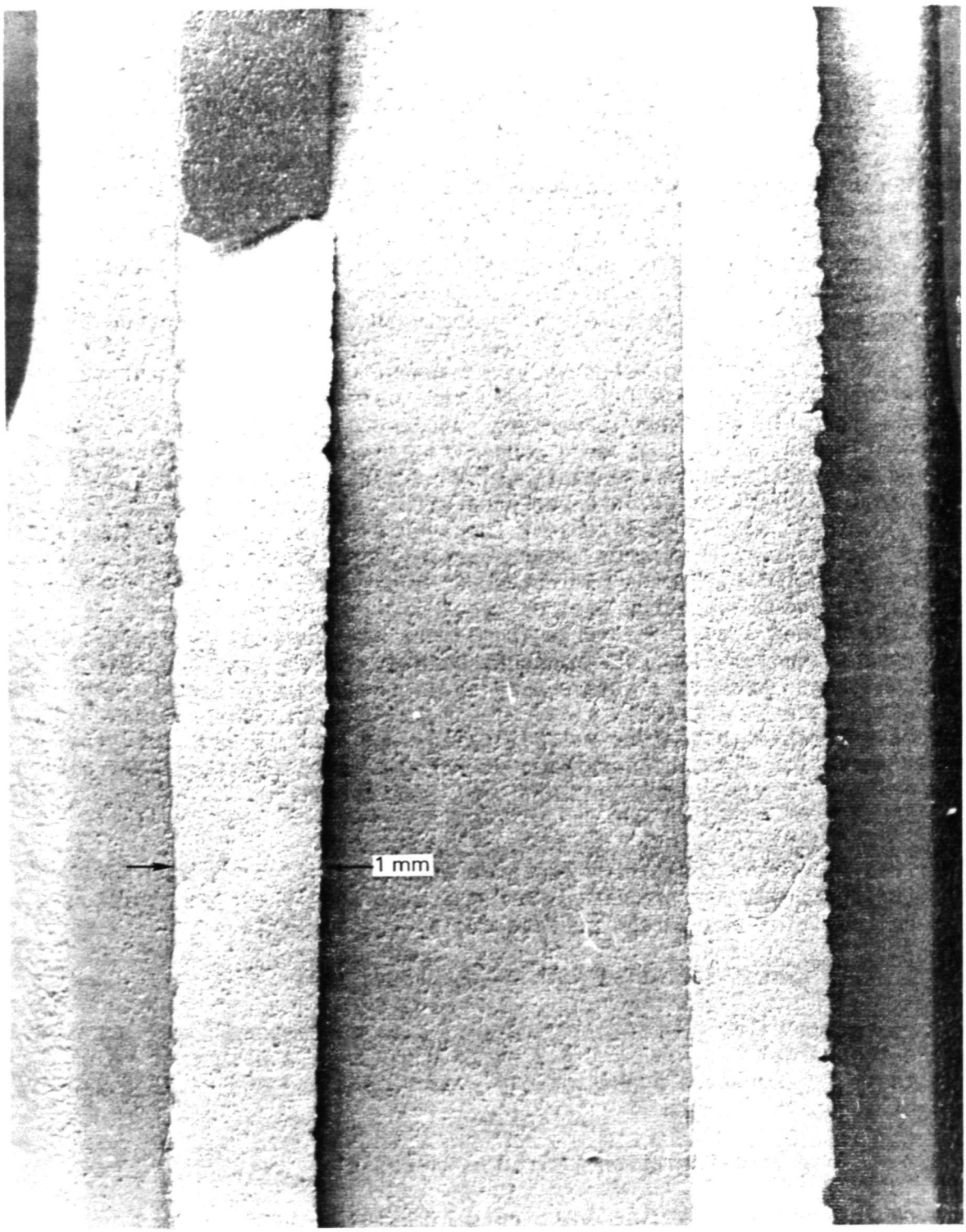

Figure 17B Sputtered Pt/10%Rh Films, Overcoated With Sputtered Si_3N_4, Are Shown Just After Sputtering of the Si_3N_4. The Pt/10%Rh films separated completely from the surface during the overcoating process.

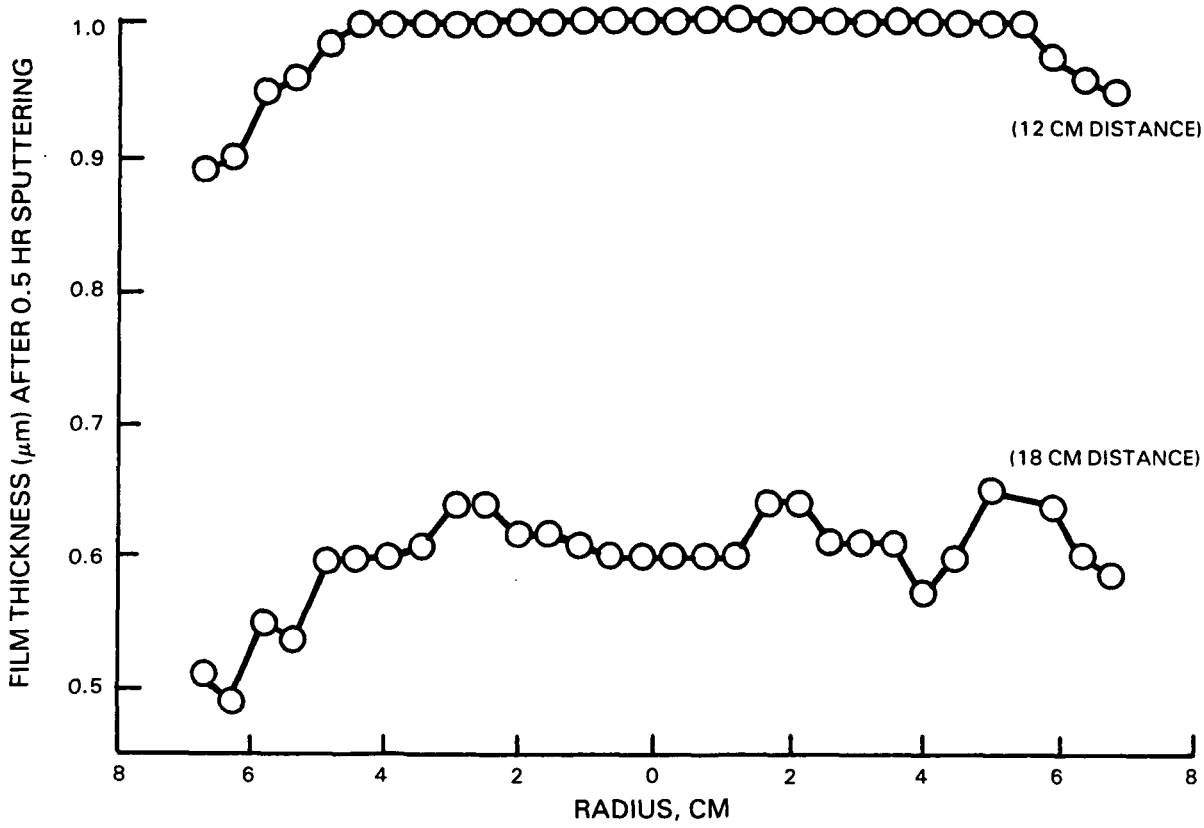

Figure 18 Film Thickness as a Function of Lateral Position on the Optical Flat. Film thickness is nearly constant over 70 percent of the radius of the disk. Sputtering time was 0.5 hours in the S-gun unit.

At the 18-cm height, film thickness behavior is similar except that there are +6 percent irregular variations in thickness even near the center portion of the disk.

7.4.3 Thickness Variation with Surface Angle (θ)

Thickness is approximately proportional to the cosine of the angle between the prism surface sputtered and the reference optical flat surface (Figure 19). This distinctly directional deposition is characteristic of S-gun performance (Reference 14, p. 126, Figure 13). Thus, for uniform coating on complex turbine blades, blade rotation or two or three successive orientations must be employed.

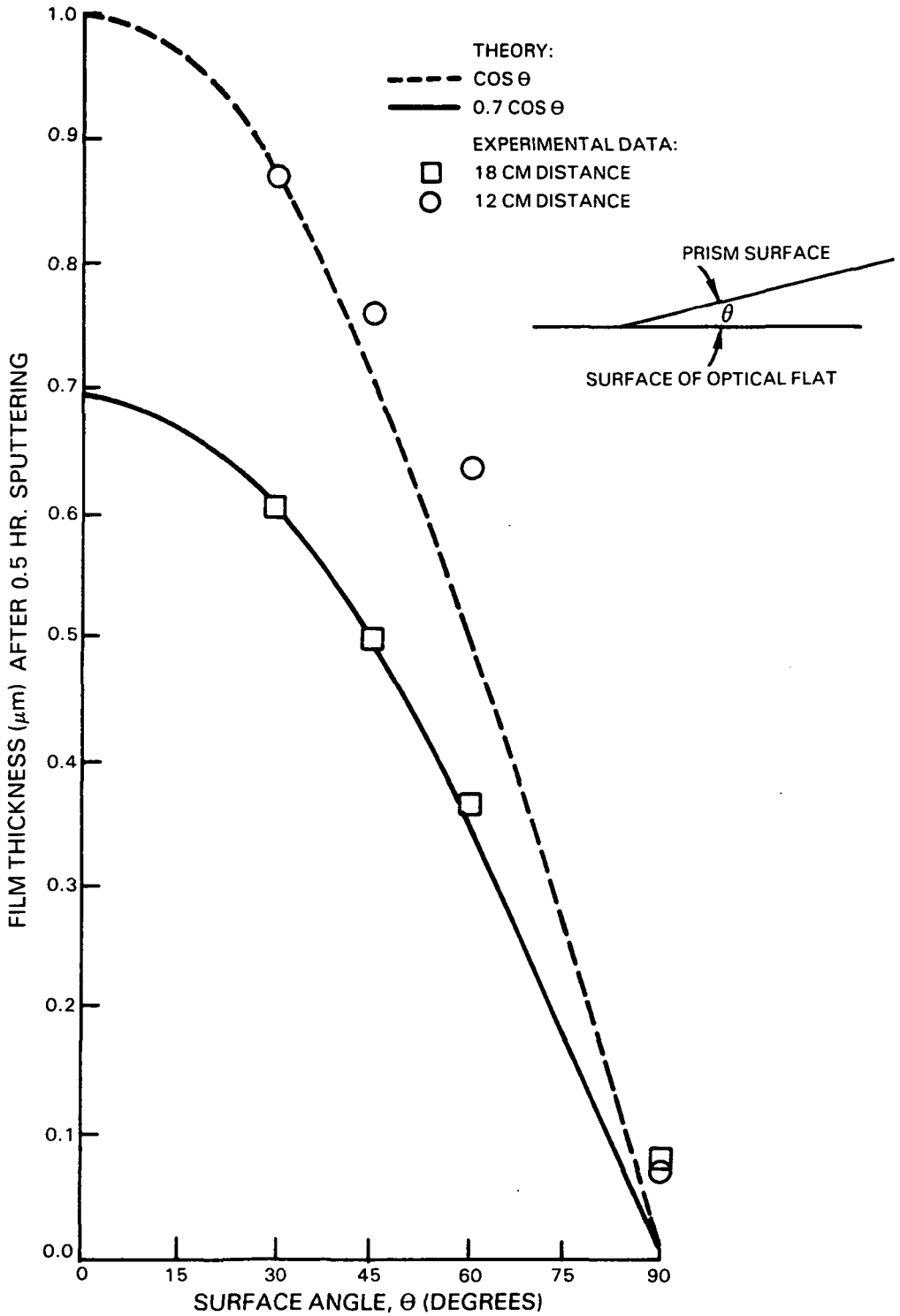

Figure 19 Film Thickness as a Function of Surface Angle. Film thickness is approximately proportional to the cosine of the angle between the prism surface sputtered and the reference optical flat surface.

Note again that the prism locations for the Figure 19 data were about 4 cm to the left and right of the specimen center and on a line that is perpendicular to the sampled traverse line for the Figure 18 data. A cosine extrapolation, to θ = 0 degrees of the Figure 19 thickness measurements at θ = 90, 60, 45, and 30 degrees, results in an estimated film thickness within 10 percent of that for the sampled traverse line of Figure 18.

7.4.4 Adherence Variations

The adherence of the platinum films on the quartz flats and prisms was poor everywhere. The films were virtually completely removed by tape testing at every location tested, including locations on both flats and all prism surfaces. No conclusions on adherence as a function of surface angles between 0 and 90° could be drawn from these tests. Some platinum became deposited on the back surfaces of the optical flats (θ = 180 degrees) during these sputtering runs, and its adherence was so poor that the films were entirely removed during routine washing in solvents used for photoresist removal.

7.4.5 Summary: Sputtering Rate vs h and

Combining the results discussed in 7.4.1 and 7.4.3, the general relation between platinum sputtering rate r (μm/hr), h (cm), and θ appears to be adequately described by the expression

$$r = 1.5\ (15/h)^{1.25} \cos\theta \qquad (1)$$

for any surface placed in the S-gun sputtering unit within the recommended sputtering region of Figure 5, with $0 < \theta < 90°$, using the standard sputtering parameters of Table IV. The height h must be measured as shown in Figure 9, from the bottom plane of the target to the point where axis A-A intersects a 30° plane touching the surface element to be sputtered.

7.5 TURBINE BLADE SENSOR INSTALLATION AND TEST PROGRAM

7.5.1 Drift as a Function of Film Thickness

Static oven drift tests were conducted as described in Section 6.7 (Table VII) on the two batches of thin film systems freshly fabricated on six turbine blades. All of these film systems were tested after heat treatment at 1370K for one hour to decompose oxides of rhodium. None of these film systems had experienced any previous exposure at high temperature other than that normally encountered during fabrication. The test results can therefore be compared directly with the earlier results shown in Figure 16. The results are plotted in Figure 20, and the data from Figure 16 are superimposed for comparison.

It is evident at once in Figure 20 that the drift rate decreases systematically as the Pt/10%-Rh film thickness is increased. In fact, for those films whose thickness is known with reasonable accuracy (Curves 1 through 9), the drift rate is inversely proportional to film thickness, within the uncertainty of the determination of film thickness.

CURVE NO.	SYMBOL	BLADE NO.	SIDE OF BLADE #	TC No.	BAR NO.	FILM NO.	Pt/10%-Rh FILM THICKNESS (um)*	T (K)	TI (K)	$\frac{T-Tsput}{T-T_1}$ AT 50 HRS.
1	●	43	CX	1			14	1320	530	.012
2	●	43	CX	3			14	1320	530	.014
3	●	46	CX	1			14	1300	780	.028
4	○				5	1	5	1230	680	
5	○				5	2	5	1230	680	
6	○				4	2	5	1230	660	
7	○				4	1	5	1230	660	
8	◇	2	CX	1			2	1210	650	.102
9	◇	2	CC	6			2	1220	710	.139
10	△	42	CC	2			2	1330	790	
11	△	43	CC	1			2	1220	641	
12	△	43	CC	2			2	1220	641	
13	△	44	CC	1			2	1250	720	.257
14	△	41	CC	1			2	1240	740	
15	△	41	CC	2			2	1240	740	

CX = Convex; CC = Concave

* Minimum, based on sputtering time and orientation

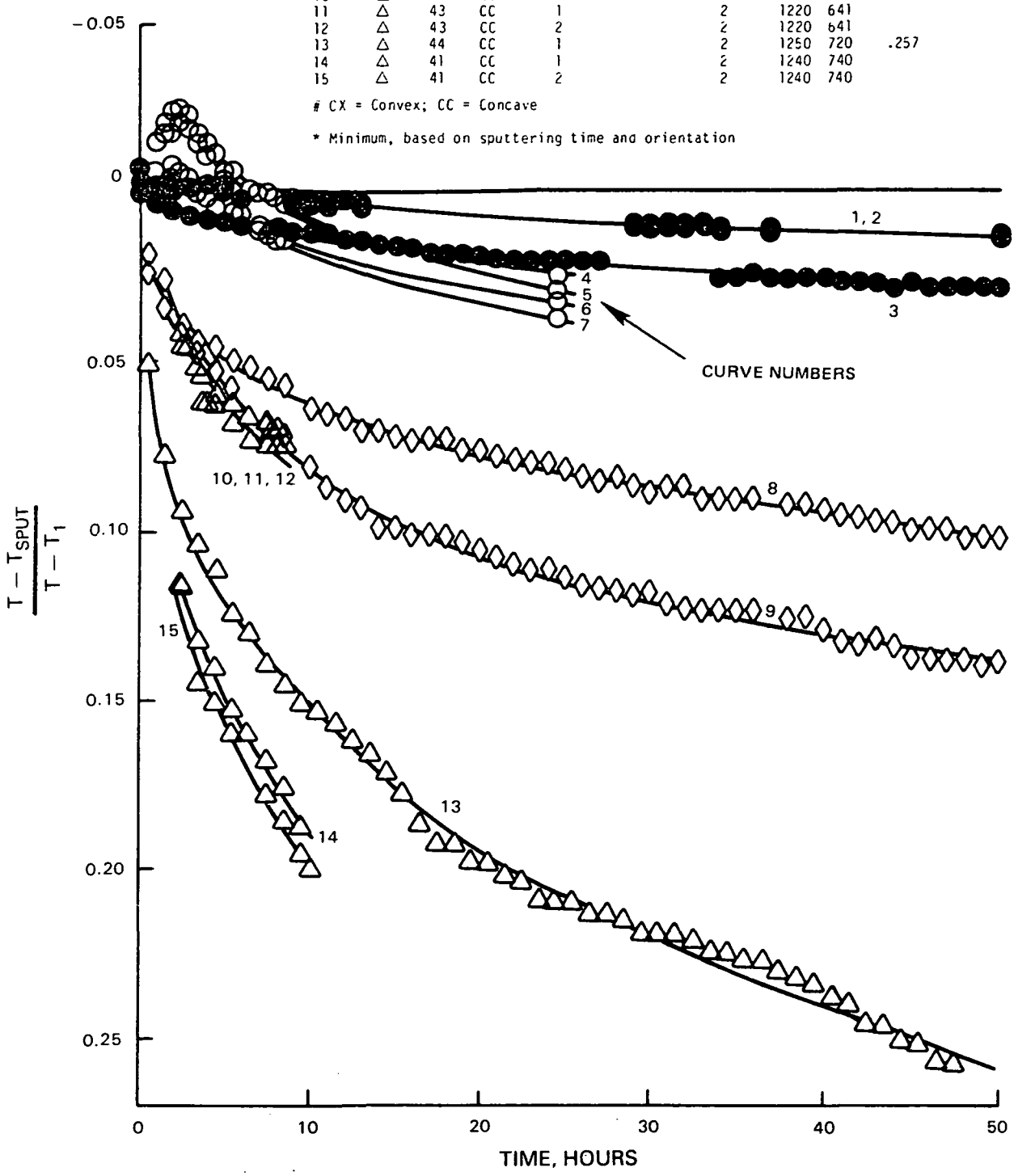

Figure 20 Comparison of Calibration Drift for 15 Thin Film Systems. Error, expressed as a fraction of the temperature gradient ($T - T_1$) imposed on the film, is plotted against time. All films were heat treated at 1366K for one hour before start.

Note that in Figure 20 the temperatures T and T_1, at the two ends of the film system, are listed for each test. The standard test procedure called for the nominal values T = 1250K, T_1 = 750K. Note that in several tests T was set somewhat higher and T_1 much lower than these standard values, in order to gain additional information on the range of temperature in which oxidation of rhodium takes place. Visual examination of the Pt/10%-Rh films after testing showed that the dark discoloration associated with oxides of rhodium extended all the way to the coolest end of the films even on the convex side of blade 43 (T_1 = 530K), indicating that the oxidation rate is significant at temperatures as low as 530K.

It is notable in Figure 20 that a reversal error in temperature indication occurs for a short time after the start of some tests (curves 1, 2,4,5,6). In all of these cases the system is Pt/10%-Rh film vs. wire and the wire diameter employed is 0.075 mm. The reversed error is believed to be due to the presence of an oxidized 0.075 mm lead wire in the return side of the thermocouple system. Note that blade 46 (curve 3) shows no reversal. This blade is identical with blade 43 (curves 1, 2) except that a 0.25 mm lead wire diameter was used (Figure 11E). In this case the lead wire surface-to-volume ratio was low enough to assure that oxidation of the lead wire did not affect the reading. Note from Table V that the surface-to-volume ratio is four times higher for a bare wire than for a thin film of the same thickness, and is also inversely proportional to thickness for either the wire or the film. The oxidation induced drift in the .25 mm bare lead wire of curve 3, Figure 20, is therefore 4.46 times less than in the 14 μm film to which it is attached.

7.5.2 Predicted Drift as a Function of Thickness and Pressure

In this section a mathematical model for prediction of error vs. time (drift in calibration) as a function of initial Pt/10%-Rh film thickness and oxygen pressure is developed. The prediction is then compared with the experimental data (at sea level) and implications for engine testing at elevated pressures are considered.

Assume first that the error E, which is defined as

$$E = \frac{T - T_{SPUT}}{T - T_1} \qquad (1)$$

is equal to the decrement in the percent rhodium concentration (x) in the Pt/Rh leg of the thin film thermocouple system. That is

$$E = 1 - \frac{x}{10} \qquad (2)$$

(This is not exactly true, since the thermoelectric emf actually decreases somewhat more slowly than x decreases, but equation (2) provides a simple and reasonably close approximation to the actual behavior.)

Assume second that the decrement in the rhodium concentration is proportional to the ratio of the oxide thickness (b) to the original Pt/10%-Rh film thickness (a). That is,

$$1 - \frac{x}{10} \propto \frac{b}{a} \tag{3}$$

This must be the case if rhodium is in fact being converted to an oxide. Combining (2) and (3) yields

$$E \propto \frac{b}{a} \tag{4}$$

It only now remains to express the oxide thickness (b) as a function of time (t) and oxygen partial pressure (p) and insert this result in equation (4) to obtain a relation describing error E as a function of a, t, and p. This may be done as follows.

The time rate of growth of the oxide thickness (at any one constant temperature below 1170K) depends on the oxygen pressure and on the oxide thickness itself. A reasonable relationship is

$$\frac{db}{dt} = A \frac{p^s}{b^n} \tag{5}$$

where A is a rate constant. A is a function of temperature and therefore a function of position along the film, but for thin film systems on turbine blades where the temperature profile is characterized by a monotonic increase from T_1 to 1 and where T_1 is well below 1170K, then A will be regarded as an absolute constant.

The exponent s in equation (5) is expected to be unity, or perhaps less if the diffusion rates of Rh and O_2 in the oxide layer increase less than linearly with pressure. The exponent n is expected to be unity for a semi-infinite solid rhodium slab but higher for Pt/Rh alloy thin films because the Rh concentration gradient decreases as the film becomes depleted. Taking the worst case (s = 1), and integrating equation (5) yields

$$\left[b^{n+1}\right]_{b_0}^{b} = (n+1)\, A \left[pt\right]_{t_0}^{t} \tag{6}$$

The change in oxide film thickness from time t_0 to time t at constant pressure and temperature is then

$$b^{n+1} - b_0^{n+1} = (n+1)\, A\, p\, (t - t_0) \tag{7}$$

If the original film thickness b_0, is zero at time t_0, then

$$b = (n+1)A^{\frac{1}{n+1}} (pt)^{\frac{1}{n+1}} \tag{8}$$

Inserting this result in (4) gives a relationship for comparison with Figure 20:

$$E = B \frac{(pt)^{1/(n+1)}}{a} \tag{9}$$

where B is a constant equal to $[(n+1)A]^{1/(n+1)}$.

If p is expressed in units of partial pressure of O_2 for standard sea level air (p = 1 in sea level air), t in hours, and original film thickness a in micrometers, then the data of Figure 20, cross-plotted in Figure 21, yield a good fit for B = 0.07, n = 2, or

$$E = 0.07 \frac{(pt)^{1/3}}{a} \tag{10}$$

In Figure 22, equation (10) is plotted for four values of a (1, 2, 5, 14 micrometers) at p = 1, and three values of p (1, 10, 20) at a = 14 micrometers. The values of p cover the range expected in engine testing.

Comparison of Figure 22 and Figure 20 shows that equation (10) describes the observed effects of film thickness and time at temperature in sea level air quite well. Of course equation (10) states the maximum expected error if all conditions are constant from the beginning of the test.

No data are available at present to confirm the effect of pressure higher than one atmosphere on error. It is interesting to note from equation (10) that the error is expected to increase only as the 1/3 power of pressure. If the 50 hour programs of Figure 20 were conducted at 10 atmospheres rather than 1 atmosphere, it is predicted that the errors observed at 50 hours in Figure 20 would be reached after only 5 hours, but that the ultimate errors after 50 hours at 10 atmospheres would be only a little more than twice the errors of Figure 20 (since $10^{1/3} = 2.15$).

To estimate the error at the end of a typical 50-hour engine test, equation (10) should be used in the form

$$E = \frac{0.07}{a} \left[p_1 (t_1 - t_0) + p_2 (t_2 - t_1) + \ldots\right]^{1/3} \tag{10a}$$

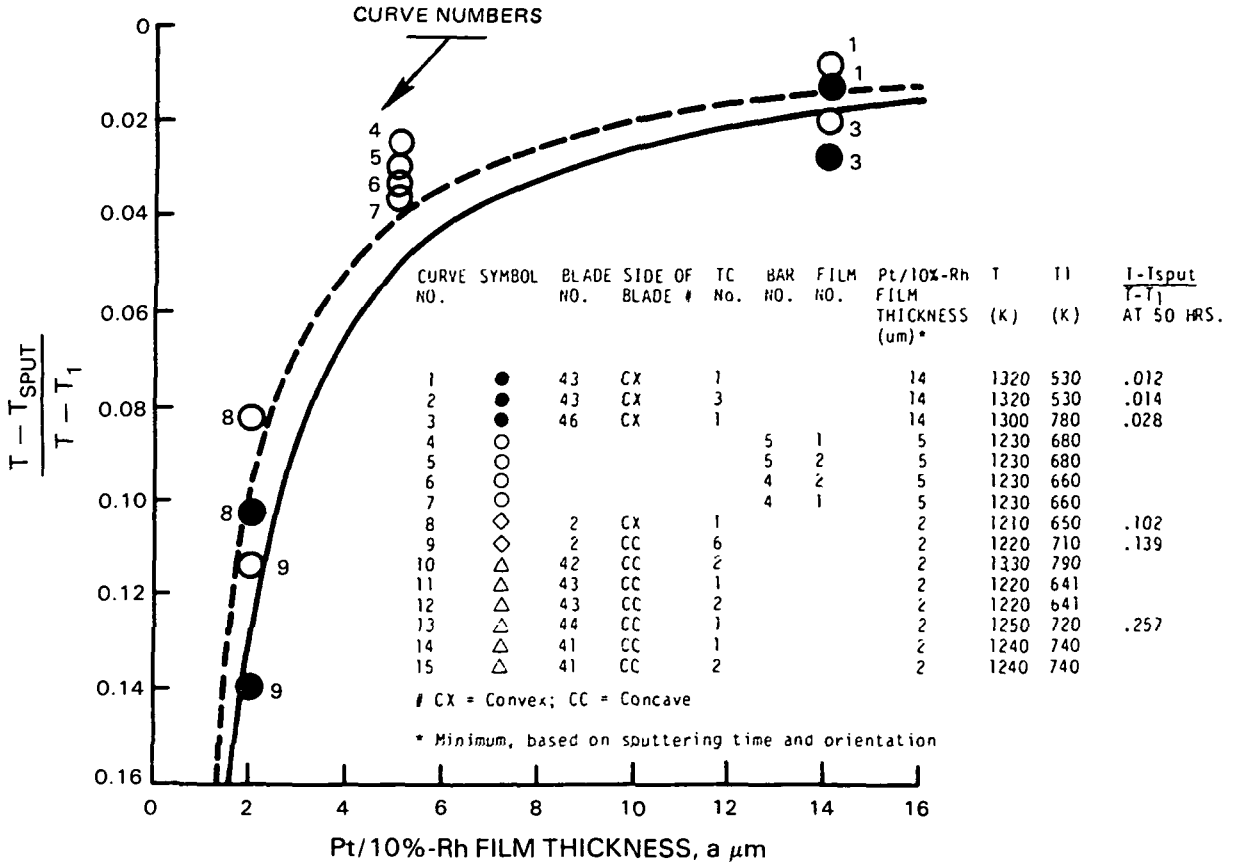

CURVE NO.	SYMBOL	BLADE NO.	SIDE OF BLADE #	TC No.	BAR NO.	FILM NO.	Pt/10%-Rh FILM THICKNESS (um)*	T (K)	T1 (K)	$\frac{T-T_{sput}}{T-T_1}$ AT 50 HRS.
1	●	43	CX	1			14	1320	530	.012
2	●	43	CX	3			14	1320	530	.014
3	●	46	CX	1			14	1300	780	.028
4	○				5	1	5	1230	680	
5	○				5	2	5	1230	680	
6	○				4	2	5	1230	660	
7	○				4	1	5	1230	660	
8	◇	2	CX	1			2	1210	650	.102
9	◇	2	CC	6			2	1220	710	.139
10	△	42	CC	2			2	1330	790	
11	△	43	CC	1			2	1220	641	
12	△	43	CC	2			2	1220	641	
13	△	44	CC	1			2	1250	720	.257
14	△	41	CC	1			2	1240	740	
15	△	41	CC	2			2	1240	740	

CX = Convex; CC = Concave

* Minimum, based on sputtering time and orientation

Figure 21 Error After 25 Hours and 50 Hours as a Function of Pt/10%Rh Film Thickness. The data points are from Figure 20. The curves are predicted values from equation (10).

where p_1 is the oxygen pressure during the time interval $t_1 - t_0$, and so forth. As an example, consider a 50-hour engine test consisting of three segments; using 14 μm films:

5 hours at 1 atmosphere
35 hours at 10 atmospheres
10 hours at 20 atmospheres

$$\text{Then } E = \frac{0.07}{14} \left[(1)(5) + (10)(35) + (20)(10)\right]^{1/3}$$

$$E = 0.04$$

For $T-T_1$ = 500K the error in temperature reading would be between 0 and 20K at the end of this program, resulting in an uncertainty of $\pm$10K.

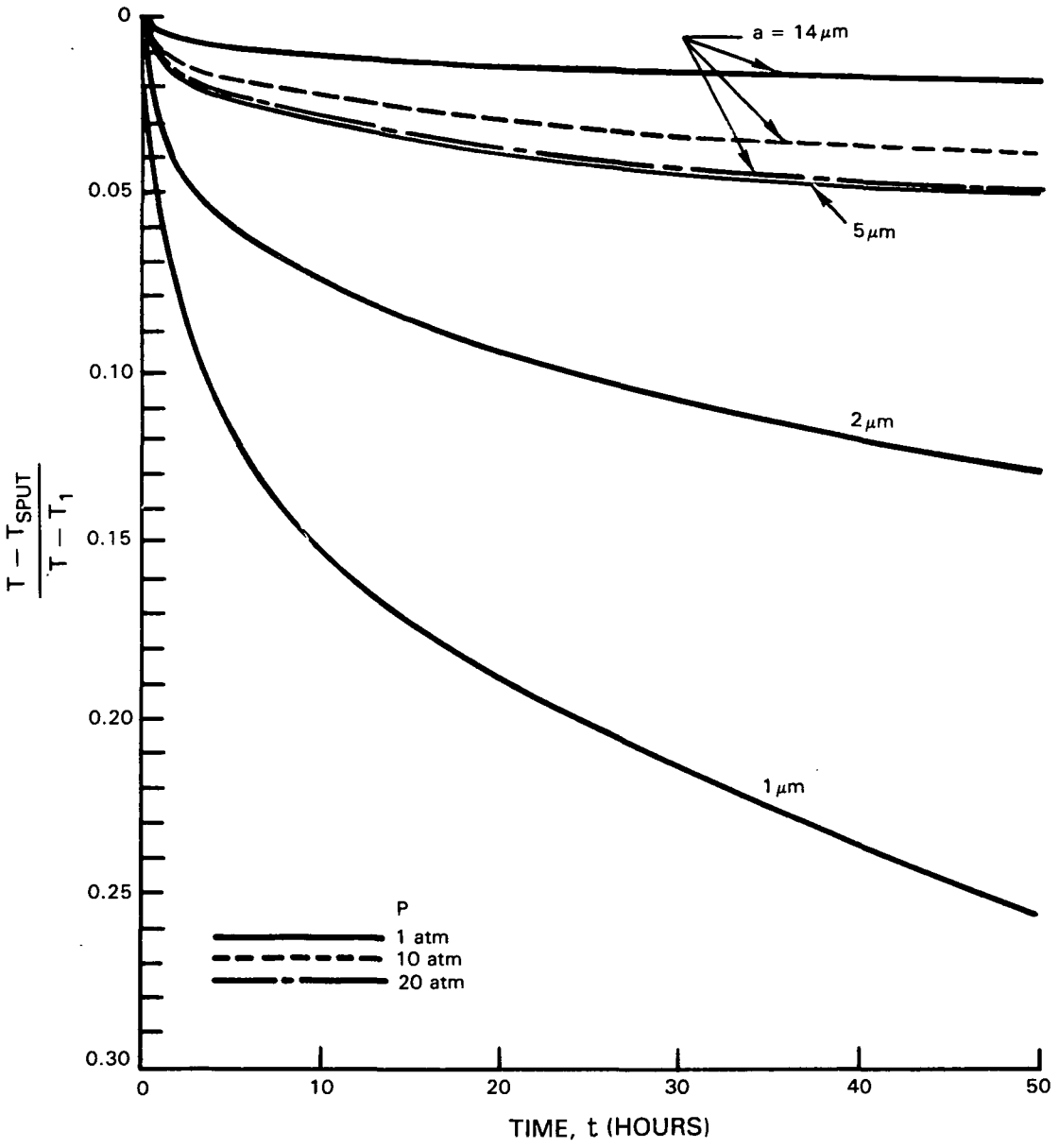

Figure 22 Predicted Drift for Several Values of Thickness (a) and Pressure (p), based on equation (10).

In preparing for an engine test using thin film thermocouples a preliminary drift test should be conducted at pressures in the range expected during the engine test, to verify equation (10a).

7.5.3 Adherence Failures on Actual Blades of Complex Shape

In the reference 1 and 2 programs (Contracts NAS3-20768 and NAS3-20831) the adherence of Pt films, and to a lesser extend Pt/10%-Rh films, was found to be critically dependent on surface cleanliness (especially freedom from adsorbed moisture), surface morphology (roughened reticulated surfaces required), and orientation with respect to the sputtering target during sputtering (avoid angles near grazing incidence).

These factors govern apparently because the Pt and Pt/10%-Rh film materials are chemically quite inactive and do not form strong chemical bonds with the underlying Al_2O_3. For example, in Contract NAS3-21262 it was found that films of strain gage alloys which are chemically more active (Ni/30%-Cr, Cu/45%-Ni) were adherent on highly polished oxide and nitride surfaces, where platinum alloy (Pt/20%-W) films were not. The importance of these factors has been discussed in Section 3.3 above and was recognized at the beginning of the present Phase III program.

In installing thin film thermocouple systems on the six blades in the present program careful attention was therefore given to surface cleanliness (including maintaining laboratory dew point below 48°F during fabrication) and correct surface morphology to promote adherence. In sputtering the first batch of films on blades 41, 42, 43, 44, however, the incorrect sputtering orientation already described in Section 6.7 (Figure 13) resulted in near grazing incidence over a major portion of the airfoil concave surface. As shown in Figure 13, the incidence angle was most disadvantageous at spanwise locations (measured from the blade root) from 15% of span to 100% of span (tip), and less disadvantageous (due to blade twist) between root and 15% of span.

A subsequent examination of the blades revealed that adherence was indeed poorest on the concave side particularly above 15% of span. Failures due to bubbled or partially raised films occurred in this area on the no. 1 thermocouple system of blade 42 and no. 2 thermocouple system of blade 44. There were no other failures in the program. These results underscore the importance of avoiding grazing incidence angles during sputtering, a lesson already learned in the reference 2 program.

Poorly adherent Pt/10%-Rh films in such regions can also affect drift and accuracy even if the films do not fail. First, the growth or decomposition of rhodium oxide can proceed twice as fast if two film surfaces are exposed in some areas due to a lifted film. Second, the lifted films may experience gas stream temperatures well above blade surface temperature.

In sputtering the second batch of film systems, on blades 43 and 46 (convex side) proper orientations were used and no adherence problems were encountered.

7.5.4 Accuracy

In this section the accuracy goals and the accuracy achieved to date are reviewed and the expected measurement error in thin film thermocouple systems under engine test conditions are reviewed. The conclusion reached is that the accuracy attained more than meets the program goals and appears adequate for highly quantitative measurements of engine turbine blade metal surface temperature under actual engine test conditions. Testing at elevated pressures was not a requirement of the present program, and accuracy at elevated pressures has not yet been verified, but only a moderate degradation in accuracy is forseen at elevated pressures.

The accuracy goal of the current three-phase program is initial agreement with reference wire thermocouples within $\pm$1.5 percent of Fahrenheit temperature and 60-hour drift of less than 5 percent of Fahrenheit temperature. If the largest gradient expected along the film is 50 percent of Fahrenheit temperature, then the goal translates to initial agreement within 3 percent of gradient and 60-hour drift of less than 10 percent of gradient.

The initial agreement actually achieved in the present program is consistently within $\pm$1.5% of gradient, and the 60-hour drift achieved in the final design is less than $\pm$2% of gradient.

In this final design the thickness of the Pt/10%-Rh films is increased to 14 μm (a value near the maximum permitted by program specifications) to suppress the effects of oxidation of Rh. Films thicker than about 25 μm might be considered intrusive in the air stream, particularly at a location on the airfoil near a boundary layer laminar-turbulent transition point or separation point, where the film could trip the boundary layer. Furthermore, in the gas stream the temperature gradient may be on the order of 1K per micrometer above the blade surface, so that increasing the film thickness much beyond 14 μm could result in increased total error. The thickness of the Pt films is increased to 8 μm to provide increased erosion resistance; since one failure attributed to erosion was reported in Reference 2.

No overcoating is employed in the final design since the coatings investigated resulted in degradation of either the mechanical or the electrical integrity of the film systems. An oxidation resistant coating on the Pt/10%-Rh films would be desirable. The Pt films do not require overcoating.

Over the duration of an actual engine test program at 10 to 20 atmospheres pressure the drift is expected to be about twice that observed in the present program (at one atmosphere), due to the increased rate of Rh oxidation. If no corrections were applied, the accuracy would therefore be degraded to $\pm$4% of gradient. On the other hand, if the temperature history at the film-to-leadwire connection were known within $\pm$100K (from approximate measurements with a reference thermocouple in the general vicinity during the engine test) then the accuracy could be improved by a factor of two. A suggested procedure is to calculate an error from equation (10a), and then correct the reading by an amount equal to one half of this calculated error. This procedure insures against over-correction by more than 2% in the event that oxidation reversals had occurred on the airfoil portions of the film system, resulting in smaller error than that calculated from equation (10a).

As mentioned in Section 7.5.2, in preparing for an engine test a preliminary drift test should be conducted on a sample film at pressures in the range expected during the engine test, to verify equation (10a). If equation (10a) is confirmed then uncertainty in temperature measurement due to drift, after correction, will not exceed $\pm$10K at 1250K throughout the program.

8.0 CONCLUDING REMARKS

The development of technology begun under the previous Phase I and Phase II Programs (References 1 and 2) for fabrication of sputtered thin film platinum vs platinum-10 percent rhodium thermocouples on turbine blades, for the purpose of measuring metal surface temperatures, was completed. The drift in calibration was reduced to 1% of Fahrenheit temperature in 50 hours (for temperature gradient on the film of 50% of Fahrenheit temperature) by increasing the platinum-10% rhodium film thickness to 14 μm. An engine installation of thin film thermocouples on turbine blades was designed. The requirements for a quantitative intercomparison test, in an engine test program, of three techniques for measurement of blade surface temperature (optical pyrometer, wire thermocouples, thin film thermocouples) were defined.

Additional drift tests were conducted at 1250K using the thin film systems fabricated on blades in Phase II. In addition 13 new thin film systems of various thicknesses from 2 μm to 14 μm were installed on four test bars and six actual turbine blades and extensively drift tested at 1250K. Some of the new systems consisted of platinum film vs platinum wire and platinum-10 percent rhodium film vs platinum-10 percent rhodium wire. The fabrication procedures developed during the Phase I and Phase II programs were used.

Two adherence failures occurred during the fabrication of the new film systems. Both occurred on blades in areas where, due to an error in orientation, grazing incidence occurred. No failures occurred during testing of the thin film systems.

The test results confirmed that the calibration drift arises entirely in the platinum-10 percent rhodium films. All of the results were in agreement with previous indications that the drift is due to the oxidation of rhodium in the temperature range 500K to 1200K and decomposition of the oxide (with recovery of the rhodium) at temperatures above 1200K. Increasing the thickness of the films to 14 μm reduced the drift to less than 1% of Fahrenheit temperature in 50 hours.

Three candidate protective coating materials (Al_2O_3, Pd/30%-Mo, Si_3N_4) were applied, by sputtering, to sample films to determine the potential for further reducing drift by overcoating. Mechanical failures were encountered in the Al_2O_3 coatings and unanticipated electrical (grounding) problems were encountered with the Pd-30Mo coatings. The Si_3N_4 coating process resulted in lifting of the platinum alloy films during the Si_3N_4 sputtering operation, with the sputtering parameters used, but Si_3N_4 remains a promising candidate for further investigation.

The effect of sputtering distance and orientation on film thickness was measured quantitatively in an S-gun sputtering unit. Thickness was found to vary as the cosine of the surface angle and slightly faster than the inverse of distance. The results confirm that attaining reasonably uniform and predictable film thickness on complex blade shapes will sometimes require continuous rotation during sputtering.

All drift testing was conducted in air at a pressure of one atmosphere. Simple theory predicts that over the 50-hour duration of the actual engine test program (at 10 to 20 atmospheres pressure) the drift is expected to total about 2% of Fahrenheit temperature and that residual error after correction will be about $\pm$1%. A preliminary drift test at elevated pressures is recommended to confirm the theory.

REFERENCES

1. Grant, H. P., and Przybyszewski, J. S., "Thin Film Temperature Sensor", NASA CR-159782, Feb. 15, 1980.

2. Grant, H. P., Przybyszewski, J. S., and Claing, R. G., "Turbine Blade Temperature Measurements Using Thin Film Temperature Sensors", NASA CR-165201, March 17, 1981.

3. Burger, H. C., and VanCitter, P. H., "Preparation of Bismuth- Antimony Vacuum Thermal Elements by Vaporization", Z. Phys., V. 66, 1930, p. 210.

4. Harris, L. and Johnson, E. A., "Technique for Sputtering Sensitive Thermocouples", Rev. Sci. Inst., 5, 1934, p. 153.

5. Benderskey, D., "A Special Thermocouple for Measuring Transient Temperatures", Mech. Engr., 1953, 75, 117.

6. Dils, R. R. and Follansbee, P. S., "Superalloy Sensors", presentation at the Third International Symposium on Superalloys, Seven Springs, PA, Sept. 1, 1976.

7. Dils, R. R. and Follansbee, P. S., "Heat Transfer Coefficients Around Cylinders in Crossflow in Combustor Exhaust Gases", 22nd Gas Turbine Conference, ASME, Gas Turbine Div., Philadelphia, PA, March 27-31, 1977.

8. Weast, R. C., Handbook of Chemistry and Physics, 48th Ed., The Chemical Rubber Company, 1968, pages D-25 and B-215.

9. Schmidt, L. D. and Wang, T.; "Morphology and Surface Composition of Alloy Particles in Reactive Atmospheres", J. of Vacuum Science Technology, 18(2), March 1981, p. 520

10. Vossen, J. L., and O'Neill, J. J., "R-F Sputtering Processes", RCA Review 29 (2) 1968.

11. Atkinson, W. H. and Guenard, R. N., "Turbine Pyrometry in Aircraft Engines", Proc. of Joint IEEE/ERA Electro/78 Convention, v. 33, Boston, MA, May 1978.

12. Atkinson, W. H. and Strange, R. R., "Pyrometer Temperature Measurements in the Presence of Reflecteds Radiation", ASME Paper No. 76-HT-74, August 1976.

13. Moffat, R. J., "Understanding Thermocouple Behavior", ISA Conference and Exhibit, New York, NY, October 28-31, 1968.

14. Vossen, J. L., et al., Thin Film Processes, Academic Press, 1978.

Page Intentionally Left Blank

APPENDIX

ENGINE TEST PLAN

1.0 PATTERN OF SENSORS AND FABRICATION OF REFERENCE WIRE THERMOCOUPLES

The sensor pattern will consist typically of four sputtered thin film thermocouples and one reference wire thermocouple on each of six blades. The thin film thermocouples will be positioned typically as shown in Figures i and ii. The position of thermocouples is such that at least two thin film thermocouples and the one reference wire thermocouple are viewed by the optical pyrometer on each blade. The pattern provides two thin film thermocouples on the pressure side and two on the suction side of each blade. The maximum dimension of each thin film temperature sensor measurement zone will not exceed 1.3 mm, as shown in Figure ii. The thin film leads from the measurement point to the thin-film-to-lead-wire connections will be 1.3 mm maximum width. The thin-film-to-lead-wire connections will be located on the under side of the platform. The thickness of the overall thin film portion of the sensor assembly will not exceed 0.015 mm.

2.0 PRELIMINARY TESTS OF THIN FILM SYSTEMS

2.1 Visual Inspection and Photographs

The physical appearance of the thin film thermocouple systems and reference wire thermocouple systems will be documented by photographs, supplemented by written descriptions and sketches based on visual examination in the case of details which cannot be clearly delineated in photographs. This documentation will include the appearance of fabricated systems on the blade airfoil, platform, platform underside, jump region, disk lead-wire region, disk hub splice region, trunk lead region in the high-pressure compressor, and connections to the telemetry modules. The height of the build-up in the region of the reference wire thermocouple junctions and lead work on each airfoil will be measured to document the effects of erosion. The documentation will be maintained step-by-step during initial assembly of the engine and again during teardown of the engine.

2.2 Electrical Tests

A low-voltage electronic ohmmeter with an applied voltage of less than 0.5 volts on the highest range will be used to measure loop resistance of each thermocouple channel and leakage resistance to the electrical ground level of the metal components in the engine. For example, it is expected that initial loop resistance readings will be on the order of 22 and 41 ohms/meter for 0.076 mm Pt and Pt-10% Rh lead wires, respectively, and 8 and 15 ohms/meter for 0.127 mm lead wires. Resistance to ground is expected to be more than 10^7 ohms initially, except in the case of the grounded reference wire thermocouples where resistance to ground measurements should correspond to the known length of lead wire between the point of measurement and the grounded

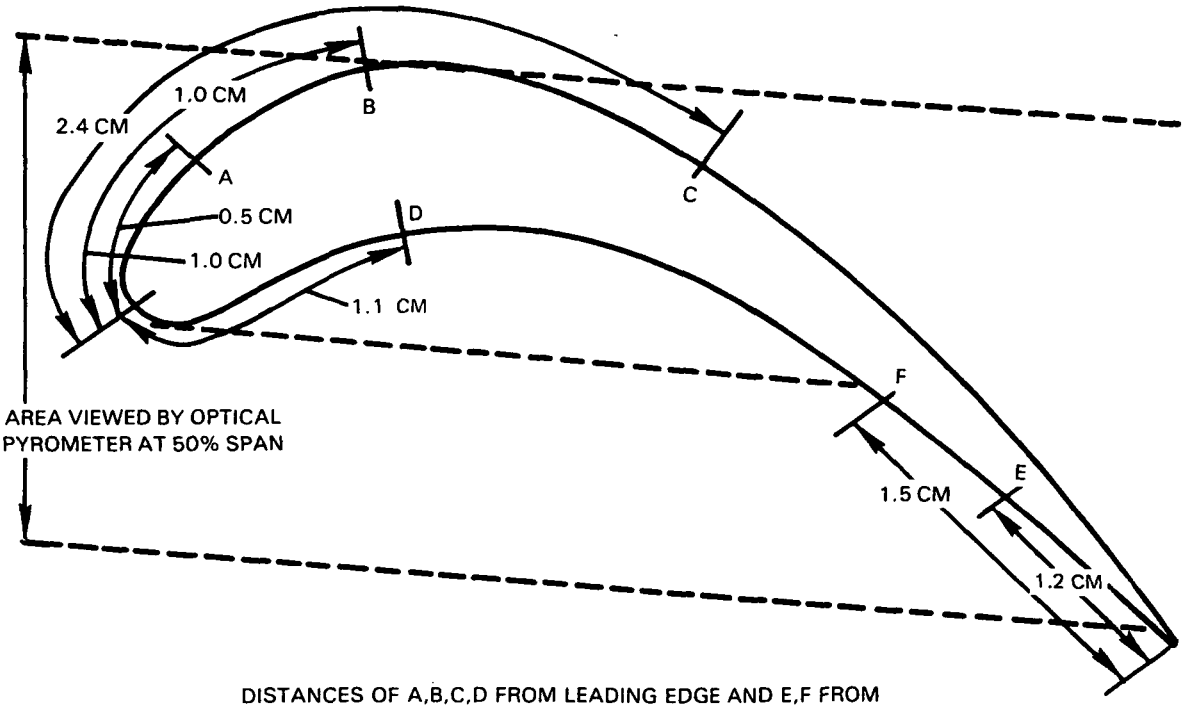

DISTANCES OF A,B,C,D FROM LEADING EDGE AND E,F FROM TRAILING EDGE ARE MEASURED PARALLEL WITH BLADE PLATFORM

LOCATION F IS AT 50% SPAN
ALL LOCATIONS ARE IN THE 41-DEGREE VIEWING PLANE OF THE OPTICAL PYROMETER, AS SHOWN IN FIGURE ii

BLADES	THIN-FILM THERMOCOUPLE LOCATIONS
1, 2 & 3	A, C, D, F
4, 5 & 6	A, B, E, F

Figure i Typical Location of Thin Film Thermocouples on High Pressure Turbine First Stage Vanes.

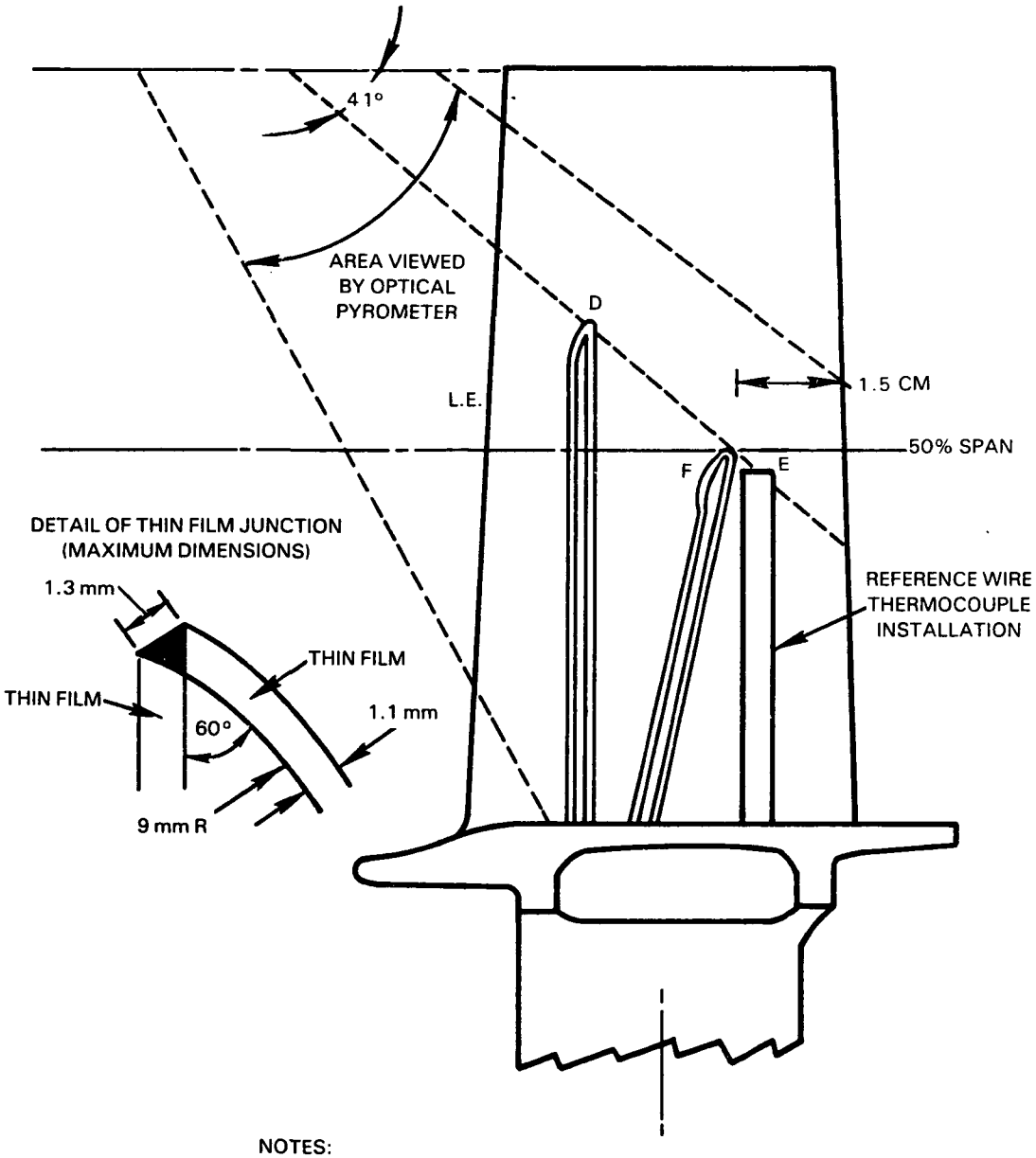

Figure ii Lateral View Showing Typical Location of Thin Film Thermocouple Installation on High Pressure Turbine First Stage Blade, Pressure Side.

thermocouple junction. Any significant change from accepted initial baseline readings obtained at time of assembly will be further investigated to determine the location and cause of the high or low reading. In the case of isolated opens or shorts to ground in the thin films on the blades, it is expected that the locations will be determined electrically within 0.5 cm, for example. The electrical measurements will be correlated with photographs and visual examinations to document any failure modes as completely as possible.

2.3 Preliminary Calibration Methods and Procedures

Calibration of each blade will be accomplished by placing the blade in a furnace, and monitoring the temperature of the thin film and wire thermocouples on a chart recorder with a temperature gradient imposed between the airfoil and the platform reference thermocouples. The temperature gradient will be at least 20% of absolute temperature on the airfoil. The furnace will be allowed to reach equilibrium for one hour or until the rate of change of the indicated temperatures is less than 1K in 10 minutes, whichever is larger. Then the temperature of each thin film thermocouple and reference wire thermocouple will be recorded from a digital readout of a Honeywell thermocouple monitor. A minimum of eight points will be recorded, with temperatures ranging from ambient to 1300K. At 1300K a drift test will be conducted on one blade for 5 hours at one atmosphere pressure plus 5 hours at a pressure of at least 6 atmospheres.

After the installation of the bladed disk in the engine is completed, testing for open circuits and for leakage to ground will be made, on the high-pressure turbine rotating module prior to splicing the disk leads to the trunk leads to the telemetry package, using a low voltage, low current, Data Precision ohmmeter model 175.

3.0 ENGINE TESTING METHODS AND PROCEDURES

3.1 Test Matrix

An optical pyrometer will be installed and pyrometer temperature data recorded. Testing will continue until a total of 50 hours have been completed.

During the 50 hours of testing, the following operating conditions are to be included:

- Twenty-five hours at intermediate power settings (30 to 80 percent of maximum rated power).
- Ten hours at a turbine inlet temperature of 1370K or higher.
- One hour at 100 percent of rated power (take-off thrust).
- Twenty start-ups and shutdowns.

After the start of the engine test if a partial teardown is scheduled to examine or change hot section components, then at this time, all instrumented blades will be physically examined, and any malfunctioning channels will be

electrically checked. This examination will isolate the failure mode (though it may not identify the precise location). A complete teardown and failure analysis will be carried out after the completion of the engine test.

3.2 Data Recording Methods

Signals from the thin film and reference thermocouples will be digitized at a rate such that a scan of all thermocouples requires only a few seconds. The data (in millivolt units) will be recorded on digital magnetic tape along with date, time, and other data to identify the engine operating condition. Monitoring of approximate indicated temperatures during engine operation will also be provided.

The optical pyrometer is a stationary sensor which detects the detailed temperature profile of all blade surfaces which pass its view. The data signal must be recorded during a full engine revolution and the blades and locations of interest identified. The flame-sprayed coating strip over the reference thermocouple leadwork on each blade will provide location reference during engine operation. The "two color" pyrometer senses infrared radiation in two spectral ranges to allow correction for reflected radiation. The linearized signal from the pyrometer detector system will be digitized and displayed using a digital storage scope. The scope capacity is typically 4000 points (about 34 points per blade). Data will be transferred to a digital magnetic disk for storage.

3.3 Data Acquisition Frequency

A recording of all thin film and reference thermocouple signals will be made at every stabilized steady state engine operating point. When the duration of an operating point exceeds 15 minutes, a recording will be made every 15 minutes. The total number of recordings during the 50 hours of testing will be at least 100.

Optical pyrometer signals, when available, will be recorded simultaneously with the thermocouple recordings.

3.4 Data Reduction Procedures

Temperature information from the thin film and reference thermocouples will be produced by computer processing of the millivolt levels recorded on digital magnetic tape. This process involves tape reading, applying the appropriate calibration curve, and printing the result (on paper) in engineering units along with test date, time, and operating condition identification. The calibration curves for the thin film thermocouples will be based on the initial laboratory calibrations plus corrections for drift.

Temperature information from the optical pyrometer data will be produced by plotting the contents of the digital magnetic disk on graph paper using a calibrated X-Y plotter. Temperatures at the desired blade locations and the magnitude of the reflected radiation correction will be obtained from these plots.

3.5 Measurement Uncertainty Due to Blade Surface Temperature Gradient in the Engine

Figure iii shows the predicted typical surface temperature distribution on a turbine blade in an engine operating at maximum power. Gradients on the order of 3 percent per centimeter in both the spanwise and chordwise directions are predicted at some locations at this extreme operating point. At lower powers all gradients will be lower, and at the location chosen for the reference wire thermocouple and optical pyrometer reference spot, the expected gradients will be less than 1.0 percent per centimeter. The distance between reference wire junction and thin film thermocouple junction typically is 3 mm. The uncertainty in location of the point sensed by the optical pyrometer is typically 2.5 mm. Uncertainty in temperature difference between thin film thermocouple and optical pyrometer due to gradients is, therefore, less than 0.3 percent at high power points and 0.15 percent at low power points. Uncertainty in temperature difference between the thin film thermocouple and the reference wire thermocouple due to surface temperature gradients will also be less than 0.3 percent at high power points and 0.15 percent at low power points.

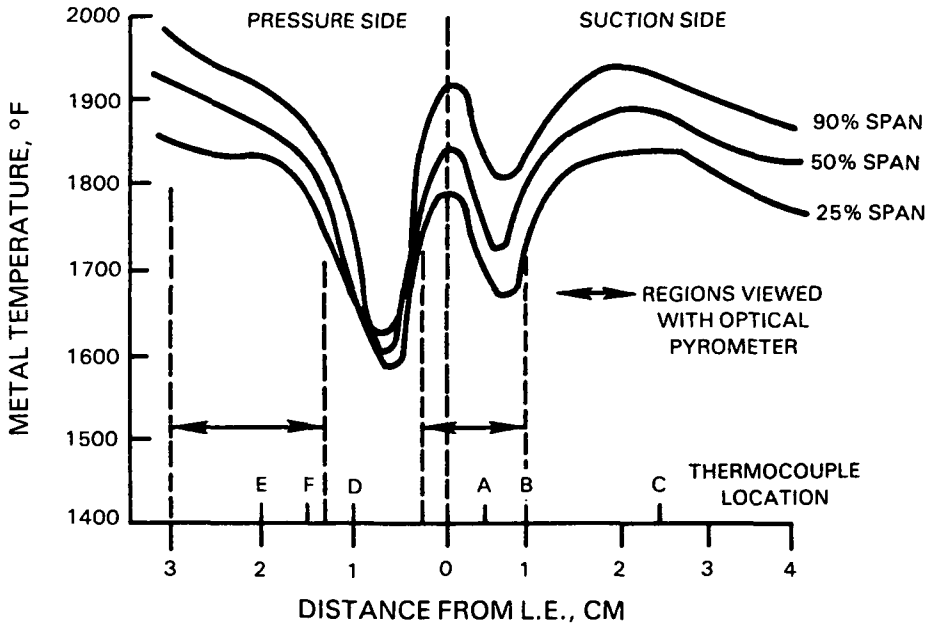

Figure iii Typical Expected Metal Temperature for Sea Level Takeoff Condition.

It is worth noting that the reference wire thermocouple will be mounted on the blade surface (not recessed into it) and, as a result, may indicate a temperature higher than the surrounding metal surface temperature as a result of hot gas flow impact on the wire thermocouple lead wires. Since the separation between thin film thermocouple and reference wire thermocouple (3.0 mm) is larger than the spot resolution of the optical pyrometer (2.5 mm), the optical pyrometer scan is expected to reveal the magnitude of this effect.

3.6 Measurement Uncertainty Due to Reference Thermocouple Wire Material

Reference wire thermocouples and thermocouple lead wires on the turbine disk are to be constructed of ANSI Type "S" wire (platinum and platinum/10 percent rhodium) certified by vendors to be of thermocouple grade with ±0.25 percent traceability to the National Bureau of Standards. Samples of each batch of wire are to be checked against laboratory transfer standards to ±0.25 percent at temperatures from 1200 to 1700K. In addition, a homogeneity check is to be carried out over sample lengths of the wire. If any sample fails to meet specifications, the entire batch is rejected. Thermocouple lead wires used on the high rotor shaft ("trunk leads") are to be copper vs copper/nickel Type S extension wire with error limit of 3.3K at 300K and 5.5K at 811K.

3.7 Automatic Data System

The temperature data from thin film thermocouples and reference wire thermocouples will be recorded at the test stand by high-accuracy d.c. automatic data system normally employed for performance data acquisition in engine tests. The uncertainty contribution in temperature measurement channels in this system is to be less than ±0.25 percent.

3.8 Optical Pyrometer System

The factors affecting uncertainty in turbine blade temperature measurement with the dual spectral area (two-color) optical pyrometer in engine testing have been discussed in References 1 and 2. The principal uncertainty contributions are the following:

Optics Cleanliness - A nitrogen purge is to be used to keep the viewing window clean, and cleanliness is to be further maintained by inspection and cleaning between engine runs. Laboratory tests indicate that measurement uncertainty from this source can be maintained below ±0.3 percent.

Blade Surface Emissivity - The black-body cavity nature of the turbine blade geometry is believed to reduce the uncertainty due to variations in emissivity to ±0.5 percent.

Blade Reflections - Radiation reflected from hotter sources, such as the combustor luminous flame, can increase the output of a conventional pyrometer by as much as 5 percent above actual blade temperature. The two-color pyrometer automatically corrects for this reflected energy and reports both the corrected temperature and the size of the correction. The uncertainty in this process is believed to be 25 percent of the correction. The uncertainty will therefore be known at each operating point and, on the basis of previous engine test data will vary from ±0.2 to ±1.2 percent.

Detector and Analyzer - Extensive laboratory testing and engine test experience show that the optical pyrometer detector and analyzer systems contribute less than ±0.25 percent uncertainty to the measurement of temperature.

4.0 POST-TEST FAILURE ANALYSIS METHODS AND PROCEDURES

Visual inspections, photographs, and electrical opens and shorts tests will be the methods employed for failure analysis. A series of base- line visual inspections, photographs and electrical tests, described in Section 2.1 will be carried out during the installation of blades in the turbine disk and installation of the disk trunk leads and telemetry system in the engine. After the completion of the engine test, a third series of inspections will be carried out. This series, contingent upon the extent of the teardown, will be as extensive as the first series, and in addition will include removal of the blades from the engine and a repeat of the oven calibrations (Section 2.3) on any instrumented blades with functioning thermocouple systems.

CONTRACT REPORT DISTRIBUTION LIST

Instrumentation R&D Branch

Each addressee will receive one copy unless indicated otherwise.

NASA Lewis Research Center
21000 Brookpark Road
Cleveland, OH 44135
Attn: R. Holanda, M.S. 77-1
(50 copies)

NASA Lewis Research Center
21000 Brookpark Road
Cleveland, OH 44135
Attn: Leonard W. Schopen, M.S. 501-11

NASA Scientific and Technical
Information Facility
P. O. Box 33
College Park, MD 20740
Attn: Acquisitions Branch
(22 copies)

NASA Lewis Research Center
21000 Brookpark Road
Cleveland, OH 44135
Attn: Library, M.S. 60-3
(2 copies)

NASA Lewis Research Center
21000 Brookpark Road
Cleveland, OH 44135
Attn: Report Control Office, M.S. 5-5

General Electric Company
Aircraft Engine Group
Evendale, OH 45215
Attn: Wayne Shaffernocker, MSH-78
Ronald Wise, MSH-78

Stanford University
Stanford, CA 94305
Attn: Dr. R. J. Moffat
Asst. Prof., Mech. Engr.
Dir. Thermoscience
Measurement Center

Air Force Wright Aeronautical
Laboratory
Wright Patterson AFB, OH 45433
Attn: R. Cox/POTC

Air Force Wright Aeronautical
Laboratory
Wright Patterson AFB, OH 45433
Attn: Everett E. Bailey/AFWAL/NASA-PO

Air Force Wright Aeronautical
Laboratory
Wright Patterson AFB, OH 45433
Attn: Deborah Finnerty/POTC

Air Force Wright Aeronautical
Laboratory
Wright Patterson AFB, OH 45433
Attn: M. Roquemore/POSF

Roto Data, Inc.
10200 Anderson Way
Cincinnati, OH 45242
Attn: David Davidson

UTRC/OATL
Palm Beach Gardens Facility
West Palm Beach, FL 33402
Attn: John T. Carroll
Bldg. 30 (MS R-23)

Lewis Engineering Company
238 Wate Street
Naugatuck, CT 06770
Attn: C. B. Stegner

Arnold Engineering
Development Center
Arnold Air Force Station, TN 37389
Attn: Marshall Kingery

Hitec Corporation
Nardone Industrial Park
Westford, MA 01886
Attn: Steve Wnuk

General Electric Company
Aircraft Engine Group
1000 Western Avenue
Lynn, MA 01910
Attn: George Leperch, A129dD

General Electric Company
Aircraft Equipment Division
50 Fordham Road
Wilmington, MA 01887
Attn: Ronald J. Casagrande

Detroit Diesel Allison
Box 894
Indianapolis, IN 46206
Attn: John Custer, W-16

Detroit Diesel Allison
Box 894
Indianapolis, IN 46206
Attn: Ken Cross

Detroit Diesel Allison
Box 894
Indianapolis, IN 46206
Attn: David Willis

Detroit Diesel Allison
Box 894
Indianapolis, IN 46206
Attn: Ralph Fox

Battelle Columbus Laboratories
505 King Avenue
Columbus, OH 43201
Attn: Ross G. Luce, Energy &
Thermal Tech. Section

Teledyne CAE
1350 Laskey Road
Toledo, OH 43612
Attn: R. Hugh Gaylord

Garret-AiResearch
P. O. Box 5217
Phoenix, AZ 85010
Attn: N. Fred Pratt

FluiDyne Engr. Corporation
5900 Olson Memorial Highway
Minneapolis, MN 55422
Attn: T. Matsuura

AVCO Corporation
Lycoming Division
550 South Main Street
Stratford, CT 06497
Attn: E. Twarog, Mgr.
Electronics and Instr.

Thermonetics Corporation
1028 Garnet Avenue
San Diego, CA 92109
Attn: H. F. Poppendiek

Battelle Columbus Laboratories
505 King Avenue
Columbus, OH 43201
Attn: M. M. Lemcoe

Peter K. Stein
5602 East Monterosa
Phoenix, AZ 85018

Pratt & Whitney Aircraft
Main Plant
P. O. Box 2691
West Palm Beach, FL 33402
Attn: John Prosser (MS C-04)

National Bureau of Standards
Washington, DC 20234
Attn: Ray Dils

National Bureau of Standards
Washington, DC 20234
Attn: George Burns
Inst. for Basic Research

General Electric Company
P. O. Box 8
Schenectady, NY 12301
Attn: Dr. David Skelley
Bldg. K-1, Rm. 3B24

Mechanical Technology, Inc.
968 Albany-Shaker Road
Latham, NY 12110
Attn: R. Hohenberg

Boeing Aerospace Company
Engineering Laboratories
Seattle, WA 98124
Attn: Darrell R. Harting

Engelhard
Engelhard Industries Div.
228 East 10th Street
Newport, KY 41075
Attn: Ronald G. Braun

Williams Research
2280 West Maple Road
Walled Lake, MI 48088
Attn: Henry Moore, Head
Instr. Dept.

Virginia Polytechnic Institute
and State University
Mechanical Engineering Dept.
Blacksburg, VA 24061
Attn: W. F. O'Brien, Jr.

Naval Post Graduate School
Department of Aeronautics (Code 67)
Monterey, CA 93940
Attn: Prof. R. P. Shreeve

Pennsylvania State University
233 Hammond Building
University Park, PA 16802
Attn: Prof. B. Lakshminarayana

Kulite Semiconductor Products, Inc.
1039 Hoyt Avenue
Ridgefield, NJ 07657
Attn: John R. Hayer

Bolt Beranek and Newman, Inc.
50 Moulton Street
Cambridge, MA 02138
Attn: Richard E. Hayden

Garrett Turbine Engine Company
111 South 34th Street
P. O. Box 5217
Phoenix, AZ 85010
Attn: Lee A. Matsch, Chief
Mech. Component Design
Engr. Sciences